Abstract

Utilizing stable isotopes $\delta^{13}C$ and $\delta^{15}N$ to analyze diet and role of mesopelagic fishes in the biological pump from the North Pacific Subtropical Gyre

By Elise Ann Easterling

Advisor Dr. Rebecca Asch

East Carolina University Department of Biology

December 2023

Several studies have sought to quantify the contribution of mesopelagic fishes to the ocean carbon cycle and the biological pump. However, to determine fish-mediated carbon transport, it is necessary to understand the behavior and ecology of mesopelagic fishes, including their foraging ecology. In this study, stable isotope analysis (SIA) was used to gather insight into mesopelagic fishes' contribution to marine food webs and their feeding behavior by interpreting $\delta^{13}C$ and $\delta^{15}N$ isotope signatures obtained from white muscle tissue. $\delta^{13}C$ and $\delta^{15}N$ represent the ratio of $^{13}C/^{12}C$ and $^{15}N/^{14}N$ isotopes relative to an international standard in a sample, in this case mesopelagic fish white muscle tissue. Mesopelagic fishes were sampled from the North Pacific Subtropical Gyre at station ALOHA. A MOCNESS net was used to sample mesopelagic fishes from depths of 0-1,000 m. From SIA results, I compared $\delta^{13}C$ and $\delta^{15}N$ isotope signatures based on fish migratory status (fishes who vertically migrate to feed or those that do not), time of day, depth sampled, variations in fish size (length/weight), and interspecific variation in isotope signatures. From this thesis, I sought to gather insight of fish dietary sources and trophic structure based on the studied parameters. In addition, how SIA results fluctuate with the chosen factors will help scientists learn how to properly interpret SIA results. The results of my study indicated that $\delta^{13}C$ and $\delta^{15}N$ isotope signatures are higher in fishes caught at deeper depths and in

those classified as non-migrators in comparison to migratory fishes. In addition, $\delta^{13}C$ was slightly higher for migratory fishes in shallower depths (<400 m) at day-time compared to other time and depth categories. An increase in $\delta^{15}N$ at night at deeper depths (>400 m) for non-migratory fishes was found to be significant. I also observed a positive trend in $\delta^{13}C$ and $\delta^{15}N$ isotope signatures with increasing fish biomass (both length and weight) for migratory and non-migratory fishes. Variation in $\delta^{15}N$ was observed amongst different species and genera of mesopelagic fishes; yet there was little fluctuation in $\delta^{13}C$ between mesopelagic fish genera/species. Based upon $\delta^{15}N$ isotope signatures, my data indicate that non-migratory fishes, who feed at deeper depths, likely feed from a detrital based food web and fishes who feed near the ocean surface feed from pelagic based food web. These sources of carbon are important to account for when quantifying fish mediated carbon contribution to the biological pump. The depth at which carbon is transported by physical or biological processes impacts the duration for which carbon is sequestered in the ocean. The deeper carbon is transported, the longer it remains sequestered and increases the chances of escaping bacterial remineralization and being released back into the atmosphere through wind and wave activity. In addition, biological factors such as fish size and their diet also impact how much carbon is injected into the ocean interior by functions such fecal pellet egestion, respiration, and mortality.

Utilizing stable isotopes $\delta^{13}C$ and $\delta^{15}N$ to analyze diet and role of mesopelagic fishes in the biological pump from the North Pacific Subtropical Gyre

A Thesis

Presented To the Faculty of the Department of Biology

East Carolina University

In Partial Fulfillment of the Requirements for the Degree

Master of Science in Biology

by

Elise Ann Easterling

Graduation December 2023

Director of Thesis: Dr. Rebecca Asch, PhD
Thesis Committee Members:
Dr. Rachel Gittman, PhD
Dr. Amanda Netburn, PhD
Dr. Fred Scharf, PhD
Dr. Siddhartha Mitra, PhD

Utilizing stable isotopes $\delta^{13}C$ and $\delta^{15}N$ to analyze diet and role of mesopelagic fishes in the biological pump from the North Pacific Subtropical Gyre

By

Elise Ann Easterling

APPROVED BY:

Director of Thesis _____

Dr. Rebecca Asch

Committee Member _____

Dr. Rachel Gittman

Committee Member _____

Dr. Siddhartha Mitra

Committee Member _____

Dr. Fred Scharf

Committee Member _____

Dr. Amanda Netburn

Chair of the Department of Biology _____

Dr. David Chalcraft

Dean of the Graduate School _____

Dr. Kathleen T. Cox

Acknowledgements

I would like to express immense gratitude for all of those who contributed to guiding me through this process. Thank you to my advisor, Dr. Rebecca Asch, who always challenged me and provided me with a depth of knowledge and suggestions for excelling in my thesis research. Thank you to Dr. Fred Scharf for your insight and allowing me access to the stable isotope facilities at UNCW. I would also like to thank Dr. Siddhartha Mitra for your instruction and use of your lab during the sample processing for stable isotope analysis. Additionally, thank you to Dr. Amanda Netburn and Dr. Rachel Gittman for fielding my questions and offering me advice along the way. Thank you to my fellow lab mates who helped assist me in my research and field collection: Naomi Jainarine, Reece Warfel, Caitlin McGarigal, Quentin Nichols, Kat Dale, and Cecilia Wood. You all were a pleasure to get acquainted with and made late night larval fish sampling more enjoyable with our conversations. Finally, a thank you to Dr. Aaron Carlisle, Helena McMonagle, and Ashley Maloney, you all provided me with so much knowledge and information to help guide me through my research.

I would also like to thank my friends and family for their support through this process. I endured many physical and mental challenges along the way. Their love and belief in me to achieve this academic goal has been extremely valuable.

Table of Contents

LIST OF TABLES……viii

LIST OF FIGURES……..x

LIST OF ABBRIEVIATIONS……...xii

CHAPTER 1: LITERATURE REVIEW

1.1 Project Overview…….1

1.2 Literature Review……....2

1.2.1 Ocean Carbon Cycle and the Biological Pump……....2

1.2.2 Passive Carbon Flux…….....5

1.2.3 Microbial Marine Processes…….....6

1.2.4 Role of Zooplankton and Micronekton in the Biological Pump……...6

1.2.5 Ecology of Mesopelagic Fishes……....9

1.2.6 Mesopelagic Fish-Mediated Carbon Export Flux……...12

1.2.7 North Pacific Subtropical Gyre (NPSG)…….....14

1.2.8 Hawaiian Ocean Time-series (HOT) Program……18

1.2.9 Stable Isotope Analysis (SIA)…….20

1.2.10 $\delta^{15}N$ Variation in Micronekton in the Mesopelagic Zone…….24

1.3 Thesis Structure…….26

CHAPTER 2: UTILIZING STABLE ISOTOPE ANALYSIS (δ13C and δ15N) TO STUDY FOOD WEB PATTERNS AND ECOLOGY OF MESOPELAGIC FISHES FROM THE NORTH PACIFIC SUBTROPICAL GYRE

2.1 Introduction…….. 27

2.2 Research Objectives and Goals…….34

2.3 Methods…….....36

2.3.1 Sample Collection…….....36

2.3.2 Mesopelagic Fish Sample Processing……37

2.3.3 Encapsulation for Stable Isotope Analysis…….....39

2.3.4 Stable Isotope Analysis……..40
2.3.5 Data Analysis……..41
2.4 Results…….....42
2.4.1 Depth Distribution……..42
2.4.2 Mesopelagic Fish Diversity and Evenness……43
2.4.3 Relationship between $\delta^{15}N$, $\delta^{13}C$, and Mesopelagic Fish Size…….....43
2.4.4 $\delta^{15}N$ and $\delta^{13}C$ and Time of Day and Sampling Depth Relationship……..45
2.4.5 $\delta^{15}N$ and $\delta^{13}C$ and Genera/Species Relationship……...47
2.5 Discussion…….....48
2.5.1 Species Composition and Depth Distribution……....49
2.5.2 Mesopelagic Fish Diversity and Evenness…….....50
2.5.3 Relationships between $\delta^{15}N$, $\delta^{13}C$ and Mesopelagic Fish Size…….....51
2.5.4 Relationships between $\delta^{15}N$ and $\delta^{13}C$ and Time of Day and Sampling Depth……..53
2.5.5 $\delta^{15}N$ and $\delta^{13}C$ and Genera/Species Relationships…….....57
2.6 Broader Implications……60
2.7 Conclusion……61
Chapter 3: PRESERVATION METHOD ANALYSIS AND ALLOMETRIC EQUATION DEVELOPMENT
3.1 Introduction…….....62
3.2 Preservation Method Hypothesis…… 66
3.3 Methods……67
3.3.1 Allometry……..... 67
3.3.2 Assessment of Preservation Method upon SIA Results…… 68
3.3.3 Fish Dissection Methods…….....69
3.3.4 Encapsulation……70
3.3.5 Stable Isotope Analysis……71
3.3.6 Data Analysis……72
3.4 Results…….....73
3.4.1 Preservation Method Analysis……..73

3.4.2 Allometry Analysis……. 75

3.5 Discussion……76

3.5.1 Preservation Method…….....76

3.5.2 Allometric Analysis……...79

3.6 Conclusion……81

CHAPTER 4: CALCULATION METHODS FOR THE GUT CONTENT CARBON FLUX OF MESOPELGIC FISHES IN THE NPSG

4.1 Introduction……..82

4.2 Methods for Calculating Micronekton Gut Flux……..82

4.3 Assumptions……86

4.4 Conclusion……....87

References……..88

Tables and Figures……..97

Chapter 2 Tables……97

Chapter 2 Figures……. 113

Chapter 3 Tables……...121

Chapter 3 Figures…….....125

Appendix……..132

List of Tables

CHAPTER 2 TABLES

Table 1 Count number of species dissected……..97

Table 2 Count of fishes pooled during dissection from each MOCNESS net……..99

Table 3 Fish species pooled during dissection from each MOCNESS net…….....99

Table 4 Linear regression of fish length and weight and SIA relationship…….....100

Table 5A ANOVA for (migrators) $\delta^{15}N$ depth and time of day variability…….....101

Table 5B ANOVA for (migrators) $\delta^{13}C$ depth and time of day variability…….....101

Table 5C Mean $\delta^{15}N$ and $\delta^{13}C$ (migrators) and time and depth variability……...101

Table 6A ANOVA for (non-migrators) $\delta^{15}N$ depth and time of day variability……102

Table 6B ANOVA for (non-migrators) $\delta^{13}C$ depth and time of day variability…….....102

Table 6C Mean $\delta^{15}N$ and $\delta^{13}C$ (non-migrators) and time and depth variability…….....102

Table 7A Tukey Kramer test (non-migrators) $\delta^{15}N$ and time and depth variability.....102

Table 7B Tukey Kramer test (non-migrators) $\delta^{13}C$ and time and depth variability.....103

Table 8A Tukey Kramer test (migrators) $\delta^{15}N$ and time and depth variability.....104

Table 8B Tukey Kramer test (migrators) $\delta^{13}C$ and time and depth variability.....104

Table 9A $\delta^{13}C$ statistics in relation to mesopelagic fish species and genera……...105

Table 9B $\delta^{13}C$ ANOVA for mesopelagic fish species and genera……..…….105

Table 10A $\delta^{15}N$ statistics in relation to mesopelagic fish species and genera…….106

Table 10B $\delta^{15}N$ ANOVA for mesopelagic fish species and genera……106

Table 11A Sediment trap data from the KM1910 cruise…….107

Table 11B Ring net data of zooplankton samples from the KM1910 cruise…….....107

Table 11C $\delta^{15}N$ and $\delta^{13}C$ benthic and pelagic data from Davenport and Bax (2002)….108

Table 12A Tukey Kramer test for $\delta^{13}C$ and species and genera…….....109

Table 12B Tukey Kramer test for $\delta^{15}N$ and species and genera……..110

CHAPTER 3 TABLES

Table 1 Description of fish specimens used to develop the allometric relationships…..121

Table 2 Descriptive statistics of carbon content (mg) for preservation analysis…….122

Table 3 Descriptive statistics of nitrogen content (mg) for preservation analysis……...122

Table 4 Descriptive statistics of $\delta^{13}C$ for preservation analysis…….....123

Table 5 Descriptive statistics of $\delta^{15}N$ for preservation analysis……...123

Table 6 Linear regression for Atlantic silversides, bay anchovies, and naked gobies for carbon content (mg) and fish weight and length……..124

List of Figures

CHAPTER 2 FIGURES

Figure 1 Map of station ALOHA……..113

Figure 2A Frequency of dissected migrating and non-migrating mesopelagic from night and day-time tows from the MOCNESS net…….....114

Figure 2B Frequency of migrating and non-migrating mesopelagic from night and day-time tows from the MOCNESS net collected aboard the research cruise……115

Figure 3A Shannon Diversity Index……...116

Figure 3B Shannon Equitability Index……...116

Figure 4A Linear regression for migratory fishes for $\delta^{15}N$ and $\delta^{13}C$ and standard length relationship……..117

Figure 4B Linear regression for migratory fishes for $\delta^{15}N$ and $\delta^{13}C$ and weight relationship…….....117

Figure 5A Linear regression for non-migratory fishes for $\delta^{15}N$ and $\delta^{13}C$ and standard length relationship……...118

Figure 5B Linear regression for non-migratory fishes for $\delta^{15}N$ and $\delta^{13}C$ and weight relationship……118

Figure 6A $\delta^{15}N$ and $\delta^{13}C$ relationship with time of day and depth variability in migratory fishes…….119

Figure 6B $\delta^{15}N$ and $\delta^{13}C$ relationship with time of day and depth variability in non-migratory fishes…….119

Figure 7A Species/genera relationship and $\delta^{15}N$……..120

Figure 7B Species/genera relationship and $\delta^{13}C$…….....120

CHAPTER 3 FIGURES

Figure 1 Standard length frequency of dissected fishes……125

Figure 2A Preservation analysis upon nitrogen content (mg) in bay anchovies……..126

Figure 2B Preservation analysis upon carbon content (mg) in bay anchovies ……...126

Figure 3A Preservation analysis upon $\delta^{13}C$ in bay anchovies…….....127

Figure 3B Preservation analysis upon $\delta^{15}N$ in bay anchovies…….....127
Figure 4A Log transformed data for carbon content (mg) and fish weight for Atlantic silversides ……128
Figure 4B Log transformed data for carbon content (mg) and fish length for Atlantic silversides ……128
Figure 5A Log transformed data for carbon content (mg) and fish weight for bay anchovies ……....129
Figure 5B Log transformed data for carbon content (mg) and fish length for bay anchovies ……129
Figure 6A Log transformed data for carbon content (mg) and fish weight for naked gobies …….....130
Figure 6B Log transformed data for carbon content (mg) and fish length for naked gobies …….…….130

List of Abbreviations

ALOHA	A Long-term Oligotrophic Habitat Assessment
DIC	Dissolved Inorganic Carbon
DOC	Dissolved Organic Carbon
DVM	Diel Vertical Migration
FME	Fish Mediated Export
HOT	Hawaiian Ocean Time-series
Migrators	Mesopelagic fishes who migrate to shallower depths to feed.
Non-migrators	Mesopelagic fishes who remain at their habitual depth full-time and do not migrate to feed.
POC	Particulate Organic Carbon
NPP	Net Primary Productivity
NPSG	North Pacific Subtropical Gyre
SIA	Stable Isotope Analysis

Chapter 1: Literature Review

1.1 Project Overview

When carbon dioxide (CO_2) is mixed into surface seawater, photosynthetic phytoplankton converts the CO_2 into oxygen and organic matter. Carbon in organic matter is transferred through the food web beginning with organisms feeding on phytoplankton and subsequently moving up each trophic level (Passow and Carlson, 2012). Carbon is also transferred into deeper water through fecal matter and sinking dead organisms in the form of particulate organic carbon. Due to their vertical migration while feeding, mesopelagic fishes are believed to be a major mechanism for transporting organic matter below the euphotic zone (Ducklow and Steinberg, 2001). After feeding at the surface, the fishes retreat to depths below 200 meters, where carbon is released through fish respiration, defecation, and mortality (Saba et al., 2021). The amount of carbon that is sequestered in the ocean column and seafloor by these processes is not well established.

The initial objective of my research was to develop and test a method of tissue analysis that quantifies the amount of carbon that is potentially sequestered in the ocean column and seafloor by measuring the carbon that is ingested as food and expelled as waste by mesopelagic fishes. Stable Isotope Analysis (SIA) was used to determine carbon content in the fish gut contents and stomach linings. I utilized data collected from a research vessel in the summer of 2019 from Station ALOHA (A Long-term Oligotrophic Habitat Assessment), which is located in the North Pacific Subtropical Gyre (NPSG). The NPSG plays a large role in nutrient cycling, carbon fixation, and contains a high diversity of fish species, which makes it an ideal location to sample mesopelagic fishes (Karl, 1999). Due to the small size of fishes caught on this research cruise, there were difficulties separating carbon in gut contents from a fish's stomach lining among the smallest fish. I attempted to overcome this challenge by developing an allometric relationship between fish size and stomach lining carbon content, so that the stomach lining could be removed from fish-mediated carbon transport calculations. However, the initial results of using local fishes to build an allometric relationship between carbon in the stomach lining and fish size (standard length/weight) did not display a strong enough relationship to justify the continuation of this line of research. As a result, I had to develop a contingency objective that used the sampled mesopelagic fishes.

Instead of calculating mesopelagic fish-mediated carbon export, I decided to interpret $\delta^{13}C$ and $\delta^{15}N$ isotope signatures, obtained via SIA, to make inferences upon mesopelagic fish feeding behavior, food web patterns, and trophic ecology. SIA was run on white muscle tissue samples extracted from mesopelagic fishes collected from station ALOHA. Analyzing $\delta^{13}C$ and $\delta^{15}N$ has been used in other ecosystems to make inferences on animal diets, foraging behavior, and food web/trophic structure analysis (Ben-David and Flaherty, 2012). With the results from SIA, $\delta^{13}C$ and $\delta^{15}N$ isotope signatures were studied with regard to how these isotopes varied with depth, time of day, genera/species, and migration status of mesopelagic fishes. From these data, we can determine what environmental and biological factors influence trophic ecology and can make inferences about mesopelagic fish feeding behaviors and ecology. It is important for scientists to understand the behavior and physiology of mesopelagic fishes to understand their role in the ocean carbon budget and their role in marine food webs (Richards et al., 2020). With increasing interest in developing fisheries upon mesopelagic fishes (St. John et al., 2016), we need to understand the impact of what potentially harvesting these fishes will have upon the environment.

In this chapter, I will discuss the literature collected pertaining to mesopelagic fishes' role in the biological pump and their contributions to marine food webs. I will also summarize how stable isotope analysis can be utilized to study marine food webs and trophic structure with an emphasis on research with mesopelagic fishes. Stable isotope analysis and its role in understanding marine food webs is also discussed in greater depth in Chapter 2.

1.2 Literature Review

1.2.1 Ocean Carbon Cycle and the Biological Pump

The ocean plays a large role in the global carbon cycle. It holds approximately 50 times more carbon than the atmosphere (Nagaraja, 2020). CO_2 is constantly exchanged between the atmosphere and ocean due to wind mixing at the surface and concentration differences between the air-sea interface (Passow and Carlson, 2012). CO_2 concentrations are a function of atmospheric and ocean CO_2 partial pressure levels. Partial pressure of CO_2 is influenced by alkalinity, temperature, photosynthesis, and respiration (Nagaraja, 2020).

The ocean carbon cycle is influenced by physical, chemical, and biological processes. The physical component of the ocean carbon cycle is collectively known as the "solubility pump." The solubility pump is the process of air mixing CO_2 from the atmosphere into the ocean's surface waters, and the CO_2 dissolving at the surface (Nagaraja, 2020). The ability of CO_2 to dissolve in seawater is an inverse function of ocean temperature. The cooler the temperature of seawater, the higher rate of solubility for CO_2. As a result, higher latitudes possess cool surface water rich in CO_2 that sinks to the deep ocean. The sinking of cold CO_2-laden water becomes part of the deep ocean circulation pattern known as thermohaline circulation (Nagaraja, 2020). CO_2 may remain entrenched in deep ocean circulation for hundreds of years (Reibeek, 2011).

The physical processes of the carbon cycle are linked to the biological carbon cycle through its control of the mixed layer, as well as through other mechanisms (Boyd et al., 2019). Variation in mixed layer depth, temperature, and nutrient flux influence phytoplankton growth. Phytoplankton productivity is a key driver of biological control of the carbon cycle. Phytoplankton flourish in environments where light and nutrients are readily available for photosynthesis (Nagaraja, 2020).

Biological processes impact dissolved CO_2 levels via phytoplankton primary production and community-wide respiration. The term "biological pump" is associated with biological activity converting dissolved CO_2 into oxygen and organic matter through photosynthesis. The biological pump begins with phytoplankton using photosynthesis to convert CO_2 and nutrients, including nitrates, phosphate, silicates, and iron, into organic carbon in the form of carbohydrates and proteins along with oxygen as a byproduct (Ducklow and Steinberg, 2001). The biological pump also includes the transformation of carbon through food web processes, physical mixing, and gravitational settling due to sinking of either phytoplankton cells, fecal pellets, or marine snow (Nagaraja, 2020). This biological process is the key link between surface ocean processes and carbon storage in the ocean interior. The biological pump also influences the sustenance of mid-water organisms (Boyd et al, 2019). Cycling of carbon in the ocean is also mediated by a set of reversible, reduction-oxidation reactions involving dissolved inorganic carbon (DIC) and organic matter with marine organisms serving as a critical catalyst. DIC is converted to organic matter via photosynthesis and respired back to DIC in the deep ocean by bacterial remineralization or by other marine biota (Karl and Lukas, 1996). Information on the rates and

methods of DIC removal from the ocean's surface via biological pathways, the export of biogenic carbon (both as organic and carbonate particles) to the ocean's interior, and the sites of remineralization and burial are all key components of the carbon cycle (Karl and Lukas, 1996). Marine burial of carbon occurs via two different pathways. DIC is removed from seawater by photosynthetic organisms and converted into organic carbon, where a small fraction makes it to the seafloor to be incorporated into ocean floor sediment or deep currents. The second method of deep carbon burial occurs through calcifying organisms using DIC to produce carbonate minerals ($CaCO_3$) for their shells. When these shelled organisms die, they sink to the seafloor and can be buried in sediment. Once carbon is buried in the deep-sea sediment, it may remain locked there for millions of years (Cartapanis et al., 2018).

Approximately 90% of the total vertical DIC gradient from the ocean's surface to the deep ocean interior is attributed to the biological pump, while the remaining 10% is attributed to the solubility pump (Boyd et al., 2019). In the upper 1,000 meters of the ocean, ~70% of CO_2 concentration differences is maintained by the export processes of the biological pump (Davison et al., 2013). The biological pump sends roughly 11 gigatons of carbon to the deep ocean each year (Gewin, 2016). Atmospheric partial pressure of carbon dioxide (ρCO_2) would be two times higher in the absence of the biological pump. Carbon principally makes it way to deep ocean storage through particle sinking in the form of fecal or detrital matter where the particulate organic matter (POM) is buried in sediment or circulated in deep ocean currents (Boyd et al., 2019).

The biological pump sequesters carbon deeper into the ocean by the means of active and passive transport in either particulate or dissolved form (Boyd et al., 2019). Passive transport refers to the sinking of organic matter through the water column. It relies on gravitational settling for organic material to reach deeper depths. Active transport is the flux of material transported by animals as they move across depth ranges on a daily or seasonal timescale (Boyd et al. 2019). The amount of organic material transported below the mixed layer by an organism depends upon the depth at which the carbon is released back into the ocean via respiration, defecation, excretion, or mortality (Saba et al., 2021). Density and size of sinking particles from excretion can also influence the ultimate depth at which they are sequestered. The next section of this

chapter provides a brief overview of passive transport; active transport will be discussed in greater detail in the following sections in this literature review.

The biologically facilitated components of the carbon cycle include the production and turnover of organic matter. Photosynthesis and the biosynthesis of organic components encompass the processes that result in net primary production (NPP). NPP is the amount of photosynthetically fixed carbon available to the first heterotrophic level in an ecosystem. NPP is an important factor in regulating carbon sinks on land and in the ocean. The ocean's NPP is dominated by photosynthetic phytoplankton, hence phytoplankton serves as the foundation of the biological pump (Field et al., 1998). Local decomposition of organic matter supplies nutrients for ocean NPP rather than relying on new nutrient sources. Yet, biologically controlled carbon sinks rely on new nutrient sources, such as upwelling, biological nitrogen fixation, deposition of nutrients from the atmosphere, and cultural eutrophication (the anthropogenic input of excess nutrients into a water body). NPP is critical in carbon and nutrient dynamics and links biogeochemical and ecological processes (Field et al., 1998). Understanding NPP is a key component to determining the strength of the biological pump.

1.2.2 Passive Carbon Flux

Approximately half of the oxygen available to terrestrial organisms is produced by marine phytoplankton (Field et al., 1998). Phytoplankton is grazed by herbivorous zooplankton. Larger zooplankton, such as some copepods, consume phytoplankton and smaller zooplankton species and egest fecal pellets. Fecal pellets can be either re-ingested or combined with other detrital matter before sinking as large aggregates to the seafloor (Anderson et al., 2018). Dissolved organic carbon (DOC) produced by phytoplankton during photosynthesis is partially consumed and respired by bacteria. Any remaining DOC is advected into and/or mixed deeper in the water column (Ducklow and Steinberg, 2001). DOC and POM are consumed by mesopelagic bacteria, zooplankton, and fishes as it sinks deeper into the water column. Following bacterial consumption, the organic carbon is then respired, reverting it to DIC. In fact, animals and bacteria in the mesopelagic zone respire 90% of organic carbon from the surface (Sommer et al., 2017). DIC remains circulated in deep ocean currents or can be buried in sediment for millions of years. Thermohaline circulation will return DIC sequestered in the deep sea (>200 meters) back to the atmosphere on a millennial time scale (Ducklow and Steinberg, 2001). This project

hopes to quantify the amount of carbon that is sequestered in the ocean interior via sinking fecal pellets egested from mesopelagic fishes.

1.2.3 Microbial Marine Processes

In this section, I turn to the role of bacteria and viruses in the carbon microbial loop. Along with the biological pump, the microbial carbon pump (MCP) contributes to the ocean's ability to act as a carbon sink. The MCP is focused upon bacterially mediated chemical transformation of DOC from rapidly to slowly degrading forms. Oligotrophic regions, dominated by small phytoplankton species, will support a microbial loop, and favor the MCP. Marine microbial loops are vital to the regeneration of nutrients in oligotrophic regions. In fact, low nutrient availability alters phytoplankton stoichiometry and yields DOC with high carbon to nitrogen and carbon to phosphorus ratios (Herndl and Reinthaler, 2013). This is because phytoplankton needs these nutrients to grow and reproduce. When nutrients are limiting phytoplankton adjust their nutrient needs, which can lead to the production of DOM resulting in high carbon to nitrogen and carbon to phosphorous ratios (Herndl and Reinthaler, 2013).

POM and DOC involved in the biological pump are subject to microbial remineralization where most organic carbon will be converted back to DIC to return to the surface via thermohaline circulation. This microbial loop occurs on a time scale of a few days to weeks and rapidly declines with depth primarily due to decreasing temperature (Boyd et al., 2019). A small fraction of POM, around ~1%, will escape mineralization to be buried in ocean sediment (Jiao et al., 2010). Marine bacteria and archaea are primarily responsible for respiration of carbon at deeper depths. Marine microbes are also responsible for providing a mechanism of DOC release in surface waters by viral lysis. Metazoan grazers may release phytoplankton cytosols as DOM, and the expelled waste of the protists and metazoans also may contain DOC (Jiao et al., 2010).

1.2.4 Role of Zooplankton and Micronekton in the Biological Pump

Zooplankton are a key prey source of mesopelagic fishes and thus an important means of transporting carbon through the marine food web. Zooplankton themselves also play a large role in active carbon transport in the biological pump (Saba et al., 2021). Many species of mesozooplankton (0.2-20 mm) migrate daily from depth to the surface to feed. Zooplankton fecal pellets sink in the water column when they defecate in surface waters. Their fecal pellets are a source of organic carbon. After feeding at the sea surface in the euphotic zone, the

vertically migrating zooplankton retreat to deeper water (Ducklow and Steinberg, 2001). This mechanism of traveling to the surface daily to feed by aquatic organisms is known as diel vertical migration (DVM). Organisms observed with a migratory feeding pattern largely swim to the surface during nighttime hours and retreat back to deeper waters during daylight. This timed behavior is performed to optimize feeding while avoiding being seen by predators (Forward, 1988). Additionally, as these vertically migrating zooplankton swim down the water column, carbon is transported deeper into the ocean interior via respiration and defecation. Zooplankton, such as copepods, also contribute carbon through bodily decomposition. When zooplankton die, their bodies carry carbon with them as they sink. Most sinking detritus is mineralized by bacteria but a portion of sinking dead organisms reach the seafloor to be buried in sediment. The deeper carbon is injected into the water column, the longer carbon is likely to be stored in the ocean's interior (Passow and Carlson, 2012).

Overall, organisms that engage in DVM contribute more to DIC contribute production and oxygen utilization in the mesopelagic zone than to the vertical POC flux (Steinberg et al., 2016). Respiration of zooplankton is often measured by oxygen utilization versus CO_2 production (Steinberg et al., 2016). This finding indicates that DVM contributions to the carbon flux are largely respiratory via ingesting carbon at the surface and respiring it at depth. Approximately 50% of carbon taken up by zooplankton is respired (Steinberg et al. 2016). Areas that have increased DVM activity will exhibit an oxygen utilization profile that does not decrease monotonically with depth as is typical in other areas. In locations where DVM is a significant contributor to DIC production, a spike in oxygen utilization at depth should be observed in the presence of migrating zooplankton (Archibald et al., 2019).

The majority of mesopelagic micronekton, which are 2-10 cm in size and include fishes, crustaceans, and cephalopods, undertake DVM to obtain food. The migratory behavior of mesopelagic organisms in the active transport of the biological pump accounts for 15-40% of particle export flux in the mesopelagic zone (Romero-Romero et al., 2019). Active transport by zooplankton and fish mediated export (FME) has been estimated at several locations (Davison et al., 2013). If the midpoint of fluxes associated with the biological pump is taken from the reported range in the literature, the mean zooplankton active transport estimate is 13.4 mg C $m^{-2}d^{-1}$, the mean FME estimate is 11.4 mg C $m^{-2}d^{-1}$ and mean passive carbon flux is 51.6 mg C $m^{-2}d^{-1}$ (Davison et al., 2013). Saba et al. (2021) estimated an annual total of FME to be 1.5±1.2 Pg

C yr^{-1}. Carbon transport by DVM contributes greatly to the functioning of deep-sea ecosystems by providing food sources for other organisms. DVM also serves to benefit of coupling between pelagic and benthic communities. Such linking of different elements in marine ecosystems improves the resilience of deep-sea benthic systems to top-down or bottom-up disturbances, such as predation or removal of a resource, which could impact the structure of marine food webs (Romero-Romero et al., 2019).

Mesopelagic micronekton are a poorly understood group of organisms due to lack of research and small commercial value. In addition, mobile mesopelagic species tend to avoid net capture and are a difficult group of organisms to study in a lab setting due to the challenge of recreating their migratory feeding patterns and keeping them alive (Anderson et al., 2018).

An estimate of active transport by mesopelagic fishes using abundance, with a correction for capture efficiency, reveals that carbon export by fishes may be as high as 28% of the total carbon flux (Davison et al., 2013). These groups of fishes play a large role in the biological pump due to their large biomass. Based on acoustic and trawl data, mesopelagic fish biomass is estimated to be approximately one billion tons worldwide, likely dominating the world's total fish biomass (Gjøsaeter and Kawaguchi, 1980; Irigoien et al., 2014). Yet, this may be an underestimate of mesopelagic biomass because mesopelagic fishes have been observed to exhibit escape reactions to nets (Davison, et al., 2013). Recent findings using acoustic data by an echosounder to track mesopelagic fishes confirm the biomass underestimation to reveal the mesopelagic zone may hold 1-20 billion tons of fishes (Martin et al., 2020). The large projected range of mesopelagic fish biomass is unclear due to uncertainty of what fraction of the detected organisms are siphonophores and cephalopods, which can have similar acoustic signatures to mesopelagic fishes (Martin et al., 2020). In addition, acoustic backscatter may have difficulty estimating the biomass of large fishes with small swim bladders, or vice versa, thus making it a potentially imprecise method for estimating mesopelagic fish biomass (Irigoien et al., 2014).

Whales and other air-breathing vertebrates may also support primary production through vertical mixing, horizontal transfer, and recycling of carbon and other limiting nutrients in the ocean (Roman et al., 2014). When diving to feed, whales deliver mechanical energy to the ocean, which may help break up otherwise stratified water columns (Roman et al., 2014). In addition, some whales transfer nutrients and benthic crustaceans (hitchhikers) from deeper water as they

dive and return to the surface during feeding sessions, which provides food for surface feeding sea birds. Whales also deliver nutrients to the surface by releasing fecal plumes and urine in feeding areas (Roman et al., 2014). This "whale pump" likely enhances primary productivity in biological hotspots (regions of high primary productivity with diverse upper trophic levels). In particular, baleen whales (or mysticetes) ingest large quantities of prey and egest their remains in the epipelagic. This recycling of nutrients to primary producers enhances the intensity and spatial extent of phytoplankton blooms (Savoca et al., 2021). Higher phytoplankton biomass provides prey for zooplankton and thus food for mesopelagic fishes. Whales also carry organic nutrients to the deeper waters as they die and sink. Whale carcasses provide food and habitat for benthic fauna in the deep sea; a single whale skeleton may support more than 200 macrofaunal species (Roman et al., 2014). Sinking whale carcasses, or whale falls, carry 190,000 tons C yr^{-1} from the atmosphere to deeper waters (Roman et al., 2014).

1.2.5 Ecology of Mesopelagic Fishes

Mesopelagic fishes refer to the group of fishes that occupies the intermediate pelagic waters between the deepest point in the euphotic zone at ~200 m and the beginning of the bathypelagic zone at ~1,000 m. This layer is classified as the mesopelagic zone. The mesopelagic zone, also referred to as the twilight zone, is where light in the ocean dwindles rapidly. These low light levels make photosynthesis impossible. The conditions of the mesopelagic are harsher than in the epipelagic zone. Light, oxygen, and temperature decrease with depth, while salinity and pressure increase. The mesopelagic zone also contains a thermocline layer, which is a transitional layer where temperature changes sharply with depth. Thermocline depth varies annually depending upon global region and the season. These abiotic factors result in little food resources in the mesopelagic zone causing many of its inhabitants to migrate to the surface to feed (Bailey, 2019).

No large-scale fisheries have been yet developed targeting mesopelagic fishes despite their large biomass (Salvanes and Kristofferson, 2001; St. John et al., 2016). Danes and Norwegians are seeking to build mesopelagic fisheries in the Indian and Arctic Oceans (St. John et al., 2016). However, technological limitations, such as finding suitable trawl nets, preserving the fish until they reach harbor, and unwanted bycatch, pose as challenges to harvesting mesopelagic fishes. Furthermore, wax esters, a type of fat commonly found in mesopelagic

fishes, are notably unpalatable to humans. Instead, fisheries are interested in harvesting mesopelagic fishes to fulfill demand for fish feed and fish oil. Mesopelagic fishery development has been proposed to raise more edible species through aquaculture for human dietary supplements (Gewin, 2016). The lack of widespread commercially valuable fisheries for mesopelagic fishes has contributed to a scarcity of research on their behavior and characteristics.

Mesopelagic fishes are found in high abundances along the continental shelf in the Atlantic, Pacific, and Indian Oceans and in deep fjords (Saba et al., 2021). However, mesopelagic fish densities decline further offshore and in Arctic and sub-Arctic waters. Regions of low mesopelagic fish density are correlated with low primary productivity due to the nature of mesopelagic food webs (Irigoien et al., 2014).

As a result of the dimly lit conditions of the mesopelagic zone, mesopelagic fishes exhibit several adaptations to thrive in low light conditions (Saba et al., 2021). Those adaptations include sensitive eyes, dark backs, silvery sides, ventral light organs that emit light on a spectrum equivalent to ambient light and reduced metabolic rates for species living at deeper depth with limited food resources (Salvanes and Kristofferson, 2001). Migrating mesopelagic fishes also tend to have muscular bodies, well-ossified skeletons, scales, a well-developed central nervous system and gills, large hearts and kidneys, and most often a swim bladder. Deeper living, non-migratory mesopelagic fishes exhibit different characteristics including reduced skeletons, higher water content in their muscles, lower oxygen consumption, lack of a swim bladder, and reduced swimming activity (Salvanes and Kristofferson, 2001).

Many features of mesopelagic fishes are morphological adaptations responding to light stimuli. Mesopelagic fishes have large eyes with pure-rod retinas, which contain a high density of photosensitive pigment (Salvanes and Kristofferson, 2001). Along with most vertically migrating mesopelagic fishes possessing a swim bladder, these fishes have a muscular organization with a large proportion of red muscle fibers. Red muscle fiber is rich in fat, mitochondria, myoglobin, glycogen, blood, and oxygen, all of which are necessary to assist fishes with the energy needed for vertically migrating (Salvanes and Kristofferson, 2001). Those mesopelagic fish species with higher proportions of red muscle fibers make the greatest vertical migrations. The amount of energy needed to construct red muscle fibers to move a fish upwards strongly influences the metabolic demands of a fish. Therefore, greater metabolic demands are

associated with mesopelagic fishes taking on longer migrations to the surface (Salvanes and Kristofferson, 2001).

Most mesopelagic fishes are small, approximately 2-15 centimeters and typically only live a few years (Romero-Romero et al., 2019). Size variation of mesopelagic fishes is explained by species, geographical region, temperature, and food availability (Salvanes and Kristofferson, 2001; Romero-Romero et al., 2019). Their small size contributes to a low fecundity, ranging from hundreds to a few thousand eggs in one reproductive event. Yet, they have higher reproductive rates in a lifetime in comparison to longer-lived epipelagic species, which have higher fecundity and a longer generation time (Salvanes and Kristofferson, 2001). Mesopelagic fishes may release hundreds to a few thousand eggs at a time, which implies low mortality in early life stages and higher mortality in adulthood in comparison to epipelagic fish species. One possible explanation for higher survival rates of larval and juvenile mesopelagic fishes than epipelagic fishes could be mesopelagic fish larvae are not known to be passively transported long distances and suffer from advective loss (Salvanes and Kristofferson, 2001).

Mesopelagic fish behavior has been studied and monitored indirectly through sound-scattering-layers by echosounders and by pelagic trawling to collect samples. The use of remotely operated vehicles (ROVs) and autonomous underwater vehicles (AUVs) has gained popularity in observing mesopelagic fish behavior (Choy et al., 2017). During the daytime hours fish can adjust their position in the water column to accommodate changing light intensity, which suggests vertically migrating fishes follow isolumes (Salvanes and Kristofferson, 2001). Isolumes are a depth-varying line of constant light intensity. Light is a key stimulus for mesopelagic fishes for when to migrate to the surface for feeding. Feeding during lower light levels serves as an anti-predatory tactic. Isolume depth is deeper in peak daylight hours; therefore, as the sun begins to set the isolume depth moves closer to the surface. In higher latitudes, where daylight is longer in the summer, optimal feeding time for these fishes is reduced. As a result, many mesopelagic fish species adapt to limited darker hours by feeding in schools (Salvanes and Kristofferson, 2001).

The families Gonostomatidae, Melanostomiatidae, Myctophidae, and Gempylidae are the most diverse types of mesopelagic fishes, having the most genera per family and highest

abundance (Salvanes and Kristofferson, 2001). Lanternfishes (family Myctophidae) and bristlemouths (family Gonostomatidae) make up 90% of fishes in the mesopelagic zone (Etnoyer, 2011). The family Myctophidae make up at least 20% of ocean ichthyofauna (Catul et al., 2010). Myctophids represent 250 species in 33 genera and inhabit all oceans, except the Arctic. Myctophids perform DVM between the mesopelagic and epipelagic zones. As their name suggests, lanternfishes give off a glowing effect due to the presence of photophores, light producing cells, around their body (Catul et al., 2010). A second group of prominent mesopelagic fish are bristlemouths. These fish rival myctophids in terms of mesopelagic fish biomass (Lambert, 2021). In fact, scientists believe bristlemouths are the most abundant vertebrate in the world (Lambert, 2021). Bristlemouths occur in tropical and subtropical regions of major oceans. Bristlemouths are noted for their large lower jaws and long bristle-like teeth. Bristlemouths prefer to typically remain at intermediate depths (below 200 meters) and most species do not migrate to the surface to feed. Like the lanternfish, bristlemouths possess photophores all over their body, which produces bioluminescence (Lambert, 2021).

1.2.6 Mesopelagic Fish-Mediated Carbon Export Flux

Mesopelagic fishes are a dominant vertebrate in the ocean both numerically and in terms of biomass. However, they are a poorly studied, and little is known of their contribution to the ocean carbon export flux (Irigoien et al., 2014). Less than eight published studies have measured the passive and active transport of carbon by fishes (Saba et al., 2021). Therefore, there is a strong need to conduct research on the mechanisms of fish-mediated transport. Variation in fish mediated carbon export flux are likely explained by regional, seasonal, and temperature differentiation, as well as variation in fish biomass estimates, taxonomic composition, and a variation in a study's method used to estimate the flux (Saba et al., 2021). Number of included sources of carbon, uncertainty in conversion factors, rates of carbon flux and fish metabolism, and the uncertainty of assumptions made for flux and metabolic rates are additional factors that produce variation in carbon flux estimates (Saba et al., 2021). Fecal pellets produced from fish can sink thousands of meters per day and are less susceptible to bacterial composition during descent to the benthos. Due to rapid sinking and slow bacterial composition in the water column, most fecal matter reaches the ocean floor in less than a day for most coastal systems (Ducklow

and Steinberg, 2001). Studies examining active transport of carbon by mesopelagic fishes largely focus upon myctophids, which comprise most of the migrating micronekton. Myctophids can migrate to the surface from depths of 400 to 1,000 meters (Anderson et al., 2018). Estimates based upon passive (fecal pellet and detrital sinking) and active (migratory and respiration) fluxes mediated by fishes are about 16.1% (±13.0%) to the total carbon flux out of the euphotic zone (Saba et al., 2021). Sediment trap data measuring passive transport (sinking of egested fecal matter and deadfall) by mesopelagic fishes (including both DVM and non-DVM fishes) contributed ~0.01-143% of particulate organic carbon (POC) flux from the euphotic zone (Saba et al., 2021). This POC flux contribution is equivalent to a yearly global carbon flux range of 0.0008-4.0 Pg C yr^{-1}. Mesopelagic fishes that undergo DVM to feed, are shown to contribute a total carbon flux of 0.3-40%, which translates to 1.7 Pg C yr^{-1} (Saba et al., 2021). Trawl surveys suggest 50% of mesopelagic fishes migrate; yet this percentage can range regionally from 20-90% depending upon species composition, temperature, turbidity, and oxygen concentration (Boyd et al., 2019). POC in the upper mesopelagic layer and euphotic layers rapidly attenuates with depth; as a result, active carbon export by mesopelagic fishes deeper in the water column becomes increasingly important with depth (Saba et al., 2021). Organic carbon introduced in the mesopelagic zone is subject to rapid feeding by bacteria and zooplankton, which reduces the efficiency of carbon export. Therefore, fishes at greater depth are more efficient at exporting carbon, and it is more likely that the carbon will be sequestered by reaching deep ocean currents or buried in sediment.

To quantify fish contributions to carbon flux, the total fish biomass, and the rate at which fish-mediated carbon transport takes place are required. Both inputs are challenging to measure, which may explain the relative scarcity of literature on this topic. Fish biomass and its contribution to the biological pump is influenced by species composition, seasonality, temperature/metabolism impact, shifts in marine species due to climate change and climate variability, variation in distribution of fish biomass in the water column, and difference in feeding behavior between populations (Saba et al., 2021). Fish behavior, such as net and gear avoidance and variation in season and vertical/horizontal distribution, yields uncertainty in quantifying fish biomass. For acoustic estimates of biomass, similarity between the acoustic signals of fishes, siphonophores, and cephalopods can be a source of uncertainty in biomass estimates unless trawls are conducted alongside acoustics surveys.

Measuring passive and active flux of carbon faces the additional challenge of monitoring multiple variables. Passive carbon flux rate requires estimates of: (1) fish biomass in a region, (2) fish fecal pellet production rate, (3) fecal pellet sinking rates, and (4) fecal organic and inorganic carbon content (Saba et al., 2021). Little-to-no data exist for quantifying these variables. Gut content analysis is useful for measuring fecal carbon content; yet assumptions of fecal pellet production still must be made. In addition, the amount of carbon in the guts may be unequal to the amount of carbon in feces since some of the carbon will be used for body maintenance, growth, and potentially reproduction (McClain-Counts et al., 2017). Fecal pellet production must assume rates stay the same within a species and assumptions are made that there is little variation between global regions, seasons, and type of prey consumed (Saba et al., 2021). To calculate active flux contribution, assumptions about energy budget components must also be made, including fish size (more of challenge with acoustic data versus physical samples), metabolic rate, swimming speed, and growth rate. Since total population estimates of such quantities must be developed, their within-population variation is ignored. To deal with this issue, size-spectrum models can organize organisms into size intervals and allometric relationships can be used to determine material fluxes between size categories (Saba et al., 2021).

1.2.7 North Pacific Subtropical Gyre (NPSG)

The North Pacific Subtropical Gyre (NPSG) is the study site used in this thesis. Subtropical gyres occupy approximately 60% of the Earth's oceanic surface, with the NPSG being the largest of these gyres. This ecosystem is home to an array of mesopelagic fish species, thus making it a good sampling site.

The NPSG is the largest circulation feature and contiguous biome on Earth. This vast gyre at the ocean's surface extends approximately 15°N to 35°N latitude and 135°E to 135°W longitude and occupies a surface area of roughly $2*10^7$ km^2 (Karl, 1999). Although this habitat is expansive, it is poorly sampled and, thus, not well understood.

The NPSG is in open ocean waters far from land. Therefore, the NPSG waters do not directly receive terrestrial run off and are considered oligotrophic, or nutrient poor. However, evidence that the NPSG presents variability in biological, chemical, and physical processes prompts the need for more research into its dynamic processes (Karl, 1999). Wind-driven currents and mesoscale eddies produce strong vertical motions that deliver sporadic short-lived

pulses of nutrients to habitats that are otherwise deprived of nutrients. Wind stress and the water circulation in the gyre lead to the creation of these eddies. Wind drag and storms also stir up nutrients to the surface to increase planktonic growth. The clockwise rotation of the NPSG due to Coriolis force leads to a doming upward of isopycnals and a shoaling of the nutricline, thus enhancing production (Karl, 1999).

The NPSG is very old dating back to the Pliocene epoch. As a result, the NPSG presents a "climax-type" community (Karl, 1999). The NPSG is characterized by warm surface waters (>24°C), low nitrate concentrations (< 50 nM), high dissolved organic nitrogen (5-6 μM), a seasonally variable surface mixed layer, low standing stocks of living organisms, and a persistent deep-water chlorophyll-a maximum layer (Karl, 1999). The NPSG's euphotic zone can sometimes be noted for having two-layers. The upper-most layer is light saturated, nutrient limited, and supports high primary production rates, while the lower layer is light limited (but not light replete), nutrient rich, and yields slower primary production rates (Karl, 1999). The constant stratification of the upper ocean and a deep permanent pycnocline (a region of rapid density change in ocean layers) largely hinder nutrient-enriched waters from entering the euphotic zone. Instead, the NPSG relies on nutrient recharge from below through vertical eddy diffusion and horizontal transport from neighboring nutrient-rich ecosystems. Nutrient flux from these sources is small, so the water in the upper 100 meters of the NPSG is chronically nutrient poor.

Despite the oligotrophic conditions, phytoplankton growth rates remain high (Rii et al., 2016). Stratification and a perennially high photosynthetically active radiation (PAR) promote the perpetual consumption of nutrients by phytoplankton to result in low concentrations of inorganic nutrients in the upper ocean. Active microbial food webs sustain primary production through rapid recycling of nutrients (Rii et al., 2016). Photosynthetic picoeukaryotes and cyanobacteria (belonging principally to the genera *Prochlorococcus* and *Synechococcus*) comprise 60-90% of plankton biomass and account for >70% of net primary productivity in the NPSG (Rii et al., 2016). The contributions of picoplankton to biomass and primary production appear to be linked to efficient nutrient acquisition and light harvesting capabilities (Rii et al., 2016). Picoplankton (species size <3μm in diameter) are the main contributor to plankton biomass and net global productivity, particularly in subtropical ocean gyres. These organisms can be both heterotrophic and autotrophic. Picoplankton are not easily captured by copepods, but

are efficiently grazed by microzooplankton (species size range of 20-200 µm), such as ciliates; thus, the microbial loop plays a large role supporting the trophic web in oligotrophic oceans (Irigoien et al., 2014). Picophytoplankton activity experience seasonal dynamics. In the summertime, blooms appear usually resulting from episodic mesoscale events, such as eddies. These summertime blooms appear to be a large contributor to particulate carbon export to the deep sea (Karl, 1996). However, limited light in the wintertime has a significant impact on the drawdown of nutrients to the lower euphotic zone and the sequestration of carbon. Limited light in the winter months prevents photosynthetic plankton from utilizing nutrients in the lower euphotic zone, resulting in the accumulation of nutrients (upwards of 36 mmol m^{-2} nitrate) in the upper ocean layers (Rii et al., 2016). Yet, as springtime provides increasing light energy, phytoplankton biomass increases, and nitrate is drawn down into deeper ocean layers (Rii et al., 2016).

The NPSG is characterized by a rich zooplankton community with low seasonal and interannual variability in plankton biomass (Sommer et al., 2017). Zooplankton in the mesopelagic zone plays an important role in marine food webs and carbon export; however, the extent of diversity of these organisms is unknown (Sommer et al., 2017). Metabarcoding, a method of using DNA/RNA to identify many taxa within the same sample, reveal mesozooplankton diversity could be ten times higher than previously recorded in the NPSG (Sommer et al., 2017). Copepods comprise the largest group of mesozooplankton. Currently 125 species of copepods have been identified in the NPSG. The biomass of copepods makes up 70-75% of the zooplankton assemblage above 1,000 meters (Karl, 1996). A study conducted on the gut contents of mesopelagic fishes in the Gulf of Mexico reveal copepods comprise the majority of mesopelagic fish diets (McClain-Counts et al., 2017). Since copepods are the dominant mesozooplankton in the NPSG, they likely consist of the bulk of mesopelagic fishes' diet in the NPSG, as well.

The vast majority of micronekton, including mesopelagic fishes, are found along the continental or insular slope regions, and around seamounts in the North Pacific. FME is estimated to be 40% of carbon export in the oligotrophic NPSG (Davison et al., 2013). FME is important in these nutrient poor waters because subtropical gyres occupy over half of the ocean's area and are the site of roughly half oceanic carbon export (Davison et al., 2013). FME is likely high in oceanic regions of warm water due to elevated metabolic rates (Davison et al., 2013).

The NPSG has high mesozooplankton biomass and growth rates along with a high annual contribution of fecal pellets to the total carbon flux (Ducklow et al., 2001).

In the NPSG, the size distribution of pelagic primary producers and the trophic structure of consumers determine both composition and the strength of the export flux of particulate materials. This concept is important to consider when examining the biological pump's ability to sequester carbon. Data from the Hawaiian Ocean Time-series (HOT) program document two major particle export fluxes in the NPSG: one in late winter and the second in the late summer (Karl, 1999). Sediment trap data suggest the two flux events are supported by different ecological processes. The winter pulse is believed to be supported by nitrate from upwelling events, while the summer pulse is supported by nitrogen via N_2 fixation (Karl, 1996). These sudden pulses of inorganic nutrients through nutricline waters into the euphotic zone select for a diatom-copepod-fish structured food web. This is the food web pattern that supports production of most mesopelagic fishes.

The ability to provide close-to-accurate measurements of primary productivity and the abundance of organisms in marine food webs are key pieces of information for correctly quantifying carbon export in the biological pump. Past measurements of primary productivity in the NPSG were uncertain and likely underestimated. The three-decade long dataset from Station ALOHA revealed the mean value of ^{14}C-based primary production to be 536.8 mg C $m^{-2}d^{-1}$, a value that is 2-3 times higher than historic estimates of ^{14}C-based primary production (Karl et al., 2021). In August 1982, the Plankton Rate Processes in Oligotrophic Oceans (PRPOOS) program confirmed that past measurements of primary productivity have been underestimated by a degree of two or threefold (Karl and Lukas, 1996). Due to the spatial and temporal variability of the NPSG, an exact estimate of overall primary productivity is challenging to quantify (Karl, 1999). Satellite data can provide estimations of primary productivity; yet, satellite observations can underestimate primary production in stratified water column when a deep chlorophyll maximum is present (Bouman et al., 2020). However, current estimates of primary productivity have improved in accuracy due to technological advances. A series of disturbances, such as mesoscale eddies and nutrient-driven upwelling events, are enough to disrupt the stability of primary production; thus, increasing primary production for years before returning to stability (Luo et al., 2012). Eddies and upwellings supply nutrients to oligotrophic waters, and due to stratified conditions nutrients are not quickly exported (Luo et al., 2012). As a result, the NPSG

experiences interannual variability of primary production. In addition, there currently remains limited information on the contributions of major groups of photosynthetic organisms to temporal variations in primary productivity at Station ALOHA, which is a long-term monitoring station located near the center of the NPSG. Data from this long-term study are bringing to light how temporal changes in the upper ocean habitat influence phytoplankton production and growth in the NPSG. For example, a recent study using water samples gathered from Station ALOHA were taken to measure photosynthetic pigments and ^{14}C-based primary production (Karl et al., 2021). Water samples were analyzed over a 30-year study period (1989-2018) to provide long time-series measurements.

Some research indicates that transfer efficiency from primary producers to microzooplankton is probably higher in warm oligotrophic ocean zones than eutrophic areas. This finding is supported by higher heterotrophic metabolic rates which increase faster than phototrophic rates with increasing temperature (Irigoien et al., 2014; Stock et al., 2017). Furthermore, with large, sensitive eyes mesopelagic fishes are visual predators who would maximize prey capture in clear, warm waters resulting in higher transfer efficiencies in less productive clear waters than turbid continental shelf and coastal waters (Irigoien et al., 2014).

1.2.8 Hawaiian Ocean Time-series (HOT) Program

To narrow my focus of sampling the vast NPSG, I will be using samples obtained from station ALOHA under the HOT program. Since October 30, 1988, a comprehensive collection of ocean measurements has been recorded at station ALOHA in the NPSG (Karl, 1999). Station ALOHA was established by a team of scientists from the University of Hawaii. Located ~100 km north of Oahu, Hawaii (22°45'N, 158°W), station ALOHA was set up as part of the National Science Foundation funded HOT program. The dynamic nature of the NPSG is one of the prime reasons for the creation of the HOT program. The site selection for the HOT oligotrophic hydrostation had to meet the following criteria: the station must be located in deep water (>4000 m), upwind (north-northeast) of the main Hawaiian Islands, and a sufficient distance from land to minimize terrestrial influences while close enough to make monthly cruises financially and logistically feasible (Karl and Lukas, 1996). Since its creation, scientists, engineers, students, and technicians from around the world have come to participate in monthly sampling expeditions to

collect data related to both anthropogenic and natural variation in ecosystem structure and function in the NPSG (Karl et al., 2018). Prior to the creation of station ALOHA, the NPSG was under-sampled and poorly understood. The HOT program was set up to evaluate and improve upon C-N-P (carbon-nitrogen-phosphorus) biogeochemical models that were previously used to evaluate NPSG. In particular, the HOT program was designed to evaluate the global carbon cycle on land and sea. Scientists argued a comprehensive knowledge of the carbon cycle would be essential to address issues related to impacts upon ecosystems, species biodiversity, biogeochemical cycles, and climate change (Karl et al., 2018). Scientists expressed the need to understand the scientific and societal issues from the threat of accumulating greenhouse gases and their impacts upon ecosystem and biogeochemical processes (Karl et al., 2018). The HOT program selected key ecosystem processes to measure via frequent sampling, such as the flux of carbon at the air-sea interface, the rates and control mechanisms of the biological pump, time dependent-changes in microbial biomass and biodiversity, and the impact of broadscale climatic forcing, such as El Niño Southern Oscillation (ENSO) (Karl, 1999).

The HOT program conducts monthly cruises to station ALOHA for measurements of thermohaline structure, water column chemistry, currents, optical properties, primary production, plankton community structure, and rates of particle export. Long time series observations of climate-related variables in the ocean are very important but unfortunately rare. Repeated measurement of oceanographic processes is vital for understanding natural phenomena that are impacted by biological, chemical, and physical influences.

Multi-decadal datasets reveal the NPSG is a unique ecosystem. Since the creation of the HOT program, new microorganisms have been discovered and scientists have been able to define major patterns and time associated processes in ocean hydrography, biogeochemistry, and controls on primary production and carbon export (Karl et al., 2018). Timeseries data have been provided from station ALOHA for almost 33 years, which helps scientists capture a snapshot of natural ocean variability and associated human impacts. These snapshots are valuable tools for measuring possible climate change impacts, as well.

Long timeseries data trends have allowed scientists to gain better estimates of primary productivity and understand planktonic community structures (Karl et al., 2021). The HOT program has obtained the longest record of ^{14}C-bicarbonate-based primary productivity (Karl and

Church, 2014). Despite small concentrations of inorganic nutrients and relatively low phytoplankton biomass, ^{14}C results indicate a moderate level of productivity (>0.5 g carbon per m^2 per day), with a peak productivity in early summer. Yet, ^{14}C-based measurement of primary production does not account for all light-dependent inorganic carbon fixation from photosynthesis or carbon losses due to respiration and grazing (Karl and Church, 2014). Export production at Station ALOHA is measured via sediment traps and has been quantified to be only a few percent of gross primary production. This finding reflects a remineralization-intensive ecosystems where most nutrients are cycled up to 30-50 times within the euphotic zone before exiting the system (Karl and Church, 2014). Additional research has shown that average concentrations of chlorophyll-a and estimated rates of primary productivity in the NPSG have doubled, while dissolved silicate and phosphate have decreased over the past 30 years (Karl et al., 2001). Furthermore, scientists have documented increased concentrations of chlorophyll-b, which suggests a shift in planktonic community structure. Shifts in planktonic communities could be a result of climate change and/or a series of sporadic events, such as mesoscale eddies and upwelling. Possible changes in planktonic communities have the implication of altering marine food webs. For example, a shift in size distribution of the herbivore population from small crustaceans to protozoan zooplankton would lead to a more complex food web and reduced energy and carbon transfer to higher trophic levels (Karl et al., 2001). Primary productivity rates would decrease and consequently fish production would decrease as a product of less efficient energy transfer in food-web interactions. Furthermore, alterations of marine food webs such as these could modify the biological pump (Karl et al., 2001). This finding highlights the need for intensive research on the mechanics of the biological pump to project future carbon sequestration scenarios. Little research has been conducted on phytoplankton community shifts in response to climate change in the NPSG. Most studies are projected scenarios and rely on the ability to accurately predict future atmospheric CO_2 concentrations (Basu and Mackey, 2018). However, with the need to understand the response of the ocean to climate change, more research in phytoplankton community shifts is being investigated, but there is still a lack of data specific to the NPSG.

1.2.9 Stable Isotope Analysis (SIA)

One technique for learning how mesopelagic fishes contribute to carbon export is SIA. Many elements on earth have isotopes, which contain the same number of protons, and hence

have the same atomic number, but vary in the number of neutrons. This difference in the number of neutrons in the nucleus of an atom results in different atomic masses for the same element. The difference in isotopes reveals itself in their physical behaviors due to variation in atomic mass. The isotopes of an element each can behave slightly differently during physical and chemical processes which are mass dependent. This is termed "fractionation" (Ben-David and Flaherty, 2012).

One of the many uses of stable isotope data is to investigate the foraging ecology of organisms. SIA can be used to determine an organism's key food sources by examining isotope ratios (Hopkins and Ferguson, 2011). Isotope ratio distributions are compared between organismal tissue and the food source after correcting for fractionation using a 'fractionation factor.' Fractionation is a reaction or process that favors one of the isotopes in a particular element. Isotope ratios are the proportion of heavy to light isotopes. If the reaction selects for the heavier isotope, the reaction product is considered 'heavy', while the remaining reactant is the 'light' isotope (Ben-David and Flaherty, 2012). The fractionation factor is derived as $\alpha=R_{reactant}/R_{product}$, where R is the ratio of heavy to light isotopes.

The first step in SIA requires converting organic compounds into their gaseous forms using an isotope ratio mass spectrometer. The compounds are combusted with oxygen and a metal catalyst in high temperatures (Ben-David and Flaherty, 2012). The gaseous form of inorganic molecules is injected into the source of the mass spectrometer where they are ionized and placed into a flight tube. A strong magnet separates the molecules based on mass. The separated ionized gaseous molecules are collected in Faraday cups at the end of the flight tube. A computer records the electric current created during the collection of the gases. When quantifying the amount of each isotope, the total across all isotopic groups will provide information on the total carbon or nitrogen contained in a tissue sample.

Sample ratios of heavy to light isotopes as it relates to internationally set standards are expressed in this form:

$$\delta X=((R_{sample}-R_{standard})/R_{standard})*1{,}000$$

where δ (delta) is the isotopic notation, X is the element in its heavy form (e.g., ^{13}C, ^{15}N), and R is the ratio of heavy to light isotopes. The sample isotope ratios are compared to an international standard: Vienna Peedee Belemnite for carbon ($\delta^{13}C$), background atmosphere for nitrogen

(δ^{15}N), Vienna Standard Mean Ocean Water for hydrogen and oxygen (δD and δ^{18}O), Vienna Cañon Diablo Meteorite Troilite for sulfur (δ^{34}S), and United States Geological Survey *Tridacna* for strontium (^{87}Sr:^{86}Sr) (Ben-Davids and Flaherty, 2011). International standards are set so data collected around the world are comparable. If the sample is higher than the international standard, then the sample is considered 'enriched.' If the isotopic sample is less than the international standard the sample is termed 'depleted' (Ben-David and Flaherty, 2012).

Ratios of heavy-to-light isotopes are expressed in a unit of measurement of parts per thousand (denoted as ‰ or per mil) (Ben-David and Flaherty, 2012). Many isotopic geochemists encourage prefacing the δ value with a sign, even when positive, to distinguish between a true positive value and a δ value that may be missing its sign. There are many ways to descriptively compare the δ values of two materials: 1) high vs. low values, 2) more/less positive vs. more/less negative, 3) heavier vs. lighter, and 4) enriched vs. depleted (what isotope is in short supply must be stated and indicate the enrichment or depletion is because of a reaction process) (Kendall and Caldwell, 1998).

Spatial and temporal variation in the prevalence of heavy and light isotopes in ecosystems on Earth allow scientists to track the flow of nutrients, trophic positions, species interactions, animal diets, and migrations (Ben-David and Flaherty, 2011). Isotope signatures of organisms reflect the isotope ratios of the substrates they consume. Therefore, it is important that the isotope ratios of all potential food sources be understood. Additionally, to trace diet and trophic relationships, isotope signatures must be distinct between diet sources and accurate estimates of consumer-diet fractionation are needed (Prado et al., 2012). SIA provides an integrated diet history of an organism whereas gut content analysis provides only a snapshot of what an organism eats in one day. Isotope ratios generally provide information on a species' diet of the past six months to a year (Prado et al., 2012). A strength of SIA is the ability to examine an organism's food source without analyzing the gut contents. No matter if an animal's stomach is full or completely empty, SIA provides a historical integrated record of prey selection. Additionally, SIA helps avoid morphologically based identification of partially digested prey, which can be extremely difficult. However, measuring the incorporation rate of isotopes in organism tissue poses challenges. Isotopic signatures vary based on organism size, age, nutritional status, type of tissue sampled, macromolecule composition of diet, and assimilation efficiency (Ben-David and Flaherty, 2011; Sharp, 2017). For example, younger animals of the

same species have the tendency to incorporate dietary isotope signatures faster than older animals due to faster growth rates and quick cell turnover. Newly developed analytic tools may reduce some of these challenges such as: 1) stable isotope mixing models to determine prey composition in a consumer's diet, 2) statistically based interpretation of spatio-temporal data used to assess movement and migratory patterns, 3) single- versus multiple-compartment models for evaluating isotopic incorporation rates, 4) and the use of spatial metrics to depict community-level variation in trophic structure across space and time (Ben-David and Flaherty, 2011; Newsome et al., 2012; Prado et al., 2012).

Isotopes $\delta^{13}C$ and $\delta^{15}N$ are used to evaluate dietary sources and trophic interactions among species, which I will discuss more below in the literature review section exploring SIA and food web studies and in Chapter 2. Over the past decade, SIA has become increasingly used to study food web patterns in marine ecosystems (Fanelli et al., 2011). The ratio of $^{15}N/^{14}N$ can be used to infer trophic position of an organism, which increases approximately 2.5-3.4‰ per trophic level, with fish and invertebrates averaging a 2‰ increase per trophic level (Ben-David and Flaherty, 2012: McClain-Counts et al., 2017). A species' primary food source can be inferred from the isotopic ratio of $^{13}C/^{12}C$. After fractionation, $\delta^{13}C$ values enrich ~1‰, with an average of 0.4 ‰, between trophic levels (Ben-David and Flaherty, 2012; McClain-Counts et al., 2017). In marine ecosystems, these carbon isotope values are beneficial in determining if an organism's carbon source is chemosynthetically based, as found around benthic cold seeps or hydrothermal vents, or photosynthetically based. During photosynthesis, plants discriminate against $\delta^{13}C$ due to small differences in mass. As a result, this discrimination can be used to assign plants to different photosynthetic groups (O'Leary, 1988). Isotopic fractionation can allow the ability to differentiate between photosynthetic sources, such as phytoplankton or salt marsh grass (O'Leary, 1988). Distinct $\delta^{13}C$ ranges are known for phytoplankton to fall between -22 to -16 ‰, while chemosynthetically derived organic matter ranges from -75 to -28‰ (McClain-Counts et al., 2017). The degree of fractionation of isotopes may be mediated by diet nutritional quality. A meta-analysis across taxa in terrestrial and aquatic organisms found that $\delta^{15}N$ enrichment increased in diets of poor nutritional quality (Vanderklift and Ponsard, 2003; Robbins et al., 2005). Nutritional stress was linked with higher metabolic rates of nitrogen, thus increasing $\delta^{15}N$ enrichment (Vanderklift and Ponsard, 2003). Lower ^{15}N isotope ratios were observed in carnivorous animals over herbivores, likely due to carnivores feeding on high quality

protein that is like their own tissue. Animals consuming an omnivorous diet will vary in isotopic fractionation depending on the availability of plant and animal resources. Omnivores expressed greater wider ranges of $\delta^{13}C$ due to more diverse prey items than carnivores and herbivores (Fanelli et al., 2011). The meta-analysis also revealed that animals feeding on high-quality prey had smaller changes in $\delta^{13}C$ values between trophic levels than organisms that starved or fed on lower quality diets. Higher $\delta^{13}C$ and $\delta^{15}N$ value`s observed in organisms with poor diets suggests a reallocation of internal resources for sustenance (Prado et al., 2012). Isotopic fractionation also depends on the type of tissue being sampled. Variation of $\delta^{15}N$ in tissue is attributed to rates of protein synthesis or degradation and to the requirements of essential versus non-essential amino acids subjected to additional metabolic pathways. Higher protein turnover rates yield higher $\delta^{15}N$ as observed in muscle tissue (Prado et al., 2012). $\delta^{13}C$ values are observed to correspond to metabolic rate. High metabolically active tissues, such as fat and liver tissue, have greater carbon turnover rates and lower isotopic signatures than less metabolically active tissues, such as blood and muscle. Carbon isotopic signatures may also be influenced by protein abundance and amino acid composition (Prado et al., 2012). Lipids are typically depleted in $\delta^{13}C$ in comparison to protein, thus any variation in lipid content may confound diet interpretations. To remedy this issue, lipids can be extracted before SIA is performed. Chloroform-methanol, a toxic solvent, is the most common agent used for lipid extraction (Elliot and Elliot, 2016). Due to low isotopic variability and low-fat composition, white muscle tissue is most frequently used by scientists in ecological studies (Curry et al., 2014). However, SIA data can be confounded by a host of factors, which are discussed in further depth in Chapter 2. For SIA to be interpreted correctly, a thorough understanding of how biological and environmental sources of variation influence isotope values of consumers is greatly needed (Richards et al., 2020).

1.2.10 $\delta^{15}N$ Variation in Micronekton in the Mesopelagic Zone

Not all micronekton migrate to feed, which challenges interpretation of SIA results from mesopelagic fishes. Whether or not micronekton migrates to obtain food has an impact on its trophic ecology and, thus, the $\delta^{15}N$ value of the metazoan. The $\delta^{15}N$ within a species depends upon the base of the organism's food web. For example, $\delta^{15}N$ of suspended and sinking material increases with depth as a result of microbial degradation (Romero-Romero et al, 2019). Therefore, larger $\delta^{15}N$ isotope signatures are found in organisms in deep-benthic communities that feed on sinking matter regardless of an organism's trophic level (Romero-Romero et al.,

2019). Consequently, migrating mesopelagic micronekton feeding at the surface are likely to exhibit $\delta^{15}N$ values consistent with $\delta^{15}N$ of epipelagic non-migrators, which reflects the $\delta^{15}N$ of surface plankton. On the other hand, non-migrating micronekton have $\delta^{15}N$ values that increase with depth, which is consistent with $\delta^{15}N$ found in zooplankton and sinking detrital matter. This confirms zooplankton and sinking detritus inhabiting mesopelagic depths as the main prey resource for non-migrating micronekton (Romero-Romero et al., 2019). Additionally, higher ^{15}N values may be observed in consumers feeding on larger particles (Mayr et al., 2011). It has also been observed that $\delta^{15}N$ enrichment increases with progressive size class of POM (Mayr et al., 2011). The lowest $\delta^{15}N$ values were related to nano- and picoplankton, while higher $\delta^{15}N$ values corresponded to larger particles independent of season (Mayr et al., 2011).

Seasonality also has a large impact on $\delta^{15}N$ within a species of migrating versus non-migrating mesopelagic fishes. Seasonally, the range of $\delta^{15}N$ for migrating micronekton was higher than the range for non-migrators, which can be attributed to migrators having higher tissue turnover rates and a higher metabolism (Romero-Romero et al., 2019). A new diet change would be faster to detect in migrating micronekton due to a higher cell turnover rate. Results collected during the summer at station ALOHA showed an increase in $\delta^{15}N$ values in zooplankton with depth due to $\delta^{15}N$ enrichment at the base of the food web and a higher trophic level for deep water plankton. Among migratory micronekton, only rayed-finned fishes (class Actinopterygii), as opposed to cephalopods and migratory crustaceans, showed an increase in $\delta^{15}N$ values with night-time depth (Romero-Romero et al., 2019). This finding suggests that the proportion of total feeding performed at night by migrating fishes depends on the depth range they reach within the epipelagic zone. Furthermore, micronekton migrating closer to the surface to feed are less likely to rely on ingesting organic matter at depth (Romero-Romero et al., 2019). This observation indicates that taxonomic groups may differ in food habits within migrating micronekton.

In the mesopelagic zone, where photosynthetic primary production is non-existent, mesopelagic species may have evolved specific traits and feeding patterns to exploit different resources, a variety of depths, and avoid direct competition with other organisms (Aparecido et al., 2023). As a result, mesopelagic fishes can serve as an important intermediate between linking primary and secondary production, by feeding heavily on zooplankton, with top predators such tuna, sharks, and billfish (Richards et al., 2020). Therefore, it is important to be able to measure

mesopelagic fish biomass to predict prey fields for top predators (Woods et al., 2023). Furthermore, through DVM, mesopelagic fishes represent an important source of connectivity between the epipelagic, mesopelagic, and bathypelagic zones and are a source of prey throughout the entire water column (Richards et al., 2020). As a result, there is need to understand the ecology and behavior of these fishes in marine food webs to comprehend their environmental significance. In chapter 2, I discuss further the significance of mesopelagic fishes in marine food webs and energy pathways.

1.3 Thesis Chapter Structure

This thesis is divided into four chapters. Chapter 1 provides a literature review pertaining to the biological pump, background information about the sample location, stable isotope analysis, and the behavior and ecology of mesopelagic fishes. Chapter 2 provides the methodology and the results of utilizing stable isotope analysis to make inferences about mesopelagic fishes' role in marine food webs and their feeding patterns. Chapter 3 overviews the methodology and results of the process of building an allometric relationship between carbon in the stomach lining in relation to fish size (standard length/ weight) using fishes caught in North Carolina. In addition, Chapter 3 also analyzes the impact of preservation method (ice versus ethanol) upon stable isotope analysis results in fishes. This preliminary analysis of preservation method was used to determine if a correction factor was needed to adjust $\delta^{13}C$ isotope values in fish tissue if ethanol did significantly alter the amount of $\delta^{13}C$ in fish tissue. Chapter 4 focuses on the methodology to calculate the amount of carbon expelled in fecal pellets (carbon gut flux) of the sampled mesopelagic fishes and then scale up the results to estimate the total gut flux contribution of mesopelagic fishes in the NPSG. Tables and Figures for Chapters 2 and 3 are both included following the reference section of this document.

Chapter 2: Utilizing stable isotope analysis ($\delta^{13}C$ and $\delta^{15}N$) to study food web patterns and ecology of mesopelagic fishes from the North Pacific Subtropical Gyre

2.1 Introduction

Understanding the relationship between organisms in a food web is vital for recognizing how matter is cycled within an ecosystem. Predation serves not only as a factor for regulating energy pathways, but also the species composition between an ecosystem (Carreon-Martinez and Heath, 2010; Cirtwill et al., 2018; Kwak and Park, 2020). Linkages between trophic levels provide a route for the flux of organic matter within a diverse array of organisms and allows for the transfer of nutrients and energy from organisms at lower trophic levels to higher levels. Therefore, all species within an ecosystem are linked. The removal or decline of one species can provide either food or energy for another species or lead to the decline of an associated species. It is important that we understand the intricacies of various food webs in our environment to detect any changes that may have large impacts on the ecosystem overall.

The volume of species that live in the ocean is vast due to its large size, resulting in an array of diverse and complex marine ecosystems. A group of small fishes living in the 200-1,000m depth range, collectively known as mesopelagic fishes, have been observed to be an influential intermediate link between primary and secondary producers and larger predatory species (Boyd et al., 2019; Saba et al., 2021). It has been estimated that 1 billion tons of mesopelagic fishes occupy the world's ocean biomass and are believed to be the largest group of vertebrates in the world (Irigoien et al., 2014). This biomass is likely underestimated due mesopelagic fishes' ability to avoid net capture and difficulty in sampling the mesopelagic zone (Drazen et al., 2011; Irigoien et al., 2014). Many groups of zooplankton and mesopelagic fish species display daily variations in their vertical distribution in the water column, thus increasing the possible interactions amongst trophic levels, resulting in the complexity of the food web structure (Bernal et al., 2015). In addition, due to the underestimation of their biomass, the efficiency of the energy transferred, from primary and secondary producers to top predators in the open ocean through the process of migrating may be higher than reported from previous studies (Bernal et al. 2015; Davison et al., 2013). Unfortunately, there is limited information on the feeding ecology of mesopelagic fishes (Bernal et al., 2015; Saba et al., 2022). Therefore, there is a great need to study the prey components of mesopelagic fishes. Determining the diet of mesopelagic fishes is

important to establish the structure of pelagic food webs, the flows of biomass across trophic levels, and assess the impact of environmental changes on pelagic systems with the use of ecosystem models such as Ecopath (Bernal et al., 2015).

These fishes carry out valuable ecosystem services of great importance to both humans and the environment. As a result, they have attracted the attention of fisheries as source of fish meal and oils (John et al., 2016; Paoletti et al., 2021). However, due to their importance in marine ecosystems more research is needed to assess the ecological impact of developing a large-scale fishery targeting mesopelagic fishes. Mesopelagic fishes also serve an important role as an intermediate between transferring energy from primary producers, such as phytoplankton, to higher trophic levels. Zooplankton feed upon phytoplankton, and the mesopelagic fishes prey upon zooplankton. In fact, myctophids have been known to remove more than 10% of the surface zooplankton biomass per night (Bernal et al., 2015). These fishes can display selective feeding upon certain types of prey and exert a top-down control on the zooplankton community structure in the open ocean (Bernal et al., 2015). Many top predators such as sharks, marine mammals, swordfish, and tuna graze directly on micronekton; thus, mesopelagic fishes help support many commercially valuable fisheries (Choy et al., 2015). Knowledge of where mesopelagic fishes tend to aggregate would help assist fisheries where to locate commercially valuable fisheries (Drazen et al., 2011). Furthermore, mesopelagic fishes' role in ocean carbon sequestration is an ecosystem service that is receiving more attention. Harvesting mesopelagic fishes for commercial use may have a substantial impact on ocean carbon sequestration and thus climate regulation (John et al., 2016). I will discuss the role of mesopelagic fishes in carbon sequestration below.

Due to their migratory behavior to obtain food, many species of mesopelagic fishes are a key player in the ocean's ability to transfer carbon from the ocean surface into the deep ocean for storage. The ocean's ability to store carbon is vital for the sustenance of life. The ocean sequesters approximately 25-33% of human carbon emissions originating from fossil fuel oxidation, deforestation, and cement manufacturing each year (Passow and Carlson, 2012). Without ocean carbon storage, atmospheric temperatures and carbon-dioxide concentrations would be twice as high (Boyd et al., 2019). The biological component that facilitates the transfer of carbon from the ocean surface to the deep ocean interior is referred to as the "biological pump" (Boyd et al., 2019). During the night, mesopelagic fishes and other small micronekton

migrate from the mesopelagic zone (200-1,000 meters) to the ocean's surface to graze upon phytoplankton and zooplankton (Archiald et al., 2019). Upon daylight, these organisms retreat to the mesopelagic zone to avoid being seen by predators. This migratory pattern is known as diel vertical migration (DVM) (Forward, 1988). This feeding tactic allows for the transfer of carbon to deeper ocean layers through fish respiration, defecation, and mortality (Saba et al., 2021). The deeper carbon is transported into the water column, the longer carbon is likely to be stored in the ocean's interior (Passow and Carlson, 2012).

The North Pacific Subtropical Gyre (NPSG), the largest circulatory system and biome on earth, is home to an array of mesopelagic fish and micronekton species (Karl, 1999). This vast biome is highly under researched (Karl and Church, 2017). The remoteness of this habitat and the difficulty of sampling its inhabitants have contributed to a dearth of information on the function and structure of this ecosystem. Few studies have focused on the NPSG mesopelagic zooplankton and micronekton communities (Gloeckler et al., 2018; Saba et al., 2021). Nonetheless, it has been observed that mesopelagic fish species are not uniformly distributed throughout the tropical and subtropical Pacific Ocean. Clearcut assemblages of mesopelagic fishes with characteristic species have been observed throughout the NPSG (Barnett, 1984). It is hypothesized these assemblages aggregate around regions of high primary productivity, which correlates with sources of food (Barnett, 1984). This observation leads to the need for research on how fish mediated carbon transport varies throughout the NPSG (Barnett, 1984; Saba et al., 2021). Variation in fish assemblages have also been possibly linked to oceanographic and bathymetric features such as mesoscale eddies and seamounts (Drazen et al., 2011). This variability in mesopelagic fish biomass further complicates quantifying total estimates of biomass globally. Therefore, there is a need to further investigate where these fishes tend to aggregate to assist in quantifying mesopelagic fish biomass.

It is estimated that the biological pump sends roughly ~5 Gt C yr^{-1} as particulate organic carbon (POC) to the mesopelagic zone (Cavan et al., 2019). Model generated carbon flux estimates predict that 1.5 ± 1.2 Gt C yr^{-1} is sequestered by fishes worldwide (Saba et al., 2021). Based on these two statistics, it is estimated that fish may mediate 30% of the transport of carbon through the biological pump. Fish mediated carbon sequestration varies spatially and seasonally due to fish and zooplankton diversity, climate, water temperature, and primary productivity (Cavan et at., 2019). Few studies have lent focus to quantifying fish mediated carbon flux in the

NPSG. Most previously conducted studies have focused on the passive flux of the biological pump versus the component of the active flux (Davison et al. 2013; Saba et al. 2022; Steinberg et al., 2008) The NPSG is known to possess nutrient poor waters; yet supports a relatively stable community of phytoplankton species (Karl and Church, 2017). It is these phytoplankton that provide nutrients to support micronekton and other marine life in the NPSG. The NPSG is home to an array of mesopelagic fish species: primarily migratory myctophids and non-migratory gonostomatids (Cavan et al., 2019). The top five mesopelagic fish families, in order of most to least abundant, that dominate the NPSG are: Myctophidae, Gonostomatidae, Photichthyidae, Sternoptychidae, and Melamphaidae (Barnett, 1984).

The research in this thesis chapter will use samples obtained from station ALOHA under the Hawaiian Ocean Time-series (HOT) program. Station ALOHA is a circle with a 6-mile radius located approximately 100 km north of Oahu, Hawaii (Figure 1). Station ALOHA, short for A Long-term Oligotrophic Habitat Assessment, was established in 1988 under a team of National Science Foundation (NSF) funded scientists as part of the HOT program (Karl et al., 2018). The HOT program was set up to monitor trends in the North Pacific Ocean; the dynamic nature of the NPSG is one the prime reasons for the creation of the HOT program. Since its creation in 1988, teams of scientists, engineers, students, and technicians from around the world have participated in monthly sampling expeditions to observe and record data related to both anthropogenic and natural variation in ecosystem structure and function in the NPSG (Karl et al., 2018).

Stable isotope analysis (SIA) has been widely used in the studies of food web dynamics. This form of analysis can provide information of an organism's diet over the course of weeks or months (Romero-Romero et al., 2019). This is due to carbon and nitrogen isotope composition in animal tissues acting as a record of diet during tissue synthesis. SIA utilizes the ratio of heavy to light naturally occurring stable isotopes of carbon ($^{13}C/^{12}C$) and nitrogen ($^{15}N/^{14}N$) within an animal's tissues, and these standardized ratios are expressed as $\delta^{13}C$ and $\delta^{15}N$ (Lerner et al., 2018). Stable isotope values are expressed using delta notation (δ) in parts per thousand (‰), where $\delta X=(R_{sample}/R_{standard} -1)*1{,}000$, where R_{sample} and $R_{standard}$ indicates the molar ratios of C^{13}/C^{12} and N^{15}/N^{14} of the sample and the standard reference material (Cloyed, 2015). During tissue synthesis, the heavier isotopes of carbon and nitrogen are favorably assimilated into the consumer's tissues in a process called discrimination. Samples enriched in the heavy isotope ($\delta^{13}C$ and $\delta^{15}N$) are "heavier" than other samples and have a "higher" or "less negative" isotope

value. In contrast, samples depleted in the isotope are "lighter" and have a "lower" or "more negative" isotope value (Ben-David and Flaherty, 2012). The amount by which $\delta^{13}C$ and $\delta^{15}N$ values increase in a consumer with each progressive trophic transfer is referred to as a trophic enrichment factor (TEF) (Lerner et al., 2018). The TEF can vary depending on consumer species, prey item and type of consumer tissues (Lerner et al., 2018). In nitrogen isotopes ($\delta^{15}N$) a 2.5‰ to 3.4‰ increase is observed from diet to consumer, which provides a useful measurement of an organism's trophic position, while carbon isotopes ($\delta^{13}C$) provide insight of an organism's diet and foraging ecology (Romero-Romero et al., 2019). Animals have a carbon isotope composition similar to their diets and are enriched by carbon by only 1‰ or less. An average of 0.4‰ is observed between trophic levels (McClain-Counts et al., 2017). This small enrichment factor between the animal and diet source makes $\delta^{13}C$ a good indicator of diet (Davenport and Bax, 2001). The ratio of $^{13}C/^{12}C$ can be used to identify a consumers' reliance on primary producers with different photosynthetic pathways (example: C3, C4, or CAM) (Ben-David and Flaherty, 2012). In other words, the $\delta^{13}C$ value in the consumer's tissue will reflect the $\delta^{13}C$ value of the primary producer in the food web to which the consumer belongs. It is important to understand what external and environmental factors may influence stable isotope results to properly interpret values.

In a marine or coastal ecosystem, there are several potential sources of carbon with unique $\delta^{13}C$ signatures such as macroalgae, seagrasses, marine phytoplankton, and terrestrial outflow (Davenport and Bax, 2001). While carbon and nitrogen isotopic values provide a useful measure of food web ecology, a variety of factors can alter these isotopic values. Feeding depth, seasonality, and spatial variability all have an influence on $\delta^{15}N$ and $\delta^{13}C$ values. The majority of primary producers in aquatic ecosystems rely on Rubisco pathways during photosynthesis; however, large differences in $\delta^{13}C$ exist between intertidal and pelagic oceanic systems (Ben-David and Flaherty, 2012). This occurrence is attributed to differences in temperature, levels of dissolved CO_2, phytoplankton growth rates, and whether the system is fueled by phototrophs or chemotrophs. Distinct $\delta^{13}C$ ranges are known for marine phytoplankton (−22‰ to −16‰) and chemosynthetic derived organic matter (−75‰ to −28‰) (McClain-Counts et al., 2017). These two aquatic ecosystems also differ in $\delta^{15}N$ (Ben-David and Flaherty, 2012). Consequently, $\delta^{13}C$ can be used to infer to which ecosystem an organism resides or where to forage for food.

More specifically in the mesopelagic zone, organisms residing below the euphotic zone heavily rely on detrital based diets rich in $\delta^{15}N$ and $\delta^{13}C$ (Steinberg et al., 2008). As a result, concentrations of $\delta^{15}N$ and $\delta^{13}C$ are expected to increase (i.e., become more enriched) with trophic position and depth (Kobari et al., 2022). In addition, due to the high diffusion resistance of CO_2 in water, phytoplankton in the upper ocean layers will assimilate normally discriminated ^{13}C (France, 1995). However, as water turbulence decreases with increasing depth, CO_2 experiences higher diffusive boundary layer resistance, thus enriching primary producers in ^{13}C relative to ^{12}C (France, 1995). The contribution of carnivores to total abundance and biomass is higher at mesopelagic depths than in the epipelagic layer (Richards et al., 2020; Kobari et al., 2022). Diets of mesopelagic organisms residing full time at depth are highly reliant on molts and carcasses of other organisms; thus, resulting in higher dietary $\delta^{15}N$ and $\delta^{13}C$ isotopic values (Bode and Hernández et al., 2018; Kobari et al., 2022). High variability in $\delta^{15}N$ and $\delta^{13}C$ is also expected across seasons and environments due to availability of prey items. Even an event such as a phytoplankton bloom can cause a dietary shift in prey items. For example, copepods, a popular prey item of mesopelagic fishes, have been observed to change their diet from diatoms and flagellates during a bloom to ciliates post bloom (Kobari, et al., 2022). In addition, prey availability is also impacted by the mixed layer depth. The mixed layer depth range varies across seasons and locations throughout the NPSG, which impacts nutrient availability, thus influencing the phytoplankton community (Karl, 1999; Kobari et al., 2022). The NPSG is characterized by a relatively deep permanent pycnocline and nutricline, and shallow mixed layer depth. This feature results in low nutrient availability throughout the NPSG (Karl and Lukas, 1995). Consequently, primary production is supported in the euphotic zone through the local regeneration of simple forms of elements from the metabolic activities of metazoan and microbial processes, and through the influx of nutrients drawn up to the euphotic zone from greater ocean depths by upward advection and diffusion, by horizontal transport, or by atmospheric deposition (Karl, 1999). Consumers in the NPSG, identified by SIA, could be considered omnivores, which feed on autotrophic, heterotrophic, and mixotrophic components of the microbial food web (Hannides et al., 2009). Low zooplankton $\delta^{15}N$ values have been observed to indicate a greater reliance on N_2-fixation and recycled nitrogen sources generated from microbes. On the other hand, higher $\delta^{15}N$ values in zooplankton have been observed when nitrogen is sourced from the biological fixing of atmospheric nitrogen gas and nitrate (Hannides et al., 2009).

Variation in isotopic values can also be observed within the same species. $\delta^{15}N$ and $\delta^{13}C$ isotopic concentrations in animal tissue are also dependent on the size and age of an organism, nutritional status, and whether it is primarily an herbivore, omnivore, or carnivore. Additionally, the tissue sampled, the macronutrient composition of the diet (carbohydrates, amino acids, and fatty acids), and assimilation efficiency also have an impact on the $\delta^{15}N$ and $\delta^{13}C$ isotopic concentrations observed in an organism (Ben-David and Flaherty, 2012). For example, younger organisms will incorporate dietary isotopic values faster than older organisms of the same species due to higher metabolism and faster tissue turnover rates (Ben-David and Flaherty, 2012).

Not all species residing in the mesopelagic migrate from their residual depth to feed in the epipelagic zone. These non-migratory species rely on a more detrital based food web by feeding on falling debris such as fecal pellets and sinking dead organisms, collectively known as the "marine snow" (Gloeckler et al., 2017). These non-migrating species likely represent different trophic linkages than migrating mesopelagic organisms (Romero-Romero et al., 2019). Non-migratory mesopelagic fishes are highly understudied. As a result, non-migrators' trophic ecology is poorly understood in comparison to migrating mesopelagic organisms (Romero-Romero et al., 2019). Observing $\delta^{15}N$ concentrations, obtained via SIA, is not only a useful tool for determining an organism's trophic position, but also determining whether a species migrates to feed or remains at depth. The $\delta^{15}N$ values of suspended and sinking particulate organic matter have been observed to increase with depth due to microbial degradation (Gloeckler et al., 2017; Romero-Romero et al., 2019). Therefore, organisms feeding on sinking detrital manner will present higher $\delta^{15}N$ values in their tissue in comparison to mesopelagic species who feed near the ocean surface (Romero-Romero et al., 2019). $\delta^{13}C$ has also been observed to be highly depleted in POM in epipelagic environments compared to areas with less turbulent conditions with increasing water depth (France, 1995). Few studies address how $\delta^{15}N$ varies between non-migrating and migrating mesopelagic fishes, which would be useful to infer differences in dietary sources and feeding habits between non-migrating and migrating mesopelagic fish species. However, Romero-Romero et al. (2019) and Richards et al. (2020) observed increases in $\delta^{15}N$ concentrations in mesopelagic fish tissue for non-migrators in comparison to migrating mesopelagic fish species. Furthermore, the Romero-Romero et al. (2019) study observed that there is a positive correlation between fish size and $\delta^{15}N$ concentrations in migrating

mesopelagic fish species; yet this relationship was not significant in non-migrating mesopelagic fish species. There is a need to expand upon this study in observing how $\delta^{13}C$ isotope concentrations change with depth, body size, and between migrating and non-migrating mesopelagic fish species to further demystify mesopelagic fish feeding ecology (Sweeting et al., 2007).

2.2 Research Objectives and Goals

The goal of this study is to gain a better understanding of the role of mesopelagic fishes in marine food webs with the use of stable isotope analysis (SIA). Mesopelagic fish are an important bridging link between lower trophic species and top predators, providing a vital role in the transfer of energy through marine ecosystems. There is a need to assess mesopelagic feeding ecology to better understand their role in marine food webs. Few studies address the active component of fish mediated carbon flux. Therefore, there is a need for research in determining how mesopelagic fishes feed to measure parameters such as fecal pellet production and respiration rate to quantify the active carbon flux in the ocean (Davison et al., 2013; Saba et al., 2022). My research aims to shed light on how mesopelagic fish feeding behavior may vary based upon genera/species, body size, time of day, and with depth. These potential variations in feeding ecology could allow scientists to determine how fish mediated carbon flux changes based upon variations in biological and environmental factors. In addition, few studies have utilized SIA to study the diets of mesopelagic fishes. Past research has focused on the use of $\delta^{15}N$ to study trophic position and dietary sources; however, there is little research employing the use of $\delta^{13}C$ isotope signatures to infer mesopelagic fish feeding behavior. The use of $\delta^{13}C$ provides the benefit of studying the original dietary source of carbon. Consequently, variations in $\delta^{13}C$ in mesopelagic fishes can be used to assess how diets vary spatially and with depth. With my results, I aim to provide information on what factors could cause fluctuations in $\delta^{13}C$. This research is important to fully understanding how to interpret SIA results. A variety of cofactors may confound SIA results when trying to decipher an organism's diet. Therefore, it is important to understand what may influence SIA results when drawing conclusions from SIA data. In addition, there is a lack of research of mesopelagic feeding ecology and role in marine food webs in the NPSG (Gloeckler et al. 2017 and Saba et al., 2022). Furthermore, these fishes are thought to play a vital role in deep sea carbon sequestration. Due to their ability to avoid net capture and current low commercial value, mesopelagic fishes present a great need for further investigation. I

aim to provide information on the diet and ecology of mesopelagic fishes in the NPSG. It is important to understand how feeding behavior and food web dynamics of these fishes change throughout the world's oceans. Spatial and temporal awareness of mesopelagic fish ecology will help scientists ultimately better understand their role in the biological pump.

I will use $\delta^{15}N$ and $\delta^{13}C$ isotope signatures to infer how dietary sources change with variables such as depth and fish body mass and length. Additionally, I intend to decipher the primary producer of the marine food web to which mesopelagic fishes belong using SIA. The use of SIA has become a useful tool to study food webs and trophic positions; yet many external factors may influence an isotope signature. I intend to examine the impact of depth, migratory vs. non-migratory mesopelagic fish species, and fish size upon $\delta^{15}N$ and $\delta^{13}C$ values. Species who do not migrate will likely have higher $\delta^{15}N$ and $\delta^{13}C$ values due to feeding on a largely detrital based food web, while migratory species will likely have lower $\delta^{15}N$ and $\delta^{13}C$ due to feeding on a phytoplankton-based food web.

Based on previous research, I hypothesize to observe a positive correlation in $\delta^{15}N$ isotope values with increasing body mass [standard length (mm) and weight (g)] in migrating mesopelagic fishes and a weak relationship between $\delta^{15}N$ isotope values and non-migrating mesopelagic fishes. This hypothesis is attributed to the observation that migrating mesopelagic fishes have a wider prey availability, while non-migrating mesopelagic fishes tend to be more generalist feeders and graze upon a limited prey selection (Romero-Romero et al., 2019; Kobari et al., 2022). I will also observe if $\delta^{13}C$ varies with fish body mass [standard length (mm) and weight (g)]. Across all genera, I expect a minimal relationship with $\delta^{13}C$ and fish body mass due to the small enrichment factor observed in $\delta^{13}C$ between producer and consumer; additionally, fish metabolism, age, and nutritional status may cofound this relationship (Sweeting et al., 2007). Given the little research on $\delta^{13}C$ variability across mesopelagic fish genera and species, I seek to evaluate this hypothesis.

Next, I also hypothesize $\delta^{13}C$ isotopic concentrations will be higher in non-migrating mesopelagic fishes due to feeding on a detrital based diet, which is richer in $\delta^{13}C$ than a phytoplankton-based diet, due to slightly increasing $\delta^{13}C$ enrichment with progressive trophic levels (McClain-Counts et al., 2017; Kobari et al., 2022). Additionally, $\delta^{13}C$ will be used to determine prey abundance and diet history of mesopelagic fishes in the NPSG. Small isotopic

enrichment occurs in the $\delta^{13}C/^{12}C$ per trophic level; therefore, I can use these ratios to compare dietary sources between non-migrating and migrating mesopelagic fishes. It can take weeks to months to note dietary changes in an organism; therefore, observing isotopic ratios provides a useful measure to compare diets of migrating and non-migrating species (Gloeckler et al., 2017 and Romero-Romero et al., 2019). Consequently, this observation could provide information on if a fish migrates to feed or largely remains at its residual depth full time.

I hypothesize to observe higher variability in $\delta^{13}C$ dietary isotope values in migratory mesopelagic fishes than non-migrators. This projection is attributed to migrating mesopelagic fishes having access to a wider prey selection than non-migrators. In addition, noting changes in $\delta^{13}C$ with depths can be used to decipher how diet sources change with depth in mesopelagic fishes. $\delta^{13}C$ can be used to determine if a fish feeds on a phytoplankton or detrital based food web (Romero-Romero et al., 2019). I project increasing $\delta^{15}N$ and $\delta^{13}C$ dietary isotope values with increasing depth will support that mesopelagic fishes rely on a more carnivorous and/or detrital based diet at deeper ocean depths. Most studies have utilized $\delta^{15}N$ in studying mesopelagic fish trophic levels (Gloeckler et al., 2017; Romero-Romero et al., 2019); thus, the use of $\delta^{13}C$ in mesopelagic fish trophic level studies and dietary source changes with depth warrants investigation.

Finally, I will compare how $\delta^{15}N$ and $\delta^{13}C$ isotope values vary between mesopelagic fish genera. I anticipate observing variation in isotopic values dependent upon fish's migratory feeding patterns. Understanding variation in SIA results will help not only in studying mesopelagic fish behavior but also provide a baseline for documenting any trends in food web dynamics such as response to environmental changes, food availability, prey competition, and habitat changes (Ben-David and Flaherty, 2012).

2.3 Methods

2.3.1 Sample Collection

The NPSG was selected as the sampling location for this study due to its vast size and unique assemblage of micronekton and zooplankton. Furthermore, the NPSG houses the deep-water station ALOHA. Data used in this research were collected at Station ALOHA (Figure 1) by the R/V Kilo Moana during a cruise on June 16-22, 2019 (cruise name: KM1910). Five multi-depth tows to collect mesozooplankton and micronekton were conducted over the span of several

days during the cruise with sampling occurring at midnight (22:00-02:00) and mid-day (10:00-14:00). A Multiple Opening/Closing Net and Environmental Sensing System (MOCNESS) with a 1-m^2 mouth and 202-μm mesh Nitex netting was used during the cruise to capture samples. The ability of MOCNESS nets to open and close on command offers scientists the advantage of being able to choose at what depths samples are collected. This provides the advantage of collecting samples across discrete depth strata (Leitner, 2023). Ten nets (nets 0-9) were towed at the following depths to collect samples: 0-50 m (net 9), 50-100 m (net 8), 100-200 m (net 7), 200-300 m (net 6), 300-400 m (net 5), 400-500 m (net 4), 500-600 m (net 3), 600-800 m (net 2), and 800-1000 m (net 1). Net 0 was towed across the entire depth range of 0-1000 m when the net was descending downward at the start of a tow. Therefore, species collected in net 0 are not depth specific. As a result, species from net 0 were not analyzed due to lacking a known capture depth. In addition, net avoidance is likely greater during downwards tows, thus making net 0 less quantitatively comparable to other MOCNESS nets. MOCNESS tows had a duration of up to six hours. Sensors on the net recorded data on temperature, salinity, oxygen concentration, and fluorescence while underway. In addition to these environmental data, sensors recorded flow counts and the tow angle, allowing the volume samples by each net to be calculated. Throughout all tows, an effort was made to fly the net at an angle of 45º. A speed over ground of 2 knots was generally maintained by the research vessel and the winch retrieval rate was varied to maintain the 45º angle. After the tow, the outer side of the net was sprayed with seawater to concentrate organisms in the collecting bucket. A Folsom splitter was used to divide the sample from each net in half to be used in different analyses. Fish found in one half of sample from each net were preserved while shipboard for use in the analyses described below. These fish samples for this study were frozen at -80°C until processed at the Life Sciences and Biotechnology Building at East Carolina University (ECU). Samples were frozen in cryovials or plastic bags based on the net and tow in which they were collected.

2.3.2 Mesopelagic Fish Sample Processing

a. Pre-dissection Steps

The mesopelagic fish samples obtained during the KM1910 cruise were stored in a -80°C freezer in the McRae Lab (Life Sciences and Biotechnology Building 3406). Samples were removed from the freezer and dissected one at a time to prevent thawing and refreezing of

samples awaiting dissection. Dissection tools were also sterilized with ≥90% ethanol to prevent contamination between dissections.

Prior to dissection, each fish was identified to prevent the removal of any key morphological features, such as fin rays and photophores. A compilation of identification materials (Table 1) for mesopelagic fishes, supplied by fisheries biologist Bruce Mundy (NOAA), were utilized to identify the samples. The fishes were identified using pictures to compare with identification material. An iPhone or microscope (Zeiss Stemi 508) equipped with a microscope camera (Lumenera Infinity 3) was used to photograph specimens. Larger specimens were identified using pictures from the iphone camera, while smaller samples (< 20 mm) were identified using the microscope camera. Samples were identified to the lowest possible taxonomic level.

A wet weight of each fish was taken using Mettler Toledo scale (model: ME103TE/00, precision of 10^{-3} g). Each fish was placed on a Kim wipe or paper towel first to blot any excess moisture. Weight boats were tared before weighing the fish. Fish weights were recorded in grams. Also, a standard length (SL) was recorded in millimeters for each fish. After weighing and measuring the fish, these measurements along with the net number, tow number, and capture time from which the fish was collected were recorded in a Microsoft Excel table. Since collaborators at the University of Hawaii will be extracting DNA from these specimens for metabarcoding, the samples were kept at freezing temperature for as long as possible to prevent bacteria growth that could contaminate the extracted DNA. Some thawing was needed for dissections to be feasible, but this was minimized to the greatest extent possible. Consequently, dissections were performed on a 100-mm monoplate petri dish resting on the petri dish cap filled with ice. Tissue samples for DNA barcoding were returned to the -80°C freezer for storage.

c. Dissection

White muscle tissue is best used for SIA due to its low isotopic variability and low lipid and inorganic carbonate content (Curry et al., 2013). Any variation in lipid content may lead to misinterpretation in diet studies (Elliot and Elliot, 2016). Lipids are typically depleted in $\delta^{13}C$ relative to protein. Using Vannas micro scissors, a piece of white muscle tissue along the dorsal side of fish was removed for later use in stable isotope analysis. Pectoral fins were removed prior to tissue extraction. In addition, any organ tissue that may have adhered to muscle tissue during extraction was removed. In some cases, fishes were too small (≤15mm SL) to extract enough

dorsal white muscle tissue for SIA. In these cases, the entire fish body was processed for SIA. In my analysis, there were 71 out of 251 cases where the entire fish body was used for SIA. The extracted tissue sample was placed in a glass cryovial labeled with an external label (fish number, time of sampling, tow number, and net number). Tissue samples from each fish were placed in their own vial and dried. Samples can be stored in a -20°F freezer until drying in the drying oven.

Next, these samples were prepared to undergo SIA for $\delta^{13}C$ and $\delta^{15}N$. For fish < 20 mm SL, pooling samples was often necessary to obtain the minimum weight (0.5 mg) for SIA. Pooling, when necessary, occurred during the encapsulation process (described below). Samples were pooled together by homogenizing the tissue samples by mixing after each tissue sample had been separately ground with a mortar and pestle. When pooling was necessary, fish of the same species and net number were pooled together. Only enough material from a sample was used to obtain the minimum weight required for stable isotope analysis (0.50 mg). In most cases, two fishes were the average number needed to pool together. A total of 47 fishes were subject to being pooled with other fishes (Tables 2 and 3). Some of the fishes collected during the cruise were too small (> 5 mm) to extract a tissue sample. As a result, these fishes were not processed for SIA.

2.3.3 Encapsulation for Stable Isotope Analysis

To prepare samples for SIA, the fish tissue must first undergo an encapsulation process. Encapsulation occurred at ECU in Room 233 of the Science and Technology building in the Organic Geochemistry Lab within the Department of Geological Sciences. Fish tissue was dried in a drying oven (Fisher Brand Isotemp Gravity Oven) in the Asch lab (Life Sciences and Biotechnology Building 3200) at 60°C for 24 hours. The dried tissue is ground to a powder with a mortar and pestle. Samples are weighed using an analytical balance with a precision of 10^{-6} g. Under the guidelines of the stable isotope facility at the University of New Mexico, each sample must weigh >0.5 mg dry weight for $\delta^{13}C$ analysis and a range of 0.5-1.5 mg of sample can be accommodated for conducting both $\delta^{13}C$ and $\delta^{15}N$ analysis.

Encapsulation of samples followed the University of New Mexico stable isotope facility's protocol for encapsulation. Samples were encapsulated in 5×8 mm tin capsules that

were placed in a 96 well tray for analysis. Prior to encapsulation, the tin capsule was placed on the analytical balance and tared to zero. The dry sample was scooped into the capsule to a weight of ≥ 0.50 mg. Using small, curved forceps, the top of the capsule was crimped closed. The capsule was laid on its side and crimped using forceps and an angled probe to form a sphere, being sure to pinch down any angled edges. The crimped capsule was then placed into one of the wells in the 96 well tray. Samples were loaded across rows with each row fully populated. Weights of each sample and the location the sample was placed in the well tray were recorded. A blank capsule of foil was placed every six wells to reveal any sources of error during the analysis. The location of the blank samples in the well tray was noted for the University of New Mexico's lab facilities and my own knowledge. In addition, when sufficient material was available, replicate samples were included to check SIA precision. A precision of 0.06‰, with one standard deviation, for both $\delta^{13}C$ and $\delta^{15}N$ was reported for the Thermo Scientific Delta V mass spectrometer, which is the equipment used at the University of New Mexico's stable isotope facility (The University of New Mexico, 2023). Results from SIA data indicated the spectrometer reported an R^2 of 0.997 for $\delta^{15}N$ and an R^2 of 1.000 for $\delta^{13}C$ when comparing the accepted standard value versus observed value for $\delta^{13}C$ and $\delta^{15}N$, which indicated the spectrometer generated highly precise SIA data. In this sample set, 31 samples had sufficient weight for replicates. Samples whose dried tissue weight was ≤ 0.5 mg did not have replicates made. Samples were secured by placing a silicone mat over the open wells before the lid was secured. The lid was securely closed with tape on all four sides. Next, the sealed tray was turned over and shaken to observe if any samples leaked from the capsule. All leaky capsules were re-encapsulated before shipping to the University of Mexico lab where SIA was performed.

2.3.4 Stable Isotope Analysis

Samples were shipped to the University of New Mexico's stable isotope lab for SIA. A Thermo Scientific Delta V mass spectrometer with a dual inlet and Conflo IV interface connected to a Costech 4010 elemental analyzer (EA), and a high-temperature conversion elemental analyzer (TCEA) was used for $\delta^{13}C$ and $\delta^{15}N$ analysis (Sharp, 2017). The samples were combusted at 1,000°C in a reactor packed with chromium oxide and silvered copper oxide. After combustion, oxides were removed in a reduction reactor (reduced copper at 650°C). The helium carrier flowed through a water trap where magnesium perchlorate and phosphorous

pentoxide are used to trap moisture from gas. Before entering the spectrometer, N_2 and CO_2 were separated on a Carbosieve GC column (65°C, 65 mL/min) (The University of New Mexico, 2023).

During analysis, samples were interspersed with at least four different reference materials that have been calibrated against recognized international reference materials including: IAEA-600, USGS-40, USGS-41, USGS-42, USGS-43, USGS-61, USGS-64, and USGS-65. The sample's existing isotope ratio was measured relative to a reference gas peak analyzed with each sample. These values were finalized after correcting the values of the entire sample batch against known values of the laboratory reference materials. Standard deviation of isotopic values is ± 0.2‰ for $\delta^{13}C$ and 0.3‰ for $\delta^{15}N$. Final delta values were recorded relative to the international standards VPDB (Vienna Pee Dee Belemnite) and air for carbon and nitrogen, respectively (Sharp, 2017).

2.3.5 Data Analysis

Following dissections, total counts of each species were made; furthermore, based upon literature for classification, the fishes were classified as migratory or non-migratory (Table 1). This information will help interpret the results of SIA. Next, I analyzed how many migratory and non-migratory species at each depth range were dissected and the time of day of which these species were captured. Species diversity and species evenness were also calculated below and above 400 meters at day and night-time tows. The Shannon-Wiener Diversity Index was used to calculate species diversity, while the Shannon Equitability Index was used to calculate species evenness. This boundary depth was selected to examine species diversity due to the observation that many of the sampled fishes congregated around this depth at both day and night-time tows. Tows conducted at 400 m or below represents the diversity of non-migrating taxa, as well as the day-time distribution of migrators, whereas tows shallower than this predominantly contained migrating taxa collected at night. Samples from above 400 m tows were classified as depth ranges 0-400 m, whereas samples from below 400 m depth ranges were designated to 400-1,000 m. Next, a two-way ANOVA was performed to observe isotopic variation in both $\delta^{13}C$ and $\delta^{15}N$ from both day- and night-time tows and across variations in depth (above or below 400 meters) with depth and time of tow as an interaction term. Separate two-way ANOVAs were performed for migratory and non-migratory taxa. A Tukey-Kramer post-hoc test was also performed to

examine what treatments were responsible for any statistically significant differences encountered. I proceeded to also analyze how $\delta^{13}C$ and $\delta^{15}N$ varied for fish body mass (both length and weight) for migratory and non-migratory fishes. This body mass analysis was conducted using a linear regression. An R^2 value ≥ 0.50 and a p-value ≤ 0.05 were considered a strong relationship when correlating fish length/weight with $\delta^{13}C$ and $\delta^{15}N$ (Dormann et al., 2013). The slope (m) was also used to assess the strength of the relationship between fish length/weight and $\delta^{13}C$ and $\delta^{15}N$. Finally, I analyzed how $\delta^{13}C$ and $\delta^{15}N$ varied with mesopelagic fish species or genera. I selected genera from my dissected population to analyze where there were ≥ 4 samples (Table 1). However, the genus *Cyclothone* was broken down to species level due to *Cyclothone signata* being a migratory species and *Cyclothone acclinidens* and *Cyclothone pseudopallida* are non-migratory species (Gon, 1990a). The other analyzed taxa all fit into the category "migratory" or "non-migratory" within their genera. This criterion of ≥ 4 samples allowed for the analysis of *Cyclothone acclinidens, Cyclothone pseudopallida, Cyclothone signata, Diaphus* spp., *Diogenichthys* sp., *Gonostoma* spp., *Stenobrachius* sp., *Electrona* sp., *Valenciennellus* sp., and *Sternopytx* sp. A one-way ANOVA was used to test how $\delta^{13}C$ and $\delta^{15}N$ changed between species or genera. Finally, a Tukey-Kramer test was conducted to analyze where the variability existed between species or genera and $\delta^{13}C$ and $\delta^{15}N$.

2.4 Results

A total of 32 species and genera or family were identified in the sampled population of mesopelagic fishes from the NPSG (Table 3). Some of the sampled fishes lacked distinguishing features, which could have been lost during preservation, to identify them to species level. As a result, these fishes were classified to the lowest taxonomic level possible. From this point, these fishes were then classified as migratory or non-migratory and processed for SIA.

2.4.1 Depth Distribution

For both day- and night-time tows, the majority of migrating and non-migrating mesopelagic fishes remained below the 400 m depth profile (Figures 2A-B). Non-migrating mesopelagic fishes that were dissected in this dataset were found largely in the 500-600m and 600-800m depth profile range for both day- and night-time tows. The migrating mesopelagic fishes that were dissected were also found fairly deep in the water column during day- and night-

time tows. There was a high presence of dissected migrators at the 400-500 m and 500-600 m range during day-time tows, while the night-time tows also presented a high occurrence of dissected migrators at the 400-500 m range and 500-600 m range. However, I observed more dissected migrators in the 400-500 m range during the day and a larger number of dissected migrators in the 500-600 m range at night. In conclusion, although both non-migrating and migrating mesopelagic fishes remained largely below 400 m at day and night, I observed non-migrating mesopelagic fishes tend to inhabit deeper depths than the migrating mesopelagic fishes in both the day and night. Despite that the majority of fishes were sampled below 400m, I still found it important to analyze fishes found in shallower depths to learn what genera/species reside in shallower depths, which is still important information in the study of mesopelagic fish behavior.

It should be noted that the abundance of fishes dissected (Figure 2A) differed from the density and frequency of fishes collected aboard the ship (Figure 2B). Dissected fishes only considered the frequency of fishes at each depth range, whereas shipboard measurements considered the density (abundance/sampling effort) at each depth range. The difference between dissected fishes and shipboard measurements is also attributed to the number of fishes that could not be dissected due to being too small (>5mm) for dissection and the number of fishes were not preserved well aboard the ship that were not viable for dissection. A third source of discrepancy is that the data in Figure 2B (total number of fishes collected from the MOCNESS nets) account for differences in the volume of water sampled during each tow and number of fishes per 1,000m^3; whereas the number of sampled fishes dissected (Figure 2A) and processed for SIA do not account for differences in volume of water sampled and fishes collected per 1,000m^3 of seawater sampled.

2.4.2 Mesopelagic Fish Diversity and Evenness

The Shannon-Wiener Diversity Index revealed the order of highest to lowest diversity of mesopelagic fishes: 1) > 400 m day-time; 2) < 400 m day-time; 3) < 400 m night-time, and; 4) > 400m night-time (Figure 3A). There is an overlap in upper 95% confidence intervals between all of these categories, implying that mesopelagic fish diversity across these categories does not significantly differ.

The Shannon Equitability Index revealed the species evenness from highest to lowest: 1) < 400 m day-time; 2) < 400 m night-time; 3) > 400 m day-time, and; 4) > 400 m night-time (Figure 3B). Like the Shannon-Wiener Index, there is an overlap in upper 95% confidence intervals between all categories, which leads to the conclusion that evenness among these groups was not statistically different.

2.4.3 Relationship between $\delta^{15}N$, $\delta^{13}C$, and Mesopelagic Fish Size

Overall, migrating mesopelagic fishes (Figure 4A) were observed to have a marginally stronger linear relationship than the non-migrators (Figure 5A) when comparing the relationship between $\delta^{13}C$ and $\delta^{15}N$ and fish standard length. Migratory mesopelagic fishes measured a length range of 8-50mm and a weight range of 0.014-0.757 g. SIA results for migrators revealed a mean of $\delta^{13}C$: -20.4‰ and $\delta^{15}N$: 6‰. In comparison, non-migratory mesopelagic fishes measured a length range of 5-216 mm (there were three large fishes that increased the size range, minus the 3 outlier fishes, non-migratory fishes ranged in length: 5-58 mm) and weight range of 0.035-14.598g. SIA results for non-migrators revealed a mean of $\delta^{13}C$: -20.6‰ and $\delta^{15}N$: 8‰. This trend was observed in both isotope fractions when comparing the relationship between $\delta^{13}C$ and $\delta^{15}N$ isotopes variation with fish standard length (Table 4). Non-migrating mesopelagic fishes $\delta^{13}C$ and standard length have a statistically significant relationship ($m=0.011$, $p=0.0007$, $R^2=0.141$), while the relationship between $\delta^{15}N$ and standard length is statistically unsignificant ($m=0.013$, $p=0.292$, $R^2=0.015$) (Table 4). On the other hand, migrating mesopelagic fishes also presented statistically significant relationships between length and both $\delta^{13}C$ ($m= 0.029$, $p\geq0.0001$, $R^2=0.224$) and $\delta^{15}N$ ($m=0.116$, $p\geq0.0001$, $R^2=0.451$). Larger amounts of variance were explained by this relationship as indicated by the higher R^2 values and slightly larger slopes than the equivalent relationship for non-migrators (Table 4).

When comparing fish wet weight and $\delta^{13}C$ and $\delta^{15}N$ isotopes, migrating mesopelagic fishes (Figure 5B) also presented a stronger linear relationship than non-migrating mesopelagic fishes (Figure 6B) for both isotopes. For both $\delta^{13}C$ ($m= 0.699$, $p=0.0009$, $R^2=0.115$) and $\delta^{15}N$ ($m= 2.010$, $p=0.0007$, $R^2=0.118$), the relationship with migrator weight was determined to be statistically significant (Table 4). Furthermore, migrating mesopelagic fishes presented the highest slope in the linear regression analysis for $\delta^{15}N$ and weight ($m=2.010$) than the other observed time and depth categories when comparing migratory versus non-migratory fishes

(Table 4). For non-migrators, the relationship between $\delta^{13}C$ and fish weight was determined to be statistically significant (m= 0.106, p=0.001, R^2=0.134) (Table 4). In addition, the relationship between $\delta^{15}N$ and fish weight was observed to have a negative slope in the linear regression analysis (m=-2.190) (Table 4), but this relationship was not statistically significant (m= -2.190, p=0.062, R^2=0.046) (Table 4). The presence of outliers was likely the cause for the observed negative slope seen among the non-migrators for $\delta^{15}N$ and fish weight (Figure 4A-B; Figure 5A-B).

Based upon analyzing R^2 values, $\delta^{13}C$ and $\delta^{15}N$ isotope fractions have a slightly stronger linear relationship with fish standard length versus wet weight in both migrating and non-migrating mesopelagic fishes (Table 4). However, non-migrators demonstrated a stronger relationship with $\delta^{15}N$ in fish weight over length (Table 4). The results of this study suggest we do see an increase in $\delta^{15}N$ values with increasing fish length and weight for both migrating and non-migrating mesopelagic fishes (Figures 4A-B and 5A-B). Furthermore, less depleted $\delta^{13}C$ values can be observed for both non-migrating and migrating mesopelagic fishes with increasing fish weight and length (Figures 4A-B and 5A-B). The relationship with fish weight was stronger for $\delta^{13}C$ than for $\delta^{15}N$ in both migratory and non-migratory fishes as indicated by higher R^2 values (Table 4). However, higher R^2 values were observed for $\delta^{15}N$ than for $\delta^{13}C$ when examining migratory fish length, indicating a stronger relationship between $\delta^{15}N$ and fish length (Table 4). Non-migratory fishes displayed the opposite relationship: the R^2 was higher in $\delta^{13}C$ than $\delta^{15}N$ when comparing isotopic ratios to fish length. As a result, migratory fishes have a stronger relationship with fish length in $\delta^{13}C$ than $\delta^{15}N$ (Table 4).

2.4.4 $\delta^{15}N$ and $\delta^{13}C$ and Time of Day and Sampling Depth Relationship

Almost no variation was observed in $\delta^{13}C$ between day- and night-time tows in migrating mesopelagic fishes, with a mean $\delta^{13}C$ of -20.48‰ at night-time and -20.26‰ during the day (Figure 6A, Table 5C). This observation also held true for depth differences in migrators when observing $\delta^{13}C$ differences above (shallow) and below (deep) 400 m; there was no variation in $\delta^{13}C$ between these two depth layers with a mean $\delta^{13}C$ of -20.28‰ in shallow depths and -20.51‰ in deeper depths (Figure 6A, Table 5C). Non-migrating mesopelagic fishes also did not express any variation in isotopic composition of $\delta^{13}C$ between day and night-time tows, with a mean δ13C of -20.22‰ at night-time and -19.78‰ during the day (Figure 6B, Table 6C). Like

the migrators, non-migrating mesopelagic fishes did not present variability in comparing $\delta^{13}C$ above and below 400m, with a mean $\delta^{13}C$ of -19.98‰ in shallow depths and -20.28‰ in deeper depths (Figure 6B, Table 6C). These observations are consistent with the overlap in 95% confidence intervals for $\delta^{13}C$ in the studied variables for migrating and non-migrating mesopelagic fishes. On the other hand, $\delta^{15}N$ appears to be higher at night in migrators versus day with a mean $\delta^{15}N$ of 6.18 at night and 5.12 during the day-time (Figure 6A, Table 5C). However, there is an overlap in 95% confidence intervals comparing these two groups; thus, this difference in $\delta^{15}N$ between day and night-time tows in migratory fishes is not statistically significant at $p < 0.05$. Little variability was observed in $\delta^{15}N$ above and below 400 meters in migrators. This observation is confirmed by the overlap in 95% confidence intervals.

Non-migrating mesopelagic fishes presented a similar trend to the migrators with $\delta^{15}N$ in respect to differences in day- and night-time tows and depth differences. $\delta^{15}N$ was observed to be higher at night than the day in non-migrators, with a mean $\delta^{15}N$ of 8.15‰ at night and 7.13‰ at day-time (Figure 6B, Table 6C). Even so, the overlap in 95% confidence intervals does not find this difference to be of statistical significance. Furthermore, $\delta^{15}N$ was higher in non-migrators collected above 400 m than those collected below 400 m (Figure 6B). Nevertheless, there is a small overlap in 95% confidence intervals revealing this difference is not statistically significant.

The results of the two-way ANOVA comparing $\delta^{13}C$ and $\delta^{15}N$ in migrators and non-migrators examining time of day, depth, and the interaction between these factors revealed that there is minimal statistical significance when comparing these variables (Table 5A-B and Table 6A-B). Yet, non-migrators presented a statistically significant relationship between $\delta^{15}N$ and depth ($p=0.019$, $F=5.780$) (Table 5A). Furthermore, there was a significant interaction between the effects of depth and time of day when examining $\delta^{15}N$ variability ($p=0.029$, $F=4.990$) (Table 5A). Yet, the results of the Tukey-Kramer post-hoc test applied following the ANOVA suggested that the only relationship of marginal statistical significance existed with $\delta^{15}N$ in non-migrating mesopelagic fishes when comparing fishes above and below 400 m depth ranges. This finding supports depth as a significant factor in $\delta^{15}N$ changes among non-migratory mesopelagic fishes (Table 7A).

In conclusion, when comparing overall $\delta^{13}C$ and $\delta^{15}N$ isotope values between migrators and non-migrators, there are a few trends to note. The average $\delta^{13}C$ isotope values remained

constant with minimal variability when comparing day and nighttime tows and depth with migrators and non-migrators. The results of ANOVAs and comparisons of 95% confidence intervals support this non-statistically significant relationship (Table 5A, Table 6). However, the mean $\delta^{15}N$ was observed to be higher for non-migrators (above 400 m: 7.49‰; below 400 m: 8.43‰) versus migrators (above 400 m: 5.97‰; below 400 m: 6.30‰). In addition, when comparing day-time and night-time measurements, non-migrators also presented higher mean $\delta^{15}N$ isotope values (day: 7.13‰; night: 8.16‰) compared to the migrators (day: 5.12‰; night: 6.18‰).

2.4.5 $\delta^{15}N$ and $\delta^{13}C$ and Genera/Species Relationship

When comparing $\delta^{13}C$ and $\delta^{15}N$ isotopic signatures across genera and species, the greatest isotopic variation was observed in $\delta^{15}N$ among genera and species (Figure 7A). On average (except for *Gonostoma* spp.), genera and species classified as migrators had higher $\delta^{15}N$ than non-migrators (Table 8A). For both $\delta^{15}N$ and $\delta^{13}C$, *Cyclothone pseudopallida* and *Cyclothone acclinidens* were noted to be statistically different (more depleted $\delta^{13}C$ and higher $\delta^{15}N$) from *Diaphus* spp. and *Electrona* sp (Table 9A-10A). Non-migrating genera and species exhibited less variability in $\delta^{15}N$ than those genera and species classified as migrators. This finding was supported by the results of the Tukey-Kramer test and the 95% confidence intervals (Figure 7A). The results of the one-way ANOVA further support that there is a statistically significant relationship between genera and species and $\delta^{15}N$ ($F=6.346$, $p\leq0.0001$) (Table 9B). Less variability in $\delta^{13}C$ than $\delta^{15}N$ was observed when comparing genera and species (Figure 7B). Average $\delta^{13}C$ remained in a close range between genera and species (Table 9A). However, those genera and species classified as migrators did present more negative $\delta^{13}C$ isotope values than non-migrators (Table 9A). The relationship between $\delta^{13}C$ among genera and species was shown to be of statistical significance based on the one-way ANOVA ($F=2.331$, $p=0.018$) (Table 9B). Yet, this relationship was not strong as the variability between $\delta^{15}N$ and genera/species. The results of the Tukey-Kramer test further suggested that greater variability between species/genera was observed in $\delta^{15}N$ than $\delta^{13}C$ isotopes (Table 12 A-B).

$\delta^{13}C$ and $\delta^{15}N$ isotope samples from fishes collected from the research cruise were compared with the isotope values for phytoplankton and particulate organic matter (POM) collected by previous studies (Davenport and Bax, 2002, Table 11B) in the NPSG and sediment

trap data collected by Ashley Maloney aboard the KM190 cruise. Per trophic level, there is an enrichment of ~3.0 ‰ for $\delta^{15}N$ and ~1.0 ‰ for $\delta^{13}C$ (Choy et al., 2015; McClain-Counts et al., 2017). Depending on a species' diet, there are 1-2 trophic levels between POM and mesopelagic fishes (McClain-Counts et al., 2017; Richards et al., 2020). Isotopic signatures for both $\delta^{15}N$ and $\delta^{13}C$ from the fishes reflected data collected in the sediment traps during the cruise (Table 11A) once these rates of enrichment across trophic levels were considered. Observed genera and species in this study exhibited $\delta^{13}C$ values in the range of -19.98‰ to -21.25‰ (Table 9A). The sampled genera and species in this study exhibited $\delta^{15}N$ values ranging 3.81‰ to 8.71‰ (Table 10A). Davenport and Bax (2002) reported phytoplankton, sediment, and POM data for $\delta^{13}C$ and $\delta^{15}N$ collected in the benthic and pelagic zones of the water column (Table 11B). The $\delta^{13}C$ isotope values reported by Davenport and Bax (2002) were consistent with the $\delta^{13}C$ isotope values collected from sediment traps and for zooplankton sampled from ring net tows aboard the KM1910 cruise (Table 11B-C). However, $\delta^{15}N$ isotope signatures from Davenport and Bax (2002) were much greater than the $\delta^{15}N$ collected from POM and zooplankton samples aboard the cruise (Table 11B-C). Davenport and Bax (2002) also reported $\delta^{13}C$ isotope values consistent with what was reflected in the tissue of our collected mesopelagic fishes; yet $\delta^{15}N$ isotope signatures from Davenport and Bax (2002) were too high to be consistent with our sampled fishes. This finding highlights the importance of considering temporal and spatial variability when interpreting isotope signatures. It is important to see if $\delta^{13}C$ and $\delta^{15}N$ vary across the NPSG.

2.5 Discussion

Sampled mesopelagic fishes for this study were largely obtained from the 400-500 m and 600-800 m depths for both migrating and non-migrating species at day and nighttime tows. The abundance of mesopelagic fishes collected from the 400-800m depth range collected from the KM1910 cruise is consistent with the average depth range observed in other studies (St. John et al., 2016; Olivar et al., 2022; Woods et al., 2023). Shipboard data (total collected fishes from each MOCNESS net) from the research cruise did reflect a higher frequency of fishes collected in shallower depth ranges (0-200 m) at night than what was reported in the subset used in this study. Nonetheless, mesopelagic fishes are notoriously difficult to capture at all depths due to net avoidance and escapement (Davison et al., 2013; Saba et al., 2021). It was also observed that more variability in $\delta^{15}N$ occurred than in $\delta^{13}C$. Most significant effects were seen in $\delta^{15}N$ and

depth for non-migratory fishes. Marginally significant time of day effects were observed in migratory fishes with variability in $\delta^{15}N$. Migratory fishes had the strongest relationship with $\delta^{15}N$ and fish weight; however, $\delta^{15}N$ and fish weight was observed to be statistically insignificant for non-migratory fishes. However, low R^2 values and weak slopes may suggest fish length/weight and stable isotope values may not be ecologically significant. I also observed there were more statistical differences in $\delta^{15}N$ enrichment across species and genera than $\delta^{13}C$ enrichment, which could be attributed to difference in the trophic enrichment factor for $\delta^{15}N$ and $\delta^{13}C$.

2.5.1 Species Composition and Depth Distribution

Of the sampled species, the genus *Cyclothone* spp. dominated the sample population, which included the species *Cyclothone acclinidens, Cyclothone pseudopallida, and Cyclothone signata* (Table 1). Of the total 251 dissected fishes, 175 belonged to the genus *Cyclothone* spp. This result is not surprising due to *Cyclothone* being the most abundant vertebrate on earth (Irigoien et al., 2014). Migratory fishes were more common than non-migrators in this sample population. This observation could be in light of migratory fishes' ability to inhabit a wider depth range than non-migrators, thus increasing the likelihood of their abundance in the MOCNESS nets. The relative abundance of migratory versus non-migratory fishes varies spatially and seasonally (Olivar et al., 2022; Woods et al., 2023). Species variation, temperature, and salinity may also explain variations in the assemblages of mesopelagic fishes and the degree of how much they migrate to feed (Olivar et al., 2022). Depth-related patterns related to light, temperature, and oxygen can act as a barrier for some migratory mesopelagic fishes. These factors can increase energy expenditure for fishes, limiting their range of depth migration (Aparecido et al., 2023). The observation of non-migratory fishes in shallower depths at night could be explained by certain species having the ability to swim outside their residual depth range in search of prey if food is scarce at their typical depth range (Olivar et al., 2022). Most of the mesopelagic fishes in this dissected study were observed to reside in the depths of 400-500 m and 500-600 m despite migratory status and time of day sampled. Unfortunately, many fishes were not able to be processed for dissection due to small size and poor preservation. As a result, frequency and density of fishes observed at various depth ranges differed from dissected versus shipboard counts of abundance. Shipboard data did not discriminate between migratory versus non-migratory fishes; however, there is an increased abundance of fishes observed in shallower

depth ranges at night than what is observed in the dissected fish data, which is a subset of fishes sampled from collected shipboard samples to be processed for SIA. Shipboard data provides a more accurate depiction of mesopelagic fish behavior to migrate to shallower depths at night to feed and retreat to deeper depths during the daytime. This likely reflects the fact that shipboard data were standardized by the volume of water sampled and by the number of fishes per 1,000 m^3 of seawater, whereas the dissected fish counts haven't been standardized. In addition, smaller depth strata were sampled closer to the surface (50 m sampled near surface vs. 200 m sampled at depth). As a result, standardizing fish counts per 1,000 m^3 of seawater will result in larger numbers of fish in surface samples. Dissected counts were not standardized by volume of water sampled and by area, which furthers reasoning for a smaller number of fishes dissected from surface depth strata. For future studies, monitoring water temperature and salinity would be useful to potentially understand mesopelagic fish migration and depth assemblage. We should also account for standardization of data from the field when comparing fishes processed in a laboratory setting.

2.5.2 Mesopelagic Fish Diversity and Evenness

The lack of statistical significance observed in fish diversity in depth and time of day is consistent with the behavior of migratory fishes to inhabit a variety of depth ranges. We would expect to see a variety of mesopelagic fishes throughout the water column based upon their DVM patterns. Past studies have shown that mesopelagic fishes inhabit depth ranges based upon energetic requirements, environmental variables, prey selection, and competition for resources (Aparecido et al., 2023; Olivar et al, 2023). Difficulty in sampling deeper depths may confound results (Romero-Romero et al., 2019). However, in this study, an equivalent number of samples were obtained from all depths. Furthermore, sampling bias could play a role in these results. There was a greater number of fishes analyzed from day-time versus night-time tows due to the number of available samples (151 dissected from daytime tows vs. 100 dissected from nighttime tows). Rarefaction curves could help evaluate patterns of diversity even in cases with unequal numbers of samples gathered. Including more sampling days may increase the accuracy of my results to reflect any trends in species diversity in time of day and depth variation.

Species evenness was not statistically different between any depth or time of day categories. Higher evenness means that no one genera or species dominated abundance, which

seemed to be particularly the case in the day-time above and below 400 m depth profile and the above 400 m night-time depth profile. Though the differences between depth and time of day categories were not calculated to be statistically significant for species evenness and richness, the following provides possible explanations for differences that were observed. Despite the lack of significant differences, species evenness was greatest shallower than 400 m during the daytime, which was surprising due to the number of mesopelagic fishes who are classified as migrators in this study. Fishes who perform diel vertical migration retreat to deeper depths during the day to avoid predation (Davison et al., 2013, Bernal et al., 2015; Archiald et al., 2019; Saba et al., 2021). However, energetic requirements and environmental variables may limit the range of migration to shallower depths. This finding could be explained by a low abundance of fishes and the no dominance of one species at shallower depths during the day-time. The results of the Shannon Wiener Index indicated a low diversity of fishes in shallower depths at day-time (Figure 3A), which sometimes corresponds with high evenness. My results are consistent with Aparecido et al. (2022) who found higher species evenness and richness in shallower mesopelagic depths during the day-time. Areas shallower than 400 m at night followed in highest species evenness. This result is consistent with past studies that observe the diel migratory pattern of mesopelagic fishes migrating to shallower depths to feed (Davison et al., 2013, Bernal et al., 2015; Archiald et al., 2019; Saba et al., 2021). Theoretically, with DVM into consideration, we would expect to see migratory mesopelagic fishes in shallower depths at night. With more species of mesopelagic fishes present at night in shallower depths to feed, species evenness would increase. However, the migration range, energy requirements, and environmental variables should be observed when noting trends in future studies of mesopelagic fish diversity and evenness to account for additional cofactors that may influence results in time of day and depth sampling.

2.5.3 Relationships between $\delta^{15}N$, $\delta^{13}C$ and Mesopelagic Fish Size

Although the results of the linear regression provide statistical significance with $p \leq 0.05$, low R^2 values and a small slope for all categories suggest the relationship between fish weight/length and $\delta^{13}C$ and $\delta^{15}N$ was not very strong. Thus, these relationships may not be ecologically significant.

Fish body mass reflected a positive trend in both $\delta^{15}N$ and $\delta^{13}C$ values for both standard length and weight in migrating and non-migrating mesopelagic fishes, except non-migrators

displayed a non-statistically significant relationship with $\delta^{15}N$ and body length. Annasawmy et al. (2020) noted increases in $\delta^{15}N$ with increased body length could possibly be explained by the ability of larger fish to feed further up the food chain. This observation would also explain why fish length has a stronger relationship than fish weight with $\delta^{15}N$ and $\delta^{13}C$ measured in fish tissue. Annasawmy et al. (2020) also provide a possible explanation for species that do not display a relationship between body length and $\delta^{15}N$ since there might be a trophic plateau where increases in trophic position with size are not possible due to physical constraints on the organism or lack of appropriate prey of higher trophic levels in their environment. Romero-Romero et al. (2019) also noted a positive relationship between increased fish length and $\delta^{15}N$ in migratory fishes, but not for migrators. Romero-Romero et al. (2019) attributes this finding to larger migratory fishes' ability to select larger prey items and migrators have higher energy requirements than non-migrators due to the energetic demands of vertical migration. In addition, dietary requirements shift throughout the life stages of a fish. As a fish progresses from juvenile to adult there is a change to a larger variety and size of prey items (Bernal et al., 2015). Bernal et al. (2015) also noted larger body size was also correlated to larger mouths in mesopelagic fishes, which allows for the ingestion of larger prey. As a result, larger, more mature fish within a species should display higher $\delta^{15}N$ and $\delta^{13}C$ than juveniles due to being able obtain larger prey from higher trophic levels, which is supported by the results in this study (Figure 4 A-B and 5A-B). Given that adult mesopelagic fishes are usually small in oligotrophic environments, 2-20 cm (Romero-Romero et al., 2019), it is difficult to distinguish juvenile fishes from adults within a species. The results of the linear regression reflected the relationship between fish length and weight for $\delta^{13}C$ was stronger in migratory fishes than the relationship between $\delta^{13}C$ and fish length and weight seen in non-migratory fishes. This finding could be due to the fact that migratory fishes are larger and have access to more prey items given their range of depth to feed is larger than non-migratory fishes. Larger individuals may also require less energy to vertically migrate to feed to increase access to various prey items. Furthermore, larger fish can outcompete smaller fish for prey (Annasawmy et al., 2020). Fanelli et al. (2011) and Davenport and Bax (2002) also noted more enriched $\delta^{13}C$ values in carnivorous fishes. This supports the finding that larger fish can feed from higher trophic levels.

There is a need for further research in how $\delta^{13}C$ relates to fish size, since limited previous research was found relating to this topic. Additionally, for future research, it would be beneficial

to sample fishes in a variety of size categories and life stages within a taxon (e.g., larval, juvenile, and adult) to further investigate variability in $\delta^{15}N$ and $\delta^{13}C$ and fish length and weight. Most of the sampled fishes were small (mean: 34 mm, 0.79 g). Adding larger fishes to the sample population may help support if the relationship exists or not. I also recommend removing any extreme outliers (in cases where they exist) from linear regression analysis to see if the relationship between fish weight and/or length with $\delta^{15}N$ and $\delta^{13}C$ might become stronger. The presence of outliers could weaken the relationship. Outliers of potential importance were among non-migratory fishes. There were two fishes measuring 100 mm and one fish measuring 216 mm, which were 3-6 times greater the mean length. In conclusion, I recommend repeating this study incorporating previously mentioned suggestions to confirm the strength of the relationship between fish weight/length and $\delta^{15}N$ and $\delta^{13}C$.

2.5.4 Relationships between $\delta^{15}N$ and $\delta^{13}C$ and Time of Day and Sampling Depth

Time of day in which the species was sampled had undetectable impacts on $\delta^{13}C$ isotopic values in both migrators and non-migratory mesopelagic fish species (migrators: $p=0.383$, non-migrators: $p=0.066$). In fact, migratory status had little impact on $\delta^{13}C$ on time of day sampled. Though the non-migratory species relationship between $\delta^{13}C$ and time of day exhibited a marginally significant relationship, non-migratory fishes would not be expected to exhibit time of day variability in $\delta^{13}C$ based on that these fishes remain at their residual depth throughout the day (Romero-Romero et al., 2019). The reason for $\delta^{13}C$ and time of day marginal significance in my study could possibly be explained by difference in species composition caught at day and night. Different non-migratory fishes could potentially feed from different food webs. It was not surprising that variability in time of day sampled had no impact on $\delta^{13}C$ in migrators, as well. If migrators are feeding close to the surface, their $\delta^{13}C$ values will reflect a phytoplankton-based diet, which takes weeks to months to incorporate in their tissues and will not reflect daily changes (McClain-Counts et al., 2017).

Time of day sampled also had a non-significant impact on $\delta^{15}N$ in both migratory and non-migratory mesopelagic fishes. The mean $\delta^{15}N$ higher at night versus day in both migrators and non-migrators, with a mean $\delta^{15}N$ of 8.16‰ (night) and 7.13‰ (day) in non-migrators (Table 6-A-B-C) and 6.18‰ (night) and 5.12‰ (day) in migrators (Table 5-A-B-C). Possible explanations for differences in mean $\delta^{15}N$ in mesopelagic fishes are based upon the biological

rationalizations and not statistical. In addition, SIA results cannot differentiate between time periods within a day, since weeks to months are needed to reflect isotopic changes (McClain-Counts et al., 2017). Therefore, longer-term studies using SIA would be needed to note any isotopic changes due to the duration needed for SIA to reflect any changes. Previous studies have shown that non-migratory mesopelagic fishes have a detrital and POM based diet, which reflects higher $\delta^{15}N$ than surface phytoplankton-based diets. Non-migrators are also limited to prey items based upon what is available to them at their residual depth (Gloeckler et al., 2017; Romero-Romero et al., 2019; Richards et al., 2020). From a biological standpoint, this finding provides a possible explanation as to why higher mean $\delta^{15}N$ values are observed in non-migrators versus non-migrators regardless of time of day and depth variability. Nonetheless, this observation warrants further analysis with regards to $\delta^{15}N$ and fish migratory status. Higher nighttime $\delta^{15}N$ values in migratory mesopelagic fishes could be explained by species present and body size. Also, most migratory mesopelagic fishes are nocturnal carnivores and rarely feed during the day (Bernal et al., 2015). Larger individuals and certain species of fishes migrate further to feed than other species and smaller fishes. Davison et al. (2013) and Olivar et al. (2022) found that fish size and species present throughout the day varied in the water column. In addition, larger fishes who may migrate further at night to feed have access to more prey items and ability to feed at higher trophic levels to thereby reflect higher $\delta^{15}N$ isotope values in their tissue.

Most of the migratory fishes in this study were *Cyclothone signata* (n=101). Although *Cyclothone signata* migrates from the mesopelagic zone to shallower depths, this species does not migrate in a diel migration pattern (Dewitt, 1972). *Cyclothone signata* has been known to be found throughout the water column regardless of time of day (Olivar et al., 2022), which may explain the lack of significant difference based on time of day. For this study, *Cyclothone signata* was classified as a migrator. Consequently, future studies including a broader range of species and fish sizes may help shed light on the factors influencing $\delta^{15}N$ and $\delta^{13}C$ based upon time-of-day variability in migratory mesopelagic fish trophic ecology. A longer study duration (months to a year) using SIA may be a useful tool for observing seasonal mesopelagic fish feeding patterns. However, given the duration needed for SIA to note diet changes, SIA is not the best method for observing daily diet trends. Pairing gut content analysis and DNA bar coding methods with this study may allow for a better view of shorter-term variations in mesopelagic fish diets (Paquin et al., 2014; McClain-Counts et al., 2017; Saba et al., 2021). There is a great

need for research to provide an explanation of $\delta^{15}N$ and $\delta^{13}C$ variability with regard to time of day in migratory mesopelagic fishes. Minimal research was found relating to this topic, perhaps due to the fact that stable isotope composition integrates feeding habitats over longer periods of time.

Depth did not play a significant influence on $\delta^{13}C$ in both migratory and non-migratory mesopelagic fishes. In fact, the average $\delta^{13}C$ remained fairly constant regardless of migratory status and depth range. Mean $\delta^{13}C$ was reported to be -20.23‰ in shallow depths and -20.51‰ for deeper depths in migrators and -19.98‰ in shallow depths and -20.28‰ in deeper depths for non-migrators. The lack of statistical significance observed in variation of $\delta^{13}C$ with depth in migrating and non-migrating mesopelagic fishes could suggest that the sampled fishes are feeding from similar trophic levels and may be part of the same food web rather than distinct food webs based on either primary production or detrital flux. The sampled fishes could also be opportunistic feeders and feed on a variety of prey items. This could provide a possible explanation for similar $\delta^{13}C$ values between non-migrators and migrators and as depth increases. Annasawmy et al. (2020) found similar $\delta^{13}C$ between fishes to possibly be explained by consuming different prey items with similar $\delta^{13}C$ signatures, which would also explain lack of variability in $\delta^{13}C$ between migrators and non-migrators. The results of my study contradict the findings of Davenport and Bax (2002) who found that $\delta^{13}C$ became more depleted when measured in fishes with increasing depth. However, France (1995), Richards et al. (2020), and Annsawmy et al. (2020) found that $\delta^{13}C$ increased in mesopelagic fishes with depth. These authors found that species sustained on a POM-based food web reflected higher $\delta^{13}C$ values than species feeding near the surface on a phytoplankton-based food web. For future studies, the use of isotopic mixing models, such as MixSIAR, would be beneficial to help decipher fishes who feed on multiple prey items (McClain-Counts et al., 2017). The data collected during the KM1910 cruise on the isotopic composition of POM, phytoplankton, and zooplankton could help parameterize such a model (Table 11). The use of these models may help explain $\delta^{13}C$ variability by determining which species are generalist feeders.

Depth variability and the depth and time-of-day interaction did not have an impact on $\delta^{15}N$ in migrators ($p=0.350$, $F=0.880$), but did express a statistical significance in non-migrators ($p=0.029$, $F=4.990$). Average nighttime $\delta^{15}N$ was higher at night and below 400m, compared to the other time and depth categories, regardless of migratory status [mean $\delta^{15}N$ below 400m at

night: 6.30‰ (migrators), 8.43‰ (non-migrators)] (Table 5C and 6C). Nonetheless, time of day sampled and its interaction with depth was not statistically significant for migrators. However, time of day presented a marginal significance for migrators (p=0.090, F=2.930). The results of this study are consistent with the literature in finding increases in $\delta^{15}N$ with depth particularly in non-migratory fish, since these fishes feed at deeper depths than migratory fishes. Gloeckler et al. (2017) and Romero-Romero et al. (2019) found increased $\delta^{15}N$ in species feeding in mesopelagic zone and species who did not migrate to feed. These studies explained these findings because fishes feeding at depth consumed a detrital or POM-based food web, which reflects higher $\delta^{15}N$ than fishes feeding in the epipelagic zone on a predominantly phytoplankton-based food web. In addition, Romero-Romero et al. (2019) also noted that $\delta^{15}N$ increased in zooplankton with increasing depth. Consequently, mesopelagic fishes grazing upon zooplankton at deeper depths will exhibit more enriched $\delta^{15}N$ in their tissue. Time of day sampled should not reflect variability in $\delta^{15}N$ in non-migrators since these species do not perform diel vertical migration to feed. Therefore, higher $\delta^{15}N$ values at night in this study could be possibly explained by sampling fishes at higher trophic levels at night versus day, which may reflect variations in species composition or fish size. Fishes may be also feeding on prey that vertically migrate, which also may reflect variability in feeding behavior based upon time of day. However, given the time needed for SIA integration to reflect isotopic changes, SIA may not be the most useful tool for monitoring changes in fish feeding behavior throughout the day. In addition, since the time-of-day effect was only marginally significant (p=0.066) for $\delta^{15}N$ values in non-migratory fishes, the impact may be minimal to none. Davenport and Bax (2002) and Choy et al. (2015) found that $\delta^{15}N$ increased with increasing trophic levels. In addition, Davenport and Bax (2002) and Richards et al. (2020) also noted that $\delta^{15}N$ is higher in fishes consuming a more carnivorous diet than fishes feeding on omnivorous or herbivorous diets. Therefore, the trophic guild and prey items the fishes are feeding on are indicative of $\delta^{15}N$ variability in fishes. Species of fishes caught and the type of prey they consume are likely the cause of time-of-day variability in non-migratory fishes, albeit this effect is only marginally significant. Nonetheless, the mean $\delta^{15}N$ in migratory fishes (mean $\delta^{15}N$ day-time: 5.12‰, night-time: 6.18‰) in day- and night-time sampling was still lower than the average $\delta^{15}N$ in non-migratory fishes (mean $\delta^{15}N$ day-time: 7.13‰, night-time: 8.16‰), which suggests migratory fishes feed on a different primary producer-based food web (Table 5C, 6C). Although $\delta^{15}N$ has

been used an indicator of trophic position in organisms, there are several factors (migration status, body size, and prey choice) to consider before assigning a trophic level to an organism based on their $\delta^{15}N$ value (Davenport and Bax, 2002; McClain-Counts et al., 2017; Romero-Romero et al., 2019). Choy et al. (2015) states that considering the feeding habits and migratory status of a fish is important to consider before assigning a trophic position.

Further research is needed to investigate potential reasons for variation in isotope signatures based on time of day and depth. Including more sampling days with day- and night-time tows to include a broader range of species (both migratory and non-migratory) and sizes may help explain SIA trends based on time of day and depth variability in $\delta^{15}N$.

2.5.5 $\delta^{15}N$, $\delta^{13}C$, and Genera/Species Relationships

$\delta^{13}C$ variability within species and genera was very minimal (-19.98‰ to -21.25‰), albeit statistically significant in some cases (Table 9A). Non-migratory genera and species overlapped in confidence intervals and expressed very similar $\delta^{13}C$ with other non-migratory genera and species. Marginally more depleted and variable $\delta^{13}C$ values were observed in migratory genera and species (-19.98‰ to -21.25‰) than non-migrators (-20.16‰ to -20.26‰). This result contradicts the studies of France (2015), Richards et al. (2015), and Romero-Romero et al. (2019). These studies found $\delta^{13}C$ increased in species residing in deeper depths and feeding on a sinking particle-based food web, which is characteristic of non-migratory fishes. However, Richards et al. (2015) also note that migrating mesopelagic fishes travel through a broad range of depths to allow access to more prey items and the ability to be more opportunistic feeders. In addition, migratory and non-migratory genera and species could be consuming different prey items with similar $\delta^{13}C$ enrichments, which may explain the marginal difference between genera and species based upon migratory status. Another possible explanation for marginal variability in $\delta^{13}C$ between genus and species could be competition for resources in oligotrophic environment (Bernal et al., 2015). Less overlap in $\delta^{13}C$ between fishes would be hypothesized for fishes consuming a variety of prey items. Low availability of prey may also explain migrators resorting to day-time feeding at depth versus night-time feeding at the surface to avoid competition for food and to maximize energy intake (Romero-Romero et al., 2019). For future studies, it would be beneficial to perform gut content analysis on a wider variety of mesopelagic fish species to help determine diet to further demystify SIA results (McClain-Counts et al., 2017).

Unlike $\delta^{13}C$, $\delta^{15}N$ exhibited a wider range between genera and species (3.81‰-8.53‰) (Table 9A). This wider range in $\delta^{15}N$ observed across genera and species could be indicative that $\delta^{15}N$ is more enriched across subsequent trophic levels. The enrichment of $\delta^{15}N$ (~3‰) with increasing trophic level is greater than the enrichment of $\delta^{13}C$ (~1.0‰). Also surprisingly, higher $\delta^{15}N$ values were observed in non-migratory genera and species (6.64‰ to 8.71‰) than in migrators (0.01‰ to 8.47‰). The results of my study were not consistent with Richards et al. (2015) and Romero-Romero et al. (2019) in that both $\delta^{15}N$ and $\delta^{13}C$ increases were observed among deeper dwelling mesopelagic fishes. However, my data supports their results in that higher $\delta^{15}N$ was observed in non-migratory fishes. Lower $\delta^{15}N$ in migratory fishes could be a result of fishes feeding on prey from lower trophic levels. Furthermore, migratory fishes feeding from a phytoplankton-based food web will likely reflect lower $\delta^{15}N$ isotope signatures than fishes feeding from a POM based food web. Gut content analysis would be a complementary analysis to examining $\delta^{15}N$ isotopes to help determine if trophic level of prey consumed is indicative of $\delta^{15}N$ variability. Given the small size of these fishes and difficulty with identifying partially digested prey items, a metabarcoding approach to examining gut contents may be warranted.

For both $\delta^{15}N$ and $\delta^{13}C$, *Cyclothone pseudopallida* and *Cyclothone acclinidens* were statistically different from *Diaphus* spp. and *Electrona* sp. Both *Cyclothone pseudopallida* and *Cyclothone acclinidens* are classified as non-migratory fishes in the family Gonostomatidae, while *Diaphus* spp. and *Electrona* sp. are classified as migratory fishes in the family Myctophidae. Differences in isotopic signatures between these fishes could be a result of feeding from food webs with different bases and/or belonging to different trophic levels. In addition, from my samples, fishes from the genus *Cyclothone* were on average larger in standard length than fishes from the family Myctophidae. Larger fish could possibly explain the statistical differences in $\delta^{13}C$ and $\delta^{15}N$. My data is consistent with Romero-Romero et al. (2019) who found $\delta^{15}N$ increased in mesopelagic fishes residing in deeper depths, characteristic of non-migratory fishes. Unfortunately, species and genera specific SIA data $\delta^{13}C$ for mesopelagic fishes are scarce, which warrants future research to allow for comparing data.

With the trophic enrichment factor considered, the sampled fish genera and species of this study reflected $\delta^{13}C$ (-19.98‰ to -21.25‰) and $\delta^{15}N$ (3.81‰ to 8.71‰) values collected from sediment trap data ($\delta^{13}C$: -20.86‰ to -22.32‰; $\delta^{15}N$: 0.68‰ to 3.56‰). These results are

indicative of a sinking particle-based food web. Furthermore, with the trophic enrichment factor considered, $\delta^{13}C$ and $\delta^{15}N$ isotope signatures were also reflective of zooplankton ($\delta^{13}C$: -21.08 to -21.52‰; $\delta^{15}N$: 2.07‰ to 2.11‰) collected during the research cruise. The zooplankton sampled from the KM1910 cruise were collected in the upper 200m of the water column. As a result, fishes reflecting $\delta^{13}C$ consistent with zooplankton were likely migratory mesopelagic fishes feeding from a phytoplankton-based food web. Since we observe in $\delta^{15}N$ a 2.5‰ to 3.4‰ enrichment per trophic level and less than 1‰ enrichment per trophic level for $\delta^{13}C$ (McClain-Counts et al., 2017; Romeo-Romero et al., 2019), I can further confirm sediment trap data and zooplankton samples were indicative of mesopelagic fish prey items.

Stable isotope variability within an ecosystem helps determine if there are different prey sources for mesopelagic fishes, changes in trophic dynamics, and observation of spatial variability of the fish mediated carbon flux (Saba et al., 2021). As a result, comparing my results with other similar studies (Davenport and Bax, 2002) allows for the observation if spatial-temporal variability exists within the NPSG. Given these $\delta^{13}C$ and $\delta^{15}N$ enrichment factors, the POM and zooplankton data reported by Davenport and Bax (2002) was higher than the $\delta^{13}C$ and $\delta^{15}N$ isotope values in my sampled fishes. $\delta^{13}C$ and $\delta^{15}N$ change spatially and seasonally based on the availability of prey items and primary productivity at a time and location (Richards et al., 2020). If isotope signatures of $\delta^{13}C$ and $\delta^{15}N$ in POM flux changes, it would take weeks to months to reflect this change based upon tissue turnover rate in a fish (Bernal et al., 2015). Consequently, this finding may explain the difference between the data from the KM1910 cruise and from Davenport and Bax (2002). As a result, this observation supports the need to conduct SIA on mesopelagic fishes sampled throughout the year to note seasonal variation. In addition, unfortunately, I only had SIA data for a small sample of zooplankton captured in the study area. For future studies, additional zooplankton samples should be taken to increase the sample size and taken from deeper depths. This information would have been useful to interpret SIA results of $\delta^{13}C$ to make inferences of potential prey items. Knowledge of $\delta^{13}C$ isotope signatures in potential prey of mesopelagic fishes is needed to help determine the primary producer of mesopelagic fish food webs.

Based upon the results of this study and from others, there appears to be a host of factors that influence isotopic variability when considering the genera and species of a fish. These factors include size, age, foraging ecology, migratory status, and environmental factors. As a

result, future studies need to take these circumstances into account when determining fluctuations in $\delta^{15}N$ and $\delta^{13}C$ between genera and species. In addition, for future studies, a wider range of species would be beneficial to help observe any trends. Only three of the ten genera and species with a sufficient sample size for inclusion in statistical analyses were classified as non-migrators. As a result, it is hard to draw strong conclusions on genera and species variation with a limited sample size of migratory and non-migratory fishes.

2.6 Broader Implications

Interests in marine food webs have become of increasing interest in the marine science community. Food webs have allowed a deeper understanding of the structure and function of populations and ecosystems and are ultimately key to the development of successful ecosystem models. Mesopelagic fishes have been observed to be a link between primary producers and top predators, including commercially important species, such as tuna, sharks, and billfish (Annasawmy et al., 2020). In addition, mesopelagic fishes are believed to play a large role in ocean carbon sequestration via their vertical migratory patterns to feed (Davison et al., 2013; Boyd et al., 2019; Saba et al., 2021). As a result, there is a need to analyze mesopelagic fish behavior and ecology to further understand their role in energy flow through marine food webs. The understanding of mesopelagic fish behavior is essential from an ecosystem-based management perspective and may help shed light on ecosystem responses to pressures from fisheries and impacts from climate and environmental changes. With an estimated 1 billion tons of biomass worldwide (Irigoien et al., 2014), fisheries are seeking to be developed upon mesopelagic fishes as a potential food and nutraceutical source. Furthermore, as more mineral resources are depleted from land, there is pressure to open large areas of the deep sea for mining minerals. This activity has the potential to have detrimental impacts upon deep sea and mesopelagic ecosystems (World Resource Institute, 2023). The implications of exploiting these fishes warrants further investigation to understand the ecosystem and carbon cycling impacts of harvesting mesopelagic fishes (St. John et al., 2016). SIA is a useful tool for illuminating trophic position, energy flow of nutrients, and the primary producer of an organism's food web (Ben-David and Flaherty, 2012). The use of SIA provides an array of useful information to reveal the ecology of mesopelagic fishes and can expose shifts in diet, habitat, and trophic level. Furthermore, many variables, such as location, salinity, prey type, water depth, body size, and health/age of an organism, can lead to variation in SIA (Romero-Romero et al., 2019). As a

result, it is important for scientists to understand what variables impact isotope signatures in order to properly interpret SIA results.

2.7 Conclusion

In summary, a suite of factors likely influenced the differences in $\delta^{13}C$ and $\delta^{15}N$ in mesopelagic fishes in this study. Variation in isotopes among mesopelagic fishes was related to fish size (length/weight), depth, and migratory status. Deeper dwelling non-migratory species typically reflected higher $\delta^{15}N$, which supports previous research that these fishes feed on a sinking particle-based food web. Furthermore, the conclusion can be drawn that there is a positive correlation between increasing fish size (length/weight) and more enriched $\delta^{13}C$ and $\delta^{15}N$ values. Variation in time of day of $\delta^{13}C$ and $\delta^{15}N$ warrants further investigation since SIA results did not reflect daily changes in this study. As a result, other methods to investigate mesopelagic fish feeding behavior based upon time of day may be more practical due to the integration time needed for SIA to reflect any changes in feeding behavior. Competition for prey items may be a contributing factor in time-of-day variability in $\delta^{13}C$ and $\delta^{15}N$. Fishes may be forced to seek depths outside of their normal range to forage when food is scarce, thus possibly leading to more competition for prey when these fishes overlap with other organisms in the newly sought out depth. Variation between genera and species is likely attributable to a combination of the previously mentioned factors. Furthermore, my results support that the genus *Cyclothone* dominates the mesopelagic fish community. Dominance of *Cyclothone signata* in our sample population at all times of day was likely the cause of lack of isotopic variation in daytime variability of $\delta^{13}C$ and $\delta^{15}N$. Sampling different areas in the NPSG and sampling across different seasons would support that the dominance of *Cyclothone signata* was our reason for lack of isotopic variability between day and nighttime sampling in the mesopelagic fish population in the NPSG. Also, there is a need to conduct further research examining trophic variations among different life stages of species, identify prey items, and observe seasonal variability to properly make a determination of food web pathways and the trophic level of mesopelagic fishes.

Chapter 3: Preservation method analysis and allometric equation development

3.1 Introduction

In this chapter, I will discuss how to potentially calculate fish-mediated carbon flux using gut content analysis and stable isotope analysis (SIA). The purpose of this document is to provide an explanation of how to calculate the amount of carbon potentially egested as fecal pellets from the carbon in the gut contents of the mesopelagic fishes using the concept of allometry. These calculations can be used to estimate the amount of carbon mesopelagic fishes potentially contribute to the carbon flux in the NPSG. I will also examine how the storage of my samples in ≥70% ethanol may have an impact on my SIA results. Therefore, I will analyze the effects of ice and ethanol-based preservation on estimation of $\delta^{13}C$ and $\delta^{15}N$ ratios and bulk carbon and nitrogen content in fish tissues examined using SIA This analysis will reveal if a correction factor is needed to account for changes in isotopic ratios or carbon content due to ethanol preservation of my samples.

Mesopelagic fishes play a large role in the marine food web due to their high abundances, vertical migratory behavior, and world-wide distribution (McClain-Counts et al., 2017). Mesopelagic fishes consume 5-10% of daily zooplankton production (McClain-Counts et al., 2017). A portion of this energy is transferred to higher trophic levels when larger predatory species, such as tuna, consume mesopelagic fishes (John et al., 2016). These energy-dense fishes have been recorded in the diets of cephalopods, elasmobranchs, piscivorous fishes (including tuna, salmon, and groundfish species), seabirds, pinnipeds, and cetaceans (Iglesias et al., 2016). Many species in this group of fishes undergo a process known as diel vertical migration (DVM), in which mesopelagic fishes migrate to the surface at night to feed and retreat to a deeper depth during the day to avoid predation. However, mesopelagic fishes are vulnerable to predation due to daytime, diving predators and nocturnal predators foraging near the surface (Iglesias et al., 2016). DVM has been observed to be a major mechanism of carbon transport from the pelagic layer of the ocean to deeper ocean depth where the carbon can be stored (Davison et al., 2013 and John et al., 2016). Due to their large biomass, mesopelagic fishes as a guild are believed to be a large contributor in the biological component of the carbon cycle known as the "biological pump." The term "biological pump" includes several biological processes, starting with activity associated with converting dissolved CO_2 into oxygen and organic matter through

photosynthesis. The biological pump also includes the transformation of carbon through food web processes, physical mixing, and gravitational settling (Nagaraja, 2020). However, the amount of carbon that is sequestered in the ocean column and seafloor by these processes is not well-established (Davison et al., 2013, McClain-Counts et al., 2017, Boyd et al., 2019, and Saba et al., 2021). Most previous studies focus on the role of the surface and upper layers of the ocean in carbon sequestration due to difficulty in sampling the mesopelagic zone (Cavan et al., 2019).

Mesopelagic fishes are a poorly understood group of organisms due to their relative lack of research and low commercial value (Salvanes and Kristoffersen, 2001; St. Johns et al., 2016). In addition, mesopelagic fishes tend to avoid net capture and are a difficult group of organisms to study in a lab setting since their migratory feeding patterns are a challenge to recreate in a lab (Anderson et al., 2018). Non-migratory mesopelagic fish species are also not thoroughly researched primarily due to the challenges of sampling the mesopelagic zone (Romero-Romero et al., 2019). Furthermore, recreating an experimental setting resembling the mesopelagic zone is challenging due to the need to maintain the high-pressure environment non-migratory fishes are accustomed to (Saba et al., 2021). There is need for research to investigate the magnitude of the contribution of mesopelagic fishes to the carbon flux as a result of their migratory behavior. Past studies have focused on the passive flux component of carbon sequestration and fail to study active transport of carbon mediated by migratory fishes and other marine organisms (Davison et al., 2013; Saba et al., 2021). It is this migratory behavior of mesopelagic fishes that drives a major component of the active carbon flux. To improve parameterization in regional and global coupled carbon-climate earth system models, it is important for scientists to understand all the processes that impact the biological pump (Saba et al., 2021). Furthermore, a baseline assessment of the relative contribution of mesopelagic fishes to the biological pump is needed to understand the rate and magnitude of fish-mediated carbon export and how climate change stressors and changes in food quality and quantity may alter these processes (Saba et al., 2021). There is an increased need for understanding how the biological pump will respond to increased atmospheric carbon input and warming. For this reason, fish mediated carbon transport will provide an avenue to measure temporal changes in particulate organic carbon (POC) flux to the ocean interior.

To decipher how much carbon is potentially stored in the stomach contents of mesopelagic fishes too small to dissect (<30 mm), allometry will be utilized. Allometry is a scaling relationship between the size of one body part and the size of the body as a whole (Shingleton, 2010). Essentially, body mass or size can be used to predict the size of another body part. However, recently scientists have expanded to allometry to include other scaling relationships among ecological (example: bird wing size and flight performance) and morphological traits (example: brain and body size in adult humans) (Shingleton, 2010). Coupling the principles of allometry with the nutritional requirements of an organism lends to explanation in variations in physiological mechanisms, individual behaviors, population dynamics, and evolutionary patterns (Arhonditsis et al., 2019). When plotting morphological allometric relationships on a log-log scale, they tend to have a linear form. Therefore, many allometric relationships can be described using the equation:

Equation #1 $\log y = a \log x + \log b$ **or** $y = bx^a$

where x is body size or mass, y is the morphological, ecological, or physiological trait being studied, and a and b are estimated parameter values. After log transformation, log b is the y-intercept of the linear relationship and a is the slope of the line (Shingleton, 2010; Klingenberg, 2016).

Although allometry proves to be a useful scaling relationship to predict size or mass of body part, there are several cautions scientists must heed to its use. Generally, allometry has been applied in lab-based settings and often studies have a small sample size; thus, real life settings and variations are not always accounted for (Arhonditsis et al., 2019). Allometric relationships applied to organisms in the natural world assume a community operating at a maximum physiological or metabolic rate in a resource saturated environment (Klingenberg, 2016). In addition, studies have found that body form, prey selection, and habitat of any given species are strongly related. In general, pelagic and benthopelagic fish species are observed to have a stream-lined body shape, while reef-associated species are more rounded, and demersal species have compressed (both dorsoventrally and laterally) bodies. As a result, this body form/habitat adaptation has an impact on weight to length ratios of fishes and other aspects of allometry among fishes (Paraskevi and Konstantinos, 2012). Expanding sample size and employing taxon-specific allometric equations may improve the predictive powers of allometry.

Mesopelagic fishes were sampled during a research cruise at station ALOHA (A Long-Term Oligotrophic Habitat Assessment) in the summer of 2019. Station ALOHA is a 6-mile diameter area located approximately 100 km north of Oahu, Hawaii in the NPSG. The sampled fish from station ALOHA can be utilized to understand the role of vertically migrating fish in carbon transport. To measure fish-mediated carbon export, I planned to utilize stable isotope analysis to measure carbon in the gut contents and stomach lining of the Hawaiian and North Carolinian fishes. Not only can stable isotope analysis reveal carbon in the gut contents, but it also provides information on a species' trophic level and primary food source (Ben-David and Flaherty, 2012). Gut contents were obtained by extracting the stomach contents from the stomach lining via dissection. The mesopelagic fishes captured during the cruise were very small, many less than 30 mm in total length (Figure 1). As a result, size limitations may impede separation of the stomach lining and gut contents, requiring removal and use of the whole stomach in SIA for the Hawaiian fish samples. In that case, I hypothesized that I could estimate the amount of carbon in fish stomachs by determining the allometric relationship between fish size/weight and the carbon biomass in the stomach lining using a variety of fish species sampled in Beaufort, NC to develop this initial allometric relationship. Presuming generalizability across species (Duque-Correa et al., 2021 and Lindstedt and Schaeffer, 2002), an allometric relationship from Beaufort samples could be used to derive a formula for estimating carbon content in the stomach lining of Hawaiian fishes, so that I could quantitatively estimate the amount of remaining carbon in gut contents after excluding the stomach lining. Here I assess the strength of the relationship between fish size/weight and the carbon content of the stomach contents and stomach lining. A $p \leq 0.05$ and $R^2 \geq 0.50$ was deemed to be the baseline for identifying a strong statistical relationship (Dormann et al., 2013). Due to their large biomass as an ecological guild, I anticipate mesopelagic fishes play a substantial role in providing a pathway to sequestering carbon into the deep ocean.

Local fishes used to build the allometric equation were preserved in ≥70% ethanol. Since we used SIA to determine carbon content in the stomach lining, we needed to assess if there was a significant impact from ethanol on the carbon content in the gut contents and stomach lining in our fish samples. Lipids are highly depleted in $\delta^{13}C$ and enriched in $\delta^{12}C$ in comparison to carbohydrates and muscle tissue (Jesus et al., 2015). Ethanol has been observed to enrich muscle tissue in $\delta^{13}C$ due to ethanol's lipid extraction effect on an organism's tissue (Jesus et al., 2015;

Sweeting et al., 2007; Yongfu et al., 2023). As a result, lipid extraction should be performed on tissue samples to minimize the impacts of $\delta^{13}C$ enrichment of a tissue from ethanol. Variability in lipid content in a sample has the potential to confound SIA results for $\delta^{13}C$ (Jesus et al., 2015; Yongfu et al., 2023). The range of enrichment values for ethanol has been observed to be 0.6-1.5‰, irrespective of preservation time. This range has been found to be similar for ants, octopus, kelp, fish muscle and liver, zooplankton, and bird tissues (Jesus et al., 2015).

Since ethanol could cause tissue hydrolysis and leaching, 70% ethanol may also extract certain constituents containing nitrogen from the muscle tissue in addition to lipids (Horii et al., 2015). As a result, ethanol may alter $\delta^{15}N$ isotope ratios in tissue samples (Horii et al., 2015; Jesus et al., 2015). Previous studies have shown conflicting results on the impacts of ethanol preservation on $\delta^{15}N$ in animal tissues. Although ethanol cannot add $\delta^{15}N$ to a sample, it can alter stable isotope ratios by breaking bonds with nitrogen atoms in tissues (Hajisafarali et al., 2023). Some studies have reported negligible impacts of ethanol preservation upon $\delta^{15}N$ isotopes (Sarakinos et al., 2002; Jesus et al., 2015; Hajisafarali et al., 2023), while others have reported increases in $\delta^{15}N$ in various tissues (Sweeting et al., 2004; Yongfu et al., 2023). Variation in $\delta^{15}N$ in response to ethanol preservation could be attributed to type of tissue sampled and could vary between species. Nonetheless, past research has shown that lipid extraction and using tissues with low lipid content help minimize the degradation impacts of ethanol on $\delta^{15}N$ isotope ratios (Horii et al., 2015; Jesus et al., 2015; Yongfu et al., 2023).

3.2 Preservation Analysis Hypothesis

At the outset of this study, I anticipated minimal alteration of both $\delta^{13}C$ and $\delta^{15}N$ due to using stomach lining to study the impacts of ethanol upon $\delta^{13}C$ and $\delta^{15}N$. Fish stomach lining has a low lipid content (Moraes and Christina de Almeida et al., 2020) and therefore should be enriched in $\delta^{13}C$ and $\delta^{15}N$ isotopes. I expect to see a greater enrichment impact of ethanol on $\delta^{13}C$ than $\delta^{15}N$ due to ethanol containing carbon in its composition and lacking nitrogen (Sweeting et al., 2004). I further predicted a wide variability in enrichment in both $\delta^{13}C$ and $\delta^{15}N$ isotopes in the fish's gut contents. Bay anchovies, sampled from Goose Creek State Park in Washington, NC, were the chosen species to conduct the preservation analysis upon. The bay anchovies likely have varying prey items in their guts, which would result in a variation in $\delta^{13}C$ and $\delta^{15}N$ isotope based upon the lipid content of their prey (Davenport and Bax, 2001; Jesus et

al., 2023; Yongfu et al., 2023). Bay anchovies feed primarily upon zooplankton (primarily copepods), krill, fish eggs, mollusk larvae, and fish larvae (Chesapeake Bay Program, 2023). Prey with higher lipid content, such as copepods, will result in greater enrichment of $\delta^{13}C$ and $\delta^{15}N$ from ethanol than prey with a lower lipid content (Vander Zanden and Rasmussen, 2001; Sweeting et al., 2004).

3.3 Methods

3.3.1 Allometry

Many of the Hawaiian mesopelagic fishes from the research cruise are very small, with most fishes measuring <30 mm. The size of these fishes poses the challenge for dissecting and separating stomach contents from the stomach lining to be prepared for SIA. Separation of these is needed to quantify carbon transport to depth since this is related to the carbon biomass of the fish gut contents, but not the stomach lining. To deal with this challenge, I developed an allometric relationship with fishes captured and dissected locally from three locations in North Carolina (Table 1). I utilized equation 1, as described previously, to assess allometric relationships, where:

$$\log y = a \log x + \log b \text{ or } y = bx^a$$

y is carbon in the stomach lining, a and b are estimated parameter values, and x is the size (biomass or length) of the fish (Enquist et al., 1998). From this equation, I can calculate carbon in the fishes' stomach lining when unknown (i.e., among fish of small sizes) and subtract that amount from total carbon of whole fish stomachs to determine carbon in the fish's gut content. Two separate allometric equations were developed, one where x was defined in terms of weight and another where x was based on length. The equation with the best fit across species can be applied to the fishes collected from Station ALOHA. I used Microsoft Excel to perform a log-transformed linear regression on the data to obtain estimates of parameters for the allometric equation. This allometric relationship would be used solely among fishes from station ALOHA that are too small to separate their gut contents from the stomach lining. In other cases, I could measure the carbon found in gut contents directly as described below.

3.3.2 Assessment of Preservation Methods upon SIA Results

North Carolina fish samples from Beaufort, NC were preserved in 90% ethanol as per the protocols used by the Beaufort Inlet Ichthyoplankton Sampling Program (BIISP) (Thaxton et al., 2020). Local samples were collected under the IACUC Animal Use Protocols (AUP) D361 and D379. Isotopic composition of the carbon in ethanol (C_2H_6O) may impact the isotopic composition of carbon in the fish gut contents as reflected in SIA results (Hajisafarali et al., 2023; Yongfu et al., 2023).

To determine the effect BIISP's ethanol preservation on isotopic composition of fishes, I collected additional fishes, half of which were preserved on ice and stored in the freezer at -20º C and the other half of which were preserved in the same manner as BIISP. This provides a basis for isolating the ethanol effect on isotopic composition.

For this purpose, fishes were collected for preservation method analysis at Beaufort Inlet and Goose Creek State Park located near Washington, NC. Fishes from Goose Creek State Park were sampled using a beach seine net. Seine netting involves deploying a net, typically made of nylon netting, and extending the net near shore to form a circle shape. Next both ends of the net were drawn ashore to target schools of fishes in nearshore waters. The seine net had light contact with the floor of the water body due to seine netting having the potential to stir up sediment and drag any debris in its path. A seine net with a mesh size of ~1/2-inch was used to target juvenile fish species. The seine net was dragged from 15-20 feet from shore to the beach, which took approximately 5 minutes. Fish remained in the net for up to an additional 20 minutes until samples of target species were processed and non-target species were released. Four tows were conducted to obtain my desired sample size for this analysis.

For the preservation analysis, fishes of various sizes and species were collected to be taken back to the lab (Howell Science Complex at East Carolina University) for dissection. Juvenile bay anchovies (*Anchoa mitchilli*) and Atlantic croaker (*Micropogonias undulatus*) were the predominant species collected. Not enough Atlantic croakers were captured to obtain a significant sample size (≥20 fish); therefore, only bay anchovies were used in the preservation-method analysis. Bay anchovies ranged in standard length of 45-55 mm and a weight range of 0.92-1.87 g. A sample size of 22 fish (9 ice preserved and 13 ethanol preserved) were used for

the ice vs. ethanol preservation analysis. The stomachs of the ice preserved fish were removed, and stomach contents were separated from the lining. The ice preserved fish stomach lining and gut contents were prepared for SIA. Samples were weighed and dried in a drying oven at 55°C for 1-2 days. The drying duration needed depended on sample pre-dried weight. Samples were dried until the sample's weight stabilized to ensure all moisture had evaporated. Weight measurements were conducted after 24 hours and reweighed after another 2 hours to ensure all moisture had evaporated. None of the samples needed further drying time after 26 hours of drying. Next, the samples were encapsulated in the Mitra lab at East Carolina University. Each sample was weighed to be at least 0.5 mg. All samples (n=20) required 2-3 fish to obtain the minimum sample weight for SIA (0.5 mg). Samples were pooled together based upon same preservation method (ice or ethanol) and sample contents (stomach lining or gut contents). Pooling samples involved grinding the samples with a mortar and pestle before the encapsulation process, which I will discuss below. Samples were sealed in a 96-well tray and sent to UNC-Wilmington for SIA analysis. Results from SIA for the ice and ethanol preserved samples will determine the degree ethanol affects the isotopic composition of carbon in these samples. If ethanol does not have a significant bearing upon carbon biomass and $\delta^{13}C$ in the samples, then I will be able to use previously dissected samples from BIISP for my research to determine the allometric relationship. However, should ethanol have a significant impact on carbon values, then new fish samples would need to be collected for dissection and will be preserved on ice instead of ethanol.

3.3.3 Fish Dissection Methods

To establish the allometric relationship, I dissected North Carolinian fishes. The fish species to be used in dissections were identified based upon body shape such that they are similarly shaped to the fishes sampled at station ALOHA. Additionally, a variety of sizes within a fish species were selected to help develop a strong allometric relationship. I selected Atlantic silversides (*Menidia menidia*), bay anchovies (*Anchoa mitchilli*), and naked gobies (*Gobiosoma bosc*) as the local fishes to build the allometric relationship.

I dissected 37 silversides, 75 bay anchovies, and 41 naked gobies to assess the presence of an allometric relationship. The fishes were weighed using a Mettler Toledo scale (precision of 10^{-3} g). Fish samples were blotted with kim wipes to remove excess moisture. After weighing,

the fishes were measured using standard length and divided into length classes. The following length classes were assigned: 6-10 mm, 11-15 mm, 16-20 mm, 21-25 mm, 26-30 mm, 31-35 mm, 36-40 mm, 41-45 mm, 46-50 mm, and 51-55 mm. The fish number, weight (in grams), standard length (in millimeters), and percent fullness of the stomach <25%, 25%, 50%, or >75% were logged in a Microsoft Excel spreadsheet.

During the dissection process, whole stomachs were removed, and the gut contents were extracted. Fish were dissected using micro-scissors in which the fish was cut along the bottom from the vent to the operculum. A cut was then made from the vent up towards the vertebra. Another cut was made towards the vertebra at the other end of the first cut; these two cuts will form a flap. The flap was removed with micro-scissors to expose the body cavity. Organs surrounding the stomach were removed with micro-scissors and forceps. The intestines were uncoiled and pulled from the body cavity to allow ease in visibility as to where to separate the stomach from the intestines and from the base of the esophagus. The stomach was placed into a petri dish where using micro scissors a cut from one opening of the stomach to the other opening was made to flay out the stomach wall into one panel. Forceps were used to hold the stomach lining in place. An angled probe was used to carefully scrape the gut contents from the stomach lining. Using a plastic pipette, a few drops of water was used to flush out gut contents from the stomach lining. The stomach contents were pipetted up from the petri dish and placed into a 2-ml glass vial, while the stomach lining was placed into a separate 2-ml glass vial. Glass vials were ashed at 450°C. The vials were labeled with date of collection, species name, fish number, and "gut contents" or "stomach lining." The vials were stored in a -20° C freezer in the Asch lab until the encapsulation process.

3.3.4 Encapsulation

To prepare samples for SIA, the fish stomach linings and gut contents must undergo an encapsulation process after drying in the drying oven. Encapsulation occurred in the 233 Science and Technology Building in Dr. Siddhartha Mitra's lab. The dried stomach contents and stomach lining were separately ground with a mortar and pestle. Samples were weighed using an analytical balance with a precision of 10^{-6} g. Under the guidelines of the stable isotope lab at the University of North Carolina – Wilmington (UNCW), each sample must weigh >0.5 mg dry

weight for $\delta^{13}C$ analysis. A range of 0.5-1.5 mg of sample can be accommodated for conducting both a $\delta^{13}C$ and $\delta^{15}N$ analysis. For the North Carolinian fishes, only $\delta^{13}C$ analysis was needed to test for an allometric relationship in the samples. $\delta^{13}C$ was only measured since the goal of this analysis was to build an allometric relationship to measure carbon in the fishes gut contents to estimate fish-mediated carbon transport by mesopelagic fishes. As a result, measurements of $\delta^{15}N$ were not needed for the allometric analysis. Multiple fish samples (~2-4 fish) were pooling to make the minimum sample weight requirement. When pooling was necessary, fish of the same species and length class were pooled together.

Encapsulation of samples followed the UNCW protocol. Samples were encapsulated in tin capsules that were placed in a 96 well tray for analysis. To wrap samples in the capsule, the tin capsule was placed on the analytical balance and tared to zero. The dry sample was scooped into the capsule to a weight of ~0.5 mg. Using small, curved forceps, the top of the capsule was crimped closed. The capsule was laid on its side and crimped using forceps and an angled probe to form a sphere, being sure to pinch down any angled edges. The crimped capsule was placed into one of the wells in the 96 well tray. Samples were loaded across rows with each row fully populated. Weights of each sample in the well tray were recorded to submit for SIA. A blank capsule of foil was placed every six wells to reveal any sources of error that may occur during the analysis. Records of the location of the blank samples in the well tray were noted. Samples were secured by placing an index card over the open wells before the lid was secured. The lid was securely closed with tape on all four sides. Next, the sealed tray was turned over and shaken to observe if any samples leaked from the capsule. Any leaky capsules were re-encapsulated before shipping to the UNCW lab.

3.3.5 Stable Isotope Analysis

Samples were shipped to the UNCW stable isotope lab for SIA. A Costech 4010 Elemental Analyzer paired with a Thermo Delta V plus continuous flow mass spectrometer was used to analyze samples (Reidhaar et al., 2015). The samples were combusted at 1,000° C in a reactor packed with chromium oxide and silvered copper oxide. After combustion, oxides were removed in a reduction reactor (reduced copper at 650° C). A chemical water trap (magnesium perchlorate and phosphorous pentoxide) was required to remove excess water vapor generated during combustion. Before entering the spectrometer, N_2 and CO_2 were swept over a helium

carrier gas stream to be separated on a Carbosieve gas chromatography (GC) column (65° C, 65 mL/min) (Reidhaar et al., 2015).

During analysis, samples were interspersed with at least four different reference materials that have been calibrated against recognized international reference materials including: IAEA-600, USGS-40, USGS-41, USGS-42, USGS-43, USGS-61, USGS-64, and USGS-65. The sample's existing isotope ratio was measured relative to a reference gas peak analyzed with each sample. These values were finalized after correcting the values of the entire sample batch against known values of the laboratory reference materials. Standard deviation of isotopic values for $\delta^{13}C$ and $\delta^{15}N$ depended upon the international reference used; however, standard deviation of isotopic values was typically ± 0.2 ‰ for $\delta^{13}C$ and ± 0.3 ‰ for $\delta^{15}N$. For our SIA data, USGS-40 and USGS 41 reference materials were used for $\delta^{13}C$ and $\delta^{15}N$ and the spectrometer reported a standard deviation of ≤ 0.1‰ for both $\delta^{13}C$ and $\delta^{15}N$ .All carbon and nitrogen isotopic compositions were reported in standard δ–per mil notation and were delivered as an expression relative to the international standards VPDB (Vienna Pee Dee Belemnite) and air for carbon and nitrogen, respectively (Reidhaar et al., 2015).

3.3.6 Data Analysis

a. Impacts of preservation method on SIA analysis

To assess if preservation method (ice or ethanol) had an impact on $\delta^{13}C$ content in fish tissue, descriptive statistics were calculated using Microsoft Excel. Analysis of preservation method impact on fish tissue was also performed on $\delta^{15}N$ content. Descriptive statistics were calculated using both fish stomach lining and gut contents for ice and ethanol preserved samples to assess if carbon in ethanol had a significant impact on $\delta^{13}C$ content on the sampled fish. From the descriptive statistics, I obtained the mean, standard deviation, standard error, and 95% confidence intervals for $\delta^{13}C$ and $\delta^{15}N$ content in ethanol and ice preserved samples of bay anchovy stomach linings and gut contents. Descriptive statistics were also performed on milligrams of carbon and nitrogen in my samples to further assess if ethanol had an impact on SIA results. This analysis was conducted since this parameter would be used to build the allometric relationship between grams of carbon in the stomach lining and biomass of the fish.

b. Allometry analysis

Only the stomach lining SIA results were used to assess the allometric relationship because our goal was to filter out excess carbon contained in the stomach lining among smaller size classes of fishes. Fish body mass, length, and milligrams of carbon in the stomach lining were log-transformed in Microsoft Excel. For samples that had multiple fish pooled together, an average was taken on weight, length, and total milligrams of carbon prior to log transformation. Next, a one-way ANOVA test and linear regression were conducted for fish body mass and fish length for each species of North Carolinian fish to assess if there was a strong relationship between these factors in relation to carbon content (mg) in the fish stomach lining. Additionally, linear regression was performed to obtain the intercept and slope coefficients needed to build the allometric relationship. An R^2 value ≥ 0.50 and a p-value ≤ 0.05 were deemed to be the level of statistical significance needed for a reliable allometric relationship (Dormann et al., 2013). Due to the variability of sizes and species of fishes used in this study, a regression where at least 50% of the data was explained was considered a strong relationship. Should a strong relationship exist, we would need to analyze if the relationship was the same or different across species due to the difference in species composition between the NPSG versus North Carolina. A relationship independent of species is needed to facilitate the use of the allometric relationship when examining NPSG fishes. To assess relationship across species, we would need to compare regression coefficients of each species and their standard errors to check if 95% confidence intervals overlapped or not across species.

3.4 Results

3.4.1 Preservation Method Analysis

Due to pooling of fish samples to obtain the minimum weight for SIA, I was only able to analyze seven samples for the ethanol preserved fish and nine samples for the ice preserved fish. Each sample contained the dried stomach linings and gut contents of approximately 2-3 fish.

The results of analyzing the impact of ethanol [mean (95% confidence intervals) = 0.089 (±0.038) mg] and ice preservation [mean (95% confidence Intervals) = 0.153 (±0.059) mg] on nitrogen content in the gut contents of the bay anchovies demonstrate an overlap in 95% confidence intervals. This suggests no statistically significant relationship between the two means (Table 2, Figure 2A). Nitrogen content in the stomach lining in ethanol and ice preserved

samples also presented a 95% confidence overlap; thus, there is no significant difference between the ice and ethanol preserved stomach linings (Table 3, Figure 2A).

Ethanol preserved gut contents [mean (95% confidence intervals) = 0.369 (±0.215) mg] did overlap in 95% confidence intervals with ice preserved gut contents [mean (95% confidence intervals) = 0.765 (±0.338) mg] in carbon content to provide evidence there is not a statistical difference in ice and ethanol preserved gut contents (Table 2, Figure 2B). In addition, there is some overlap in 95% confidence intervals of ethanol preserved stomach lining [mean (95% confidence intervals) = 0.233 (±0.157) mg] with ice preserved stomach lining [mean (95% confidence intervals) = 0.378 (±0.798) mg] in carbon biomass to suggest there is no statistical difference between these two groups (Table 3, Figure 2B).

The results of impacts on preservation method on $\delta^{13}C$ on gut contents in ice [mean (95% confidence intervals) = -25.33‰ (± 4.23)] and ethanol [mean (95% confidence intervals) = -25.42‰ (± 0.91)] preserved samples presented an overlap in 95% confidence intervals to suggest there is no statistical difference between ice and ethanol preserved gut contents (Table 4, Figure 3A). However, average $\delta^{13}C$ values between ice [mean (95% confidence intervals) = -25.98‰ (± 0.68)] and ethanol [mean (95% confidence intervals) = -24.54‰ (± 0.68)] preserved stomach linings in bay anchovies displayed no overlap in 95% confidence intervals to conclude that there is a statistical difference in $\delta^{13}C$ between ice and ethanol preserved stomach linings (Table 4, Figure 3A). There was an observed $\delta^{13}C$ enrichment of 1.443‰ from ethanol in bay anchovy stomach lining.

$\delta^{15}N$ in ice [mean (95% confidence intervals) =10.24‰ (±2.61)] and ethanol [mean (95% confidence intervals) = 9.50‰ (±0.36)] preserved gut contents presented an overlap in 95% confidence intervals to suggest no statistical difference in the means of these samples (Table 5, Figure 3B). There is also an overlap in 95% confidence intervals between ice and ethanol preserved stomach lining; as a result, no statistical difference exists between $\delta^{15}N$ content in ice [mean (95% confidence interval) = 10.42‰ (±0.30)] and ethanol [mean (95% confidence interval) = 11.02‰ (±0.69)) preserved stomach linings (Table 5, Figure 3B).

The results of the preservation analysis did not present a statistical difference in average carbon content (mg) for both the gut contents and stomach lining. I observed a larger difference between the means of ice preserved gut contents and ethanol preserved gut contents versus the

ice and ethanol preserved stomach lining samples (Figure 2B). Nonetheless, these averages between categories were statistically insignificant. As expected, there was little impact on preservation method on average nitrogen content (mg) for both the ice and ethanol preserved samples (Figure 2A). No statistically significant relationship was observed in any of the preservation method categories. Furthermore, I observed either no difference or very minor differences in means of $\delta^{13}C$ and $\delta^{15}N$ in both ice and ethanol preserved stomach lining and gut contents (Figure 3A-B). This observation concluded ethanol only presented a minor statistically significant relationship in the impact of $\delta^{13}C$ enrichment in the fish stomach lining; all other preservation method categories were statistically insignificant.

3.4.2 Allometry Analysis

The Atlantic silversides had a total sample size of 19. A total of 37 silversides were dissected; however, multiple fish were needed to be pooled to obtain the minimum SIA weight (0.50 mg) (Table1). A positive trend can be observed in the log transformed carbon content and, in both length, and weight of the fish (Figure 4A-B). The results of the linear regression revealed the relationship between fish weight and length and carbon content to possess a relationship of statistical significance (Table 6). However, the low R^2 score and visualization of the regression data (Figure 4A-B) reveal a widespread range of the data and weak linear relationship. The amount of explained variance (i.e., the R^2) was very similar between milligrams of carbon in the stomach lining and length and weight of the silversides (Table 6). Consequently, length or weight did not meet the threshold of desired explanation of variance ($R^2 \geq 0.50$). As a result, there is not a close enough relationship between fish length and weight and carbon content in the stomach lining to justify use of an allometric relationship in Atlantic silver sides.

Bay anchovies had a total sample size of 37. A total of 75 anchovies were dissected; however, multiple fish were needed to be pooled to obtain the minimum SIA weight (0.50 mg) (Table 1). The bay anchovies demonstrated a positive trend in log transformed carbon content with both length and weight of the fish (Figure 5A-B). The results of the linear regression revealed the relationship between both fish weight and length and carbon content to not have a relationship of statistical significance (Table 6). In addition, the bay anchovies had a low R^2 score (Table 6) and the visualization of the data (Figure 5A-B) revealed not a strong enough relationship to justify using allometry to estimate carbon content of the stomach lining in small-

sized fish. Like the Atlantic silversides, the bay anchovies also possessed a very similar R^2 between length and weight. Thus, one indicator of fish size did not outweigh the other in terms of strength of relationship to carbon content in the fish's stomach lining (Table 6).

The naked gobies had a total sample size of 15. A total of 41 anchovies were dissected; however, multiple fish were needed to be pooled to obtain the minimum SIA weight (0.50 mg) (Table 1). The naked gobies also followed the trend seen in other species where length or weight had similar strength of relationships with carbon in the stomach lining (Table 6). The results of the linear regression revealed the relationship between both fish weight and length and carbon content to have a statistically significant relationship (Table 6). The naked gobies also presented a positive relationship between fish length, weight, and log transformed carbon content in the stomach lining (Figure 6A-B). Like the other examined fish species, the low R^2 score, and visualization of the data (Figure 6A-B) did not exhibit a strong enough allometric relationship to justify extrapolating this relationship between fish length and weight and carbon in the stomach lining to examination of NPSG fishes.

3.5 Discussion

3.5.1 Preservation Method

The results of the preservation method in bay anchovies revealed inconclusive results upon carbon and nitrogen content (mg) in their gut contents and stomach lining (Figure 2A-B). The overlap in confidence intervals between the ice and ethanol gut contents and stomach lining showed no statistical difference. I expected carbon content to be higher in both the stomach lining and gut contents of the ethanol preserved samples due to the addition of carbon from the ethanol. These results could be attributed to variation in carbon content in the prey items of the fish and the weight of the gut content samples in relation to stomach lining samples when preparing the samples for SIA. For both the ice and ethanol preserved gut contents, the weight of the samples encapsulated for SIA tended to be heavier than the stomach lining samples. For replicate studies, to correct this error the samples could be standardized by dividing the carbon content by total weight of the sample. It is difficult to draw a definite conclusion on whether ethanol has an impact upon carbon content in fish tissue due to the wide variation in the SIA results. A larger sample size and variation of species used would help in future studies to draw a

more determinate conclusion. However, it must first be established if variability is attributed to the variation in biomass of the gut content samples and difference in prey items of the fishes. Another recommendation to minimize any cofactors that would influence carbon content in the fish's gut contents would be to conduct a lab-based experiment on fishes fed a diet of only one prey item.

There was a lack of published research to address the impact of preservation methods upon carbon content in organic samples. A few studies address the impact of preservation method upon $\delta^{13}C$, which I will address below. To avoid further error, attention to keeping the weight of the sample being encapsulated consistent (0.5-1.0 mg) as much as possible should be noted. This correction may help reduce variability between samples in SIA results.

As expected, nitrogen content (mg) experienced little variation from impact of preservation method (Figure 2A). The nitrogen content of ice preserved gut contents was slightly higher than the ethanol preserved gut contents, but confidence intervals between these measurements overlapped ultimately indicating no difference between them. The ethanol and ice preserved stomach linings showed very little difference in nitrogen content, which confirms nitrogen content is not altered when preserved in ethanol. There are little to no published studies examining the impact of preservation methods upon nitrogen content so these results are novel and may provide a baseline for future research on this topic.

The results of preservation method upon $\delta^{13}C$ in the stomach lining and gut contents revealed very similar means between the samples to suggest ethanol has a minimal impact upon SIA results (Figure 3A). Although the stomach lining displayed some enrichment in $\delta^{13}C$ from ethanol, the shift was slight and not significant for gut contents. However, the slight carbon enrichment of ethanol in the stomach lining was deemed statistically significant. The difference between the lower (-25.30‰) and upper (-25.21‰) confidence intervals between the ice and ethanol samples was ~0.1‰. This small difference is likely not biologically significant and is close to the detection limits of the spectrometer. The negligible impact of ethanol upon samples is likely due to the low lipid content of stomach lining and potentially low lipid content of the prey items in the gut contents. The lipid extraction from ethanol in muscle tissue has the potential to confound SIA results (Horii et al., 2015). However, stomach lining is a low-lipid muscle tissue (Sweeting et al., 2004). This finding is consistent with the literature in that organic

samples with low lipid content displayed minimal-to-no $\delta^{13}C$ enrichment from ethanol (Sweeting et al., 2004; Carabel et al., 2009). Edwards et al. (2002) also states that in many ecosystems, a carbon source can differ by greater than 2‰. If carbon sources are isotopically different by more than 2‰, a shift of less than 2‰ due to preservation may not alter any results substantially in such ecosystems. In my study, mean $\delta^{13}C$ shifts between ice and ethanol preserved samples were not greater than 1.443‰, which supports the idea that ethanol preservation would not confound SIA results by causing one to think that the isotopic composition samples could be derived from a different carbon source. For future studies, a $\delta^{13}C$ correction factor may be beneficial to apply to tissue samples in cases where the difference from primary producer to consumer is less than 1.443‰ if $\delta^{13}C$ is being used as an indicator of trophic position. On the other hand, a correction factor may not be needed if all samples being analyzed (both predator and prey) are preserved in the same method and thus share the same bias. In conclusion, ethanol displayed minimal $\delta^{13}C$ enrichment upon bay anchovy stomach lining and gut contents in comparison to the ice preserved gut contents and stomach lining. Confidence intervals indicates that these differences were not significant for gut contents and were marginally significant for stomach linings (i.e., < 1‰ difference in confidence intervals). Nonetheless, further analysis is warranted on the degree of ethanol $\delta^{13}C$ enrichment to confirm if lipid extraction or a correction factor is needed for preserved tissues. Repeating this study and/or performing this analysis on multiple species would be beneficial for future observations.

Like $\delta^{13}C$, the mean $\delta^{15}N$ displayed negligible and non-significant impacts from ethanol preservation (Figure 3B). This finding is consistent with Sarakinos et al. (2002) who found alcohol $\delta^{15}N$ shifts to range from −0.39 to 0.40‰. The difference between my samples displayed a mean shift of less than 0.74 ‰ between both the ice- and ethanol preserved stomach lining and gut contents. However, Sweeting et al. (2004) and Horii et al. (2015) found larger shifts in $\delta^{15}N$, which they attributed to ethanol extracting certain constituents containing nitrogen from the muscle tissue in addition to lipids. Mayr et al. (2011) noted that there is an average of 3.4‰ shift in $\delta^{15}N$ between trophic levels. As a result, the minor and non-significant shifts in $\delta^{15}N$ in this study, attributed to preservation method, should not impact trophic studies using $\delta^{15}N$. The ice preserved gut contents displayed a wider range in 95% confidence intervals in comparison to the other samples; however, this variability could be due to a difference in prey items consumed by the fish. Variation in $\delta^{15}N$ of prey can be observed based upon what trophic level the fish may be

feeding upon that day (Romero-Romero et al., 2019). This is especially true for gut contents, whereas the isotopic composition of the stomach lining may be stable over longer periods of time. During dissection, shrimp, small fish, zooplankton, and eggs were observed as popular prey items in the gut contents of the bay anchovies. Each of these prey items could potentially have a different $\delta^{15}N$ signature. In summary, ethanol did not display a substantial impact upon $\delta^{15}N$ signatures between my ice and ethanol preserved samples, which is further confirmed by the overlap in 95% confidence intervals between ice and ethanol preserved gut contents and stomach lining.

Based upon the preservation method analysis, for future replicate studies it may be better to focus on stomach lining tissue versus the gut contents. The stomach lining has low lipid content, which leads to less $\delta^{13}C$ and $\delta^{15}N$ alterations due to lipid extraction and tissue hydrolysis from ethanol (Sweeting et al., 2004). Variation in prey items could likely lead to high variability in $\delta^{13}C$ and $\delta^{15}N$, which is why gut contents could display high SIA variability (Vander Zanden and Rasmussen, 2001). Whether the animal consumed a carnivore, omnivore, or herbivore-based diet will impact the degree of isotope enrichment of $\delta^{13}C$ and $\delta^{15}N$ in their tissue (Vander Zanden and Rasmussen, 2001). Due to the variability in isotopic enrichment of the gut contents, we may only need to pay attention to the SIA results of the stomach lining for preservation impacts on SIA. Since we are comparing stomach lining samples within species, the impacts of preservation method are more likely to be observed and we do not have to account for varying prey items to confound SIA results as seen in the gut contents. Furthermore, this observation is validated in that for both ice and ethanol preserved samples of the stomach lining, the $\delta^{13}C$ and $\delta^{15}N$ values do not display the wide variability as seen in the gut content samples (Figure 3A-B).

3.5.2 Allometric Analysis

Results of the allometric analysis did not reveal a strong enough relationship to justify extrapolating the correlation between the amount of carbon biomass in the fish's stomach lining and the length and the weight of the fish for examining mesopelagic species. This result was observed for the Atlantic silversides (Figure 2A-B), bay anchovies (Figure 3A-B), and naked gobies (Figure 4A-B). Results of SIA did reveal a generally positive linear trend between stomach lining carbon content, fish weight and length, as further explained by low p-values for all three species ($p \leq 0.05$). However, for all three species, the low R^2 (≤ 0.27) for each regression

model for both fish weight and length did not rationalize continuing to build the allometric relationship so that it could be generalized across species.

If strong relationships between fish size and carbon content of stomach linings (R^2>0.5) had been observed amongst multiple species, I would have developed a joint regression looking at a cross-species allometric relationships. This step would be necessary to justify extrapolating this relationship across species and extending it to NPSG mesopelagic fishes. However, since allometric scaling was not sufficiently robust at the species level, I opted not to extend this analysis to examine multi-species comparisons.

For future studies, using a larger sample size with a greater sampling of each weight and size category may reveal a stronger relationship than the results obtained from my data. Due to the time of year for sampling species for dissection (late July-November), I was limited in species I could capture that would fit my size criteria (20-70 mm) and capture in large numbers. Most juvenile fishes begin to move out of estuaries and sounds by early fall, thus making capture more difficult (Arevalo et al., 2023). As a result, my sample size was limited, and certain size categories had smaller numbers of dissected fish than others due to a lack of diversity in sizes of fishes captured. For both the Atlantic silversides and bay anchovies, the 40-45 mm and 46-50 mm size categories dominated other size categories, which may have skewed the relationship by having fewer fishes dissected in other size categories. Therefore, I recommend sampling fishes for dissection throughout the year to have enough time to obtain a larger sample size of each sampled species with a greater array of fish lengths and weights. Increasing number of fish sampled in each size category and sampling larval, juvenile, and adult stages within a species could possibly provide contrast to improve claims if an allometric relationship exists or not (Lindstedt and Schaeffer, 2001). Increasing the sample size of dissected fishes in each size category may help strengthen the confidence in the fish size to stomach lining carbon content, while sampling multiple life stages within a species may help explain variability (R^2) in the stomach lining carbon content in relation to fish size. Unfortunately, the small size of some of the fishes captured for the study limited the ability to separate the gut contents from the stomach lining. Using a variety of gear types, such as minnow traps, cast nets, or a dipnet, may help with catching fish of different sizes; however, using different gear does not guarantee obtaining the desired fish sizes. Consequently, I think multiple sampling events is the best option for obtaining a wide range of fish sizes and species. Should the allometric relationship across species exist, I

would also recommend possibly sampling more than three species of fishes to further strengthen the validation of an allometric relationship. However, since our allometric relationship study did not yield data to support the allometric relationship, I would first recommend repeating our study with the same species to see if we yield the same results before examining other species. Observing multiple species of varying sizes and shapes would further validate if an allometric relationship exists if I was able to demonstrate a strong relationship between carbon in the stomach lining and fish body mass. If each of these steps yielded satisfactory results, I could then generalize this allometric relationship across species and could apply the developed allometric equation to other fish species. This recommendation can be supported by the findings of Olivar et al. (2013) who found a positive allometric relationship between length and weight in larger mesopelagic fishes such as myctophids. However, Olivar et al. (2013) observed a negative length-weight allometric relationship in slender mesopelagic fish species such as *Cyclothone braueri*. As a result, further investigation of allometry in carbon in the stomach lining in relation to fish biomass is warranted to see if variation between species and life stages within a species exists. Additional study is also needed to address how variable stomach morphology is among species. This question poses the investigation into if some fishes have larger or smaller stomachs relative to body size. If so, this might imply an allometric relationship does not exist between body size and carbon in the fish's stomach lining. Consequently, multiple allometric relationships may need to be developed based upon species and/or fish shape. Living at deep depths, non-migratory fishes often deal with food scarcity and may have evolved large mouths to accommodate a large variety of prey (Annasawmy et al., 2020).

3.6 Conclusion

In conclusion, the results of my data suggest that a strong allometric relationship between carbon content in the fish stomach lining and length or weight of the fish is equivocal. Further analysis is needed to determine if such a relationship exists.

Chapter 4: Calculation Methods for the Gut Content Carbon Flux of Mesopelagic Fishes in the NPSG

4.1 Introduction

In this chapter I will discuss the calculations necessary to scale up estimated carbon flux from the gut contents of the sampled mesopelagic fishes from station ALOHA to estimate total mesopelagic fish-mediated carbon transport out of the epipelagic zone in the North Pacific Subtropical Gyre (NPSG).

Uncertainties in mesopelagic fish biomass and proportion of these fishes who migrate is well established in the literature (Irigoein et al., 2014; St. John et al., 2016; Saba et al.,2021). However, mesopelagic fish physiology (metabolism, respiration, and digestion rates) and behavioral patterns are even less known (McMonagle et al., 2023). Fish mediated carbon transport may account for up to 30% of total biological carbon transport in the ocean (Davison et al., 2013; Saba et al., 2021). As a result, there is a need to create more accurate models to estimate fish-mediated carbon transport, especially as interest is peaking in developing fisheries around mesopelagic fishes. Previous estimates of fish-mediated carbon transport have not been designed based on direct measurements of carbon consumed by these fishes and transported to depth. I attempt to estimate carbon flux based on these more direct measurements. Hikada et al. (2001) is the only known study to estimate the gut flux of fishes by analyzing gut contents. The calculations in this chapter will focus only on estimating fish-mediated carbon flux based upon fish gut flux. To estimate total carbon flux from mesopelagic fishes, respiration, excretion, and mortality rates must also be accounted for in addition to gut flux (McMonagle et al., 2023). In addition, the calculations below pertain to potential fish-mediated carbon flux and not the amount of time that carbon will stay sequestered at depth.

4.2 Methods for Calculating Micronekton Gut Flux

Daily consumption by mesopelagic fishes was calculated using the evacuation rate model from Hudson et al. (2014), where consumption was calculated as

Equation 2: $C=24(E_r S_w)$

where 24 is 24 hours/day, E_r=Evacuation rate, and S_w=Mean dry weight of stomach contents. Both E_r and S_w are expressed in terms of carbon content (milligrams). The equation for daily consumption rate can be used to determine the amount of carbon from extracted gut contents that will be converted to fecal pellets.

The carbon content of fish stomach contents was intended to be obtained from stable isotope analysis (SIA) (See Chapter 3 for details on this approach). Therefore, the S_w term can be measured directly. Some samples may require pooling due to the small biomass of fish gut contents among mesopelagic fishes; therefore, it is important that we pool fishes in the same size class. Size classes are set in 5-mm increments (0-5 mm, 6-10 mm, 11-15 mm, etc…). This way I can average size and amount of carbon per fish in the vial. I will also note how many fish are in each vial. Naturally, fish of the same species will be pooled. Fishes must be pooled by same size classes and species to obtain accurate data from the developed allometric relationship. (See Chapter 3 for allometric equation reasoning and development). The allometric equation allows for obtaining information on carbon content in the fish's stomach lining, which is particularly important for smaller fishes where separating gut contents from the stomach lining via dissection is not possible. Pooling of samples is only necessary for smaller fishes to acquire enough sample to achieve the minimum weight for SIA (≥0.5mg).

Next the equation for consumption needs to be set up to solve for evacuation rate, since this is the unknown term in this equation:

Equation 3: $\mathbf{E_r = C/(24*S_w)}$

Hudson et al. (2014) observed the term for consumption (C) = 0.7% per day of myctophid biomass. Consumption needs to be expressed in terms of carbon content. Carbon content is obtained from SIA results. Muscle tissue makes up 11-28% of the fish's biomass, with 19% average (Venugopal & Shahidi, 1996). Muscle tissue (stomach lining) is obtained via dissection from the mesopelagic fishes. Once the muscle tissue undergoes SIA, carbon content of muscle tissue is obtained. Next to solve for consumption, we need to track how much carbon is in the muscle sample relative to body size. For example, if a tissue sample is 0.5% of the fish's body weight and has 0.2 mg of carbon, then 0.2 mg carbon * (100/0.5) = total carbon in fish assuming

that the muscle tissue is representative of carbon content in other organs. This calculation process will need to be done for each fish to sum carbon in each sampled fish's body to get entire sum of carbon biomass from all the sampled fishes. This calculation process can be generalized in the form of the equation below:

Equation 4: Total carbon biomass = (Muscle carbon biomass)/ (portion of the muscle sample's biomass relative to fish overall biomass)

Mesopelagic fishes are known to exhibit net avoidance to result in an underestimate of fish biomass in a sampled area (Davison et al., 2014 and Irigoien et al., 2014). As a result, we must account for mesopelagic biomass underestimated due to net avoidance. The total biomass from the sampled fishes will be multiplied by a factor of net avoidance (14%) (Davison et al., 2013). The fish biomass in sampled from the MOCNESS * (100/14) = total fish biomass in the sampled area. It must be assumed that the net avoidance rate is similar for all species of mesopelagic fishes (both migrating and non-migrating species). Total fish biomass should be calculated at each depth strata sampled from the MOCNESS nets (e.g., 0-100m, 100-200m, 200-300m, 300-400m, etc…). These values will be entered into my equation for consumption so a daily ingested carbon value will be calculated for each depth profile:

Equation 5: Total fish biomass at sample depth * 0.7% = Consumption

As a result, we can relate these ingested carbon values with fecal pellet sinking speeds to determine how much carbon can potentially sink to depths in the water column per day.

To reiterate the developed equation for evacuated carbon:

Equation 6: $E_r = C/(24*S_w)$

Now we have all known terms to solve for evacuation:

Equation 7: E_r**=0.007*(total fish biomass at sampled depth*100/14)/ (24* sum-total carbon in stomach contents of all sampled fish at sampled depth)**

This is the amount of carbon estimated that fish produce as fecal matter in terms of carbon (mg) per day at a given depth.

The next question is how to relate evacuation rate to carbon flux. According to the literature, mesopelagic fish fecal pellets have a sinking rate of 787 m/day (Steinberg and Saba, 2012). Steinberg and Saba (2012) noted at this sinking speed most fecal pellets would escape bacterial remineralization. From where fish are sampled in the water column, we can determine how much carbon is transported to the mesopelagic zone (200-1,000 meters) per day by multiplying the sinking rate by the total egested carbon. All carbon excreted as fecal pellets below 200 meters are considered exported. This chosen depth is selected as our export boundary due to it being below the typical mixed layer depth at Station ALOHA so wind and wave activity cannot easily resurface carbon back to the atmosphere (Hikada et al., 2001; Davison et al., 2013; McMonagle et al., 2023).

The next process is to upscale the calculations from our sampled fishes at station ALOHA to calculate fish-mediated carbon export across the entire NPSG. To determine the amount of carbon sequestered by mesopelagic fishes in the NPSG, we assume that station ALOHA is a representative area of mesopelagic fish biomass distribution across the NPSG biome. To calculate total annual fish mediated carbon flux, the following equation is used:

Equation 8: Annual Total (mg C $m^{-2}yr^{-1}$) = (Sum total egested carbon in MOCNESS samples)/ (Volume of water sampled by MOCNESS) * (Total Area of NPSG/Total area of station ALOHA) = (Total potential carbon egested by mesopelagic fishes) *365 days/year

*The term “Sum total of egested carbon in MOCNESS samples” is the total egested carbon collected across all depths sampled by the MOCNESS

From the literature, total area of the NPSG is estimated to be $2*10^{13}$ m^2 (Karl & Church, 2017), while the area of station ALOHA is 292928 m^2 (Station ALOHA, 2023).

Now that gut flux has been calculated, respiration and mortality rates should be considered with our daily egested carbon rate by mesopelagic fishes to get a daily rate of total

fish mediated carbon export. Fishes release carbon via respiration and from deadfall via mortality and decomposition of carcasses. Therefore, these forms of released carbon from fishes must also be considered when calculating fish mediated carbon export (Ariza et al., 2015; Saba et al., 2021). From the literature, mesopelagic fish respiration flux = 2.9 ± 1.0 mg C m^{-2} d^{-1} (Ariza et al., 2015) and mortality flux= 3.1-11.1 mg C m^{-2} d^{-1} (Saba et al., 2021). Respiration and mortality flux calculations need further research as the previous calculation methods pertain to carbon excreted via fish gut flux. For example, respiration and mortality contributions to fish mediated carbon export should consider how these rates vary with individual fish biomass to calculate expelled carbon more accurately.

4.3 Assumptions

While calculating fish mediated carbon export via gut flux, several assumptions must be made with the current research that is available. Seeing as 90% of migrating mesopelagic fishes are myctophids (Davison et al., 2013), I based my rates discussed above off myctophids. I assume these rates do not vary between mesopelagic fish species. This is likely not totally accurate for fishes that do not do DMV, but this seems like a necessary assumption based on available knowledge. I must also assume that seasonal, spatial, and temporal variation in the sampled area were constant when reporting fish carbon gut flux calculations in the NPSG. Due to variation in prey items, water temperature, species composition/population, and nutrient availability, fish carbon flux rates are likely to fluctuate seasonally and spatially (Annasawmy et al., 2020). Yet, for my given research, I need to assume a constant fish carbon gut flux rate given lack of comparable data from other regions and seasons. It is also assumed that mesopelagic fishes feed and excrete fecal pellets at a constant rate (Hikada et al., 2001), which is an assumption that may be violated due to diel feeding patterns. I must also assume that my sample population is representative of the NPSG population in terms of variability in gut fullness. There is evidence that downward migrants have fuller guts than those migrating up (Hidaka et al., 1999; Angel and Pugh, 2000); therefore, most mesopelagic fishes will egest fecal pellets on a downward migratory retreat and egest more fecal pellets at their daytime depth versus closer to the surface during nighttime feeding (Angel and Pugh, 2000). Most food is digested by myctophids at 400-1,000 meters during the day while the fishes are at depth (Hudson et al., 2014). As a result, all fecal pellets are assumed to be egested below 200 meters in the

mesopelagic zone (Hidaka et al., 2001). With this assumption, we can include both migratory and non-migratory mesopelagic fish species in our calculations.

4.4 Conclusions

In summary, the above calculations can be utilized to determine fish-mediated carbon export via fish gut flux. However, respiration, excretion, and mortality rates must also be used to calculate total fish-mediated carbon export. Mesopelagic fish physiological traits and patterns are highly under researched. Therefore, further research is needed to narrow the number of assumptions made for my calculations, which would help develop more accurate methods for estimating mesopelagic fish carbon gut flux.

References

Anderson, T.R.M., Lampitt, R.S., Martin, A.P., Trueman, C.N., Henson, S.A., and Mayor, D.J. (2018). Quantifying carbon fluxes from primary production to mesopelagic fish using a simple food web model. *ICES Journal of Marine Science.* 76, 690-701.

Angel, M.V. and Pugh, P.R. (2000). Quantification of diel vertical migration by micronektonic taxa in the northeast Atlantic. *Hydrobiologia.* 440, 161-179.

Annasawmy, P., Chere,Y., Romano, E.V., Le Loc'he, F., Menard, F., Ternon, J., and Marsac, F. (2020). Stable isotope patterns of mesopelagic communities over two shallow seamounts of the south-western Indian Ocean. *Deep Sea Research: Part II Oceanographic Research Papers.* 176, 1-15.

Aparecido, K.C., Frédou, T., Eduardo, L.N., Mincarone, M., Lima, S.R., Fernanda da Silva Morais, M., and Mérigot, B. (2023). Living in darkness: functional diversity of mesopelagic fishes in the western tropical Atlantic. *Frontiers in Marine Science*. 10, 1-17.

Archiald, K.M., Siegel, D.A., and Doney, S.C. (2019). Modeling the Impact of Zooplankton Diel Vertical Migration on the Carbon Export Flux of the Biological Pump. *Global Biogeochemical Cycles*. 33, 181-199.

Arevalo, E., Cabral, H.N, Villeneuve, B.,Possémé, C., and Lepage, M. (2023). Fish larvae dynamics in temperate estuaries: A review on processes, patterns and factors that determine recruitment. *Fish and Fisheries*. 24, 466-487.

Arhonditsis, G.B., Shimoda, Y., and Kelly, N.E. (2019). Allometric theory: extrapolations from individuals to ecosystems. *Elsevier*. 2, 242-255.

Ariza, A., Garijo, J.C., Landeira, J.M., Bordes, F., and Hernández-León, S. (2015). Migrant biomass and respiratory carbon flux by zooplankton and micronekton in the subtropical northeast Atlantic Ocean (Canary Islands). *Progress in Oceanography.* 134, 330-342.

Bailey, Regina. "Life in the Mesopelagic Zone of the Ocean." ThoughtCo, Aug. 2, 2021, thoughtco.com/mesopelagic-zone-4685646.

Barnett, M.A. (1984). Mesopelagic fish zoogeography in the central tropical and subtropical Pacific Ocean: species composition and structure at representative locations in three ecosystems. *Marine Biology*. 82, 199-208.

Ben-David, M. and Flaherty, E.A. (2012). Stable isotopes in mammalian research: a beginner's guide. *Journal of Mammalogy.* 93, 312-328.

Bernal, A., Pilar, O.M, Maynou, F., and Fernández de Puelles, M.L. (2015). Diet and feeding strategies of mesopelagic fishes in the western Mediterranean. *Progress in Oceanography*. 135, 1-17.

Bode, A. and Hernández-Leon, S. (2018). Trophic diversity of plankton in the epipelagic and mesopelagic layers of the tropical and equatorial Atlantic determined with stable isotopes. *Diversity*. 10, 48.

Boyd, P.W., Claustre, H., Levy, M., Siegel, D.A., and Weber, T. (2019). Multi-faceted particle pumps drive carbon sequestration in the ocean. *Nature*. 568, 327-335.

Carabel, S., Verísimo, P., and Freire, J. (2009). Effects of preservatives on stable isotope analyses of four marine species. *Estuarine, Coastal and Shelf Science*. 82, 348-350.

Carpenter, K.E. (1992) Check-list of the fishes of the eastern tropical Atlantic (CLOFETA). *Review in Fish Biology and Fisheries.* 2, 182–184.

Cartapanis, O., Galbraith, E.D., Bianchi, D., and Jaccard, S. (2018). Carbon burial in deep-sea sediment and implications for oceanic inventories of carbon and alkalinity over the last glacial cycle. *European Geosciences Union*. 14, 1819-1850.

Carreon-Martinez, L. and Heath, D.D. (2010). Revolution in food web analysis and trophic ecology: Diet analysis by DNA and stable isotope analysis. *Molecular Ecology. 19*, 25–27.

Catul, V., Gauns, M., and Karuppasamy, P.K. 2010. A review on mesopelagic fishes belonging to family Myctophidae." *Reviews in Fish Biology and Fisheries*. 21, 339–354.

Cavan, E.L., Laurenceau-Cornec, E.C., Bressac, M. and Boyd, P.W. (2019). Exploring the ecology of the mesopelagic biological pump. *Progress in Oceanography*. 176, 1-15.

Choy, C.A., Popp, B.N., Hannides, C.C.S., and Drazen, J.C. (2015). Trophic structure and food resources of epipelagic fishes in the North Pacific Subtropical Gyre ecosystem inferred from nitrogen isotopic compositions. *Limnology and Oceanography*. 60, 1156-1171.

Choy CA, Haddock, S.H.D, and Robison, B.H. (2017). Deep pelagic food web structure as revealed by in situ feeding observations. *Biological Sciences*. 284, 1.

Cloyed, C.S., Newsome, S.D., and Eason, P.K. (2015). Trophic discrimination factors and incorporation rates of carbon and nitrogen-stable isotopes in adult green Frogs, *Lithobates clamitans*. *Physiological and Biochemical Zoology*.88, 576-585.

Cirtwill, A.R., Dalla Riva, G.V., Gaiarsa, M.P., Bimler, M.D., Cagua, E.F., Coux, C., and Dehling, M.D. (2018). A review of species role concepts in food webs. *Food Webs.* 16, 2352-2496.

Curry, R.A., Gautreau, M.D., Culp, J.M. (2013). Fin tissue as surrogates of white muscle tissue when assessing carbon and nitrogen stable isotope levels for Arctic and brook char. *Environmental Biology of Fishes*.8, 627-633.

Davenport, S.R. and Bax, N.J. (2001). A trophic study of a marine ecosystem off southeastern Australia using stable isotopes of carbon and nitrogen. *Canadian Journal of Fisheries and Aquatic Sciences.* 59, 514-530.

Davison, P.C., Checkley, D.M. Jr., Koslow, J.A., and Barlow, J. (2013). Carbon export mediated by mesopelagic fishes in the northeast Pacific Ocean. *Progress in Oceanography*. 116,14-30.

DeWitt, F.A. (1972). Bathymetric Distributions of Two Common Deep-Sea Fishes, Cyclothone acclinidens and C. signata, off Southern California. *Copeia.* 1, 88–96.

Dormann, C.F., Elith, J., Bacher S., Buchmann, C., Carl, G., Carré, G., Marquéz, J.R.G, Gruber, B., Lafourcade, B., Leitão, P.J., Münkemüller, T., McClean, C., Osborne, P.E., Reineking, B., Schröder, B., Skidmore, A.K., Zurell, D., and Lautenbach, S. (2013). Collinearity: a review of methods to deal with it and a simulation study evaluating their performance. *Ecography*. 36, 27-46.

Drazen, J.C., De Forest, L.G., and Domokos, R. (2011). Micronekton abundance and biomass in Hawaiian waters as influenced by seamounts, eddies, and the moon. *Deep-Sea Research 1*. 58, 557-566.

Ducklow, Hugh W. and Steinberg, Deborah K. (2001). Upper Ocean Export and the Biological Pump. *Oceanography*. 14, 50-58.

Duque-Correa, M.J., Codron, D., Meloro, C., McGrosky, A., Schiffmann, C., Edwards, M.S. and Clauss, M. (2021). Mammalian intestinal allometry, phylogeny, trophic level and climate. *Proceedings of the Royal Society*. 288, 1-10.

Elliott, K.H. and Elliot, J.E. (2016). Lipid extraction techniques for stable isotope analysis of bird eggs: Chloroform-methanol leads to more enriched ^{13}C values than extraction via petroleum ether. *Journal of Experimental Marine Biology and Ecology*. 474, 54-57.

Eschmeyer, W.N., Herald, E.S., and Hammann, H. (1983). A field guide to Pacific coast fishes of North America. Houghton Mifflin Company. Boston, Massachusetts.

Etnoyer, Peter. (2011, February 7) "Science Weekend: They eat their young." *Deep Sea News*. http://www.deepseanews.com/2007/02/just-science-weekend-they-eat-their-young/.

Fanelli, E., Cartes, J.E., and Papiol, V. (2011). Food web structure of deep-sea macrozooplankton and micronekton off the Catalan slope: Insight from stable isotopes. *Journal of Marine Science*. 87, 79-89.

Field, C.B., M.J. Behrenfeld, J.T. Randerson, and P. Falkowski. (1999). Primary production of the biosphere: Integrating terrestrial and oceanic components. *Science*. 281, 237-240.

Forward, R.B. Jr. (1988). Diel vertical migration zooplankton photobiology and behavior. *Oceanography and Marine Biology: An Annual Review*. 26, 361-393.

Foroshchuk, V.P. and Fedorov, V.V. (1992). *Poecilopsetta normani* -- a new species of flounder (Pleuronectidae) from the Saya de Malha Bank, Indian Ocean. *Journal of Ichthyology*. 32, 37-44.

Forward, RB. Jr. (1988). Diel vertical migration zooplankton photobiology and behavior. *Oceanography and Marine Biology: An Annual Review*. 26, 361-393.

France, R. L. (1995). Differentiation between littoral and pelagic food webs in lakes using carbon isotopes. *Limnology and Oceanography*.40, 1310–1313.

Fry, B. (2006). Stable isotope ecology. Springer Science+Business Media, LLC, United States.

Gewin, Virginia. "Fishing the Deep: Is it time to start fishing the deep sea? Some scientists are urging caution." *Hakai Magazine*, Coastal Science and Societies, 8 March 2016, https://www.hakaimagazine.com/news/fishing-deep/.

Gjøsaeter, J. and Kawaguchi, K. (1980). A review of the world resources of mesopelagic fish. Bernan Press, Blue Ridge Summit, PA.

Gloeckler, K., Choy, A.C., Hannides, C.C.S., Close, H.G., Goetze, E., Popp, B.N., and Dazen, J. C. (2018). Stable isotope analysis of micronekton around Hawaii reveals suspended particles are an important nutritional source in the lower mesopelagic and upper bathypelagic zones. *Limnology and Oceanography*. 63,1168-1180.

Gon, O. (1990a). Gonostomatidae. Fishes of the Southern Ocean. J.L.B. Smith. Institute of Ichthyology, Grahamstown, South Africa.

Gon, O. (1990b). Sternoptychidae. Fishes of the Southern Ocean. *Reviews in Fish Biology and Fisheries*. 2, 344-345.

Hajisafarali, M., Taskinen, J., Eloranta, A.P. Eloranta. A.P., and Kiljunen, M. (2023). Ethanol preservation effects on stable carbon, nitrogen and hydrogen isotopes in the freshwater pearl mussel. *Hydrobiologia*. 850, 1885–1895.

Hannides, C.C.S., Popp, B.N., Landry, M.R., and Graham, B.S. (2009). Quantification of zooplankton trophic position in the North Pacific Subtropical Gyre using stable nitrogen isotopes. *Limnology and Oceanography*. 54, 50–61.

Herndl, G.J. and Reinthaler, T. (2013). Microbial control of the dark end of the biological pump. *Nature Geoscience.* 6, 718-724.

Hopkins, J.B. and Ferguson, J.M. (2012). Estimating the diets of animals using stable isotopes and a comprehensive Bayesian mixing model. *PLOS ONE*. 7, 1-13.

Horii, S., Takahashi, K., and Furuya, K. (2015). Effects of ethanol-preservation on stable carbon and nitrogen isotopic signatures in marine predators. *Plankton and Benthos Research*. 10, 91-97.

Hudson, J.M., Steinberg, D.K., Sutton, T.T., Graves, J.E., and Latour, R.J. (2014). Myctophid feeding ecology and carbon transport along the northern Mid-Atlantic Ridge. *Deep Sea Research*. 93, 104-116.

Iglesias, I.S., Santora, J.A., Fiechter, J., and Field, J.C. (2023). Mesopelagic fishes are important prey for a diversity of predators. *Frontiers in Marine Science.* 10, 1-13.

Irigoien, Xabier, Klevjer, T.A., Rostad, A., Martinez, U., Boyra, G., Acuña, J.L., Bode, A., Echevarria, F., Gonzalez-Gordillo, J.I., Hernandez-Leon, S., Agusti, S., Aksnes, D.L., Duarte, C.M., and Kaartvedt, S. (2014). Large mesopelagic fishes biomass and trophic efficiency in the open ocean. *Nature Communications*. 5, 1-10.

Jesus, F.B., Pereira, M.R., Rosa, C.S., Moreira, M.Z., and Sperber, C.F. (2015). Preservation Methods Alter Carbon and Nitrogen Stable Isotope Values in Crickets (Orthoptera: Grylloidea). *PLoS One*. 10, 1-14.

Jiao, N., Herndl, G.J., Hansell, D.A., Benner, R., Kattner, G., Wilhelm, S.W., Kirchman, D.L., Weinbauer, M.G., Luo, T., Chen, F., and Azam, F. (2010). Microbial production of recalcitrant dissolved organic matter: long-term carbon storage in the global ocean. *Nature Reviews Microbiology*. 8, 593-599.

Karl, D.M. (1999). A Sea of Change: Biogeochemical Variability in the North Pacific Subtropical Gyre. *Ecosystems*. 2, 181-214.

Karl, D. and Church, M. (2014). Microbial oceanography and the Hawaii Ocean Time-series programme. *National Review of Microbiology*. 12, 699–713.

Karl, D.M. and Church, M. J. (2018). Station ALOHA: A gathering place for discovery, education, and scientific collaboration. *Limnology and Oceanography.* 28,10-12.

Karl, D.M. and Lukas, R. (1995). The Hawaii Ocean Time-Series (HOT) program: Background, rationale and field implementation. *Deep Sea Research Part II: Topical Studies in Oceanography*. 43, 129-156.

Kendall, C. and Caldwell, E.A. (1999). Isotope Tracers in Catchment Hydrology. *Elsevier Science*. 51-86.

Klingenberg, C.P. (2016). Size, shape, and form: concepts of allometry in geometric morphometrics. *Development in Genes and Evolution.* 226, 113–137.

Kobari, T., Nakamura, R. Aita, M.N. and Kitamura, M. (2022). Mesopelagic community supported by epipelagic production in the western North Pacific Ocean based on stable isotope ratios of carbon and nitrogen. *Deep Sea Research: Part I Oceanographic Research Papers.*182, 1-11.

Kwak, I. and Park, Y. (2020). Food chains and food webs in aquatic Ecosystems. *Applied Sciences*. 10, 1-5.

Lambert, Andy H. (2021). Bristlemouth Facts, Size, Adaptations, Habitat. *PeekaPoos*. http://www.peekapoos.info/2021/08/bristlemouth-facts-size-adaptations.html. [Accessed November 10, 2023].

Leitner, A. (2023). Net gains at station ALOHA: Introducing MOCNESS-the star of the show. https://schmidtocean.org/cruise-log-post/introducing-mocness-the-star-of-the-show. [Accessed July 7, 2023].

Lerner, J.E., Ono, K., Hernandez, K.M., Runstadler, J.A., Puryear, W.B., and Polito, M.J. (2018). Evaluating the use of stable isotope analysis to infer the feeding ecology of a growing US gray seal (Halichoerus grypus) population. *PLoS One*. 13, 1-16.

Lindstedt, S.L. and Schaeffer, P.J. (2002). Use of allometry in predicting anatomical and physiological parameters of mammals. *Laboratory Animals*. 36, 1-9.

Luo, Y., Ducklow, H.W., Friedrichs, M., Church, M.J., Karl, D.M., and Doney, S.C. (2012). Interannual variability of primary production and dissolved organic nitrogen storage in the North Pacific Subtropical Gyre. *Journal of Geophysical Research: Biogeosciences*. 117, 1-12

Masuda, H., Amaoka, K., Araga, C., Uyeno, T., and Yoshino, T. (1984). The fishes of the Japanese Archipelago. Tokai University Press, Tokyo, Japan.

Martin, A., Boyd, P., Buesseler, K., Cetinic, I., Claustre, H., Giering, S., Henson, S., Irigoien, X., Kriest, I., Memery, L., Robinson, C., Saba, G., Sanders, R., Siegel, D., Vila-Alfageme, M., and Guidi, L. (2020). The oceans' twilight zone must be studied now, before it is too late." *Nature*. 580, 26-28.

Mayr, C.C., Försterra, G., Häussermann, V., Wunderlich, A., Grau, J., Zieringer, M., and Altenbach, A.V. (2011). Stable isotope variability in a Chilean fjord food web: implications for N- and C-cycles. *Marine Ecology Progress Series*. 428, 89-104.

McClain-Counts, J.P., Demopolous, A.W.J., and Ross, S.W. (2017). Trophic structure of mesopelagic fishes in the Gulf of Mexico revealed by gut content and stable isotope analyses. *Marine Ecology.* 38, 1-23.

McEachran, J.D. and Fechhelm, F.D. (1998). Fishes of the Gulf of Mexico. Volume 1: Myxiniformes to Gasterosteiformes. University of Texas Press, Austin.

Moraes, G. and Cristina de Almeida, L. (2020). Nutrition and functional aspects of digestion in fish. *Biology and Physiology of Freshwater Neotropical Fish.* 11, 251-271.

Nagaraja, M.P. Carbon Cycle. *NASA*. (2020). https://science.nasa.gov/earth-science/oceanography/ocean-earth-system/ocean-carbon-cycle. [Accessed September 24, 2020].

Nelson, J.S. (1994). Fishes of the world. Third edition. John Wiley & Sons, Inc., New York.

Newsome, S.D., Yeakel, J.D., Wheatly, P.V., and Tinker, T. (2012). Tools for quantifying isotopic niche space and dietary variation at the individual and population level. *Journal of Mammalogy*. 93, 329–341.

O'Leary, M. (1988). Carbon Isotopes in Photosynthesis: Fractionation techniques may reveal new aspects of carbon dynamics in plants. *Bioscience.* 38, 328.

Olivar, M.P., Moli, B., and Bernal, A. Length-Weight relationships of mesopelagic fishes in the north-western mediterranean. (2013). *International Commission for the Scientific Exploration of the Mediterranean Sea*. 528, 1.

Olivar, M.P., Castello, A., Sabate, A., Sarmiento-Lezcano, A., Emelianov, M., Bernal, A., Yang, Y., Proud, R., and Brierley, A.S. (2022). Variation in mesopelagic fish community composition and structure between Mediterranean and Atlantic waters around the Iberian Peninsula. *Frontiers in Marine Science*. 9, 1-22.

Paoletti, S., Nielsen, J.R., Sparrevohn, C.R., Bastradie, F., and Vastenhoud, B.M.J. (2021). Potential for mesopelagic fishery compared to economy and fisheries dynamic in current large scale Danish pelagic fishery. *Frontiers.* 8, 1-21.

Paquin, M.M., Buckley, T.W., Hibpshman, R.E., Canino, M.F. (2014). DNA-based identification methods of prey fish from stomach contents of 12 species of eastern North Pacific groundfish. *Deep Sea Research Part I: Oceanographic Research Papers*. 85, 110-117.

Paraskevi, K.K. and Konstantinos, I.S. (2012). Morphometrics and Allometry in Fishes, Morphometrics, Prof. Christina Wahl (Ed.), ISBN: 978-953-51-0172-7, InTech.

Passow, U. and Carlson, C.A. (2012). The biological pump in a high CO_2 world. *Marine Ecology Progress Series*. 470, 249-271.

Prado, P., Carmicael, R.H., Watts, S.A., Cebrian, J., and Heck, K.L. Jr. (2012). Diet-dependent C and N fractionation among sea urchin *Lytechinus variegatus* tissues: implications for food web models. *Marine Ecology Progress Series.* 462, 175-190.

Quéro, J.C., Njock, J.C., and de la Hoz, M.M. (1990). Sternoptychidae. Check-list of the fishes of the eastern tropical Atlantic (CLOFETA). *Reviews in Fish Biology and Fisheries*. 2, 182-184.

Reidhaar, P.E., Lane, C.S., Benitez-Nelson, C.R., and Gamble, D.W. (2015). Spatial and temporal variations in *Pyrodinium bahamense* cyst concentrations in the sediments of bioluminescence mangrove lagoon, St. Croix, USVI. *Estuaries and Coasts*. 39, 682-694.

Rii, Y.M., Karl, D.M., and Church, M.J. (2016). Temporal and vertical variability in picophytoplankton primary productivity in the North Pacific Subtropical Gyre. *Marine Ecology Progress Series*. 562, 1-18

Roman, J., Estes, J.A., Morissette, L., Smith, C., Costa, D., McCarthy, J., Nation, J.B., Nicol, S., Pershing, A., and Smetacek, V. (2014). Whales as marine ecosystem engineers." *Frontiers in Ecology and the Environment*. 12, 377-385

Romero-Romero, S., Choy, C. A., Hannides, C.C.S., Popp, B.N., Drazen, J.C. (2019). Differences in the trophic ecology of micronekton driven by diel vertical migration. *Limnology and Oceanography*. 64, 1474-1483.

Richards, T.M., Sutton, T.T., and David-Wells, R.J. (2020). Trophic Structure and Sources of Variation Influencing the Stable Isotope Signatures of Meso- and Bathypelagic Micronekton Fishes. *Frontiers in Marine Science*. 7, 1-15.

Saba, G.K and Steinberg, D. (2012). Abundance, composition and sinking rates of fish fecal pellets in the Santa Barbara channel. *Scientific Reports.* 2, 716.

Saba, G. K., Burd, A. B., Dunne, J. P., Hernández-león, S., Martin, A. H., Rose, K. A., Salisbury, J., Steinberg, D. K., Trueman, C. N., Wilson, R. W., and Wilson, S. E. (2021). Toward a better understanding of fish-based contribution to ocean carbon flux. *Limnology and Oceanography* 66, 1639-1664.

Salvanes, A.G.V. and Kristoffersen, J.B. (2001). Mesopelagic Fishes. *The Encyclopedia of Ocean Sciences.* 3, 1711-1717.

Sarakinos, H. C., Johnson, M. L., and Vander Zanden, M. J. (2002). A synthesis of tissue preservation effects on carbon and nitrogen stable isotope signatures. *Canadian Journal of Zoology*. 80, 381–387.

Savoca, M.S., Czapanskiy, M.F., and Kahane-Rapport, S.R. (2021). Baleen whale prey consumption based on high-resolution foraging measurements." *Nature*. 599**,** 85–90

Sharp, Z. 2017. Principles of stable isotope geochemistry 2nd edition. *Pearson Prentice Hall*. New Jersey.

Shingleton, A.W. (2010) Allometry: The study of biological scaling. *Nature Education Knowledge* 3,2.

Sommer, S.A., Van Woudenberg, L., Lenz, P.H., Cepeda, G., and Goetz, E. (2017). Vertical gradients in species richness and community composition across the twilight zone in the North Pacific Subtropical Gyre. *Molecular Ecology*. 26, 6136-6156

St. John, M.A., Guillem, A.B., Chust, G., Heath, M., Grigorov, I., Mariani, P., Martin, A.P., and Santos, R.S. (2016). A Dark Hole in Our Understanding of Marine Ecosystems and Their Services: Perspectives from the Mesopelagic Community. *Frontiers in Marine Science*. 3, 1-6.

Station ALOHA. (2023). Bathymetry of station ALOHA. https://hahana.soest.hawaii.edu/stationaloha/BathMaps.html. [Accessed November 24, 2023].

Steinberg, D.K. Van Mooy, B.A. S. Buesseler, K.O. Boyd, P.W. Kobari, T., and Karl, D.M. (2008). Bacterial vs. zooplankton control of sinking particle flux in the ocean's twilight zone, *Limnology and Oceanography*, 53, 1327-1338.

Steinberg, Deborah K. and Landry, Michael R. "Zooplankton and the Ocean Carbon Cycle." *Annual Review of Marine Science*, Vol 9, June 2016, pp 413-444, 10.1146/annurev-marine-010814-015924.

Stock, C.A., John, J.G., Rykaczewski, R.R., Asch, R.G., Cheung, W.W., Dunne, J.P., Friedland, K.D., Lam, V.W., Sarmiento, J.L., Watson, R.A. (2017). Reconciling fisheries catch and ocean productivity. *Proceedings of the National Academy of Science*. 114, 1-9.

Sweeting, C. J., Polunin, N. V. C., and Jennings, S. (2004). Tissue and fixative dependent shifts of $\delta^{13}C$ and $\delta^{15}N$ in preserved ecological material. *Rapid Communications in Mass Spectrometry.* 18, 2587–2592.

Sweeting, C.J., Barry, J.T., Polunin, N.V.C., and Jennings, S. (2007). Effects of body size and environment on diet-tissue $\delta^{13}C$ fractionation in fishes. *Journal of Experimental Marine Biology and Ecology*. 352, 165–176.

Thaxton, W.C., Taylor, J.C., and Asch, R.G. (2020). Climate-associated trends and variability in ichthyoplankton phenology from the longest continuous larval fish time series on the east coast of the United States. *Marine Ecology Progress Series*. 650, 269-287.

The University of New Mexico. (2023). Center for stable isotopes. http://csi.unm.edu/ [Accessed November 12, 2023].

Tinker, S.W. (1978). Fishes of Hawaii, a handbook of the marine fishes of Hawaii and the Central Pacific Ocean. Hawaiian Service Inc., Honolulu.

Whitehead, P.J.P. (1985). FAO Species Catalogue. Vol. 7. Clupeoid fishes of the world (suborder Clupeoidei). An annotated and illustrated catalogue of the herrings, sardines, pilchards, sprats, shads, anchovies and wolf-herrings. FAO Fish. Synop. 125(7/1):1-303. Rome: FAO.

Woods, B.L., Van de Putte, A.P., Hindell, M.A., Raymond, B., Saunders, R.A., Walters, A., and Trebilco, R. (2023). Species distribution models describe spatial variability in mesopelagic fish abundance in the Southern Ocean. *Frontiers in Marine Science*. 9, 1-19.

World Resource Institute. (2023). What we know about deep-sea mining-and what we don't. https://www.wri.org/insights/deep-sea-mining-explained. [Accessed November 14, 2023].

Vanderklift, M.A. and Ponsard, S. (2003). Sources of variation in consumer-diet δ15N enrichment: a meta-analysis. *Oeco – logia.* 136, 169−182.

Vander Zanden, M.J. and Rasmussen, J.B. (2001). Variation in δ15N and δ13C trophic fractionation: Implications for aquatic food web studies. *Limnology and Oceanography*. 46, 2061-2066.

Venugopal, V. and Shahidi, F. (1996). Structure and composition of fish muscle. *Food Reviews International*. 2, 175-197.

Yongfu, S., Mboglen, D., Yi, G., Feng, W., and Yunkai, L. (2023). Effects of ethanol storage and lipid extraction on stable isotope compositions of twelve pelagic predators. *Frontiers in Marine Science*. 10, 1-7.

Chapter 2 Tables

Table 1. Count of number of species dissected. Some species were only able to be classified to family or genus level. Fishes were also classified based on whether a species migrated diurnally (migrator) to feed or stayed at their residual depth full time (non-migrator).

Species	Count of Species	migrator/non-migrator	source
Argyropelecus hemigymnus	3	migrator	Gon ,1990b
Alepocephalidae (family)	2	non-migrator	Nelson, 1994
Argyropelecus lychnus	1	migrator	Eschmeyer et al.,1983
Bolinichthys longipes	1	migrator	Masuda et al.,1984
Clupea pallasii	1	non-migrator (pelagic species)	Whitehead, 1985
Cyclothone acclinidens	17	non-migrator	Gon ,1990a
Cyclothone pseudopallida	57	non-migrator	Gon, 1990a
Cyclothone signata	101	migrator	Gon, 1990a
Danaphos oculatus	4	migrator	Tinker, 1978
Diaphus spp.	6	migrator	Tinker, 1978
Diaphus fulgens	4	migrator	Tinker, 1978
Diaphus mollis	1	migrator	Tinker, 1978
Diogenichthys atlanticus	8	migrator	Carpenter, 1992
Electrona risso	4	migrator	Tinker, 1978
Eustomias sp.	1	only females migrate to feed	McEachran and Fechhelm, 1998
Gonostoma atlanticum	13	migrator	Gon, 1990a
Idiacanthus antrostomus	1	migrator	Eschmeyer et al.,1983
Microstomus pacificus (larva)	1	non-migrator	Tinker, 1978
Nemichthyidae (ID'd to family)	1	non-migrator	Eschmeyer et al.,1983
Nemichthys scolopaceus	2	non-migrator	Eschmeyer et al.,1983
Notolychnus valdiviae	1	migrator	Carpenter, 1992
Poecilopsetta hawaiiensis	2	non-migrator	Foroshchuk and Fedorov, 1992

Protolychnus valdiviae	1	migrator	Tinker, 1978
Pseudobathylagus milleri	1	non-migrator	Tinker, 1979
Stenobrachius leucopsarus	7	migrator	Tinker, 1980
Sternoptyx diaphana	1	migrator	Quéro et al., 1990
Sternoptyx obscura	1	migrator	Quéro et al., 1990
Sternoptyx pseudobscura	2	migrator	Quéro et al., 1990
Tactostoma macropus	1	migrator	Eschmeyer et al.,1983
Tarletonbeania crenularis	1	migrator	Nelson, 1994
Valenciennellus tripunctulatus	4	non-migrator	Quéro et al., 1990
Total	**251**		

Table 2

Count of fishes pooled during dissection from each MOCNESS net

Net Number	Count of Fishes	Number of pooled fishes
1	16	2
2	38	12
3	86	25
4	84	8
5	9	0
6	7	0
8	2	0
9	9	0
Grand Total	251	47

Table 3

Species composition of fishes pooled during dissection from each MOCNESS net

Net Number	Species	Species Count
1	*Cyclothone signata*	2
2	*Cyclothone pseudopallida*	8
2	*Cyclothone acclinidens*	2
2	*Diogenichthys atlanticus*	2
2	*Diaphus (genus)*	2
3	*Cyclothone pseudopallida*	15
3	*Cyclothone signata*	6
3	*Gonostoma atlanticus*	2
4	*Cyclothone pseudopallida*	4
4	*Diogenichthys atlanticus*	2
4	*Diaphus fulgens*	2

Table 4 Linear regression descriptive statistics of mesopelagic fish biomass [standard length (mm) and wet weight (g)] with relationship to $\delta^{13}C$ and $\delta^{15}N$.

Migrators	**$\delta^{15}N$ Weight**	**$\delta^{15}N$ Length**	**$\delta^{13}C$ Weight**	**$\delta^{13}C$ Length**
R^2	0.118	0.451	0.115	0.224
Standard Error	1.823	1.438	0.642	0.601
N	92	92	92	92
F	12.048	74.040	11.729	25.997
P-Value	p=0.0007	p≤0.0001	p=0.0009	p≤0.0001
Slope	2.010	0.116	0.699	0.029
Intercept	5.679	3.288	-20.575	-21.131
Non-Migrators	**$\delta^{15}N$ Weight**	**$\delta^{15}N$ Length**	**$\delta^{13}C$ Weight**	**$\delta^{13}C$ Length**
R^2	0.046	0.015	0.134	0.141
Standard Error	2.835	2.881	0.763	0.760
N	77	77	77	77
F	3.598	1.124	11.662	12.314
P-Value	p=0.0620	p=0.2920	p=0.001	p=0.0007
Slope	-2.190	0.013	0.106	0.011
Intercept	8.129	7.524	-20.220	-20.512

Table 5 ANOVA for migrating mesopelagic fish species to analyze the intereaction of isotope signatures for **A)** $\delta^{15}N$, and **B)** $\delta^{13}C$ with regard to depth (m) and time of day (day or night) sampled, and **C)** mean $\delta^{15}N$ and $\delta^{13}C$ at time of day and depth variability.

A)

ANOVA for Migrators: Interaction for δ15N and depth and time of day				
Source	**Sum of Squares**	**Degrees of Freedom**	**F**	**Prob>F**
Depth	7.074	1	1.960	0.164
Time of Day	10.569	1	2.930	0.090
Depth:Time of Day	3.180	1	0.880	0.350
Error	320.497	89		
Total	338.491	92		

B)

ANOVA for Migrators: Interaction for δ13C and depth and time of day				
Source	**Sum of Squares**	**Degrees of Freedom**	**F**	**Prob>F**
Depth	1.034	1	2.230	0.139
Time of Day	0.357	1	0.770	0.383
Depth:Time of Day	0.308	1	0.660	0.418
Error	41.348	89		
Total	42.870	92		

C)

Migrators		
Time of Day	**δ13C**	**δ15N**
Night	-20.481	6.179
Day	-20.264	5.118
Depth		
Above 400m	-20.278	5.973
Below 400m	-20.513	6.3

Table 6. ANOVA for non-migrating mesopelagic fish species to analyze the intereaction of isotope signatures of **A)** $\delta^{15}N$, and **B)** $\delta^{13}C$ depth (m) and time of day sampled, and **C)** mean $\delta^{15}N$ and $\delta^{13}C$ at time of day and depth variability.

A)

ANOVA for Non-Migrators: Interaction for δ15N and depth and time of day				
Source	**Sum of Squares**	**Degrees of Freedom**	**F**	**Prob>F**
Depth	45.006	1	5.780	0.019
Time of Day	0.034	1	0	0.947
Depth:Time of Day	38.829	1	4.990	0.029
Error	568.050	73		
Total	631.031	76		

B)

ANOVA for Non-Migrators: Interaction for δ13C and depth and time of day				
Source	**Sum of Squares**	**Degrees of Freedom**	**F**	**Prob>F**
Depth	0.632	1	1.020	0.316
Time of Day	2.159	1	3.480	0.066
Depth:Time of Day	0.444	1	0.720	0.401
Error	45.335	73		
Total	50.965	76		

C)

Non-Migrators		
Time of Day	**δ13C**	**δ15N**
Night	-20.216	8.155
Day	-19.780	7.127
Depth		
Above 400m	-19.979	7.495
Below 400m	-20.279	8.426

Table 7. Tukey-Kramer test to analyze variation for non-migrating mesopelagic fishes between daytime/nighttime tows and depth (above and below 400 m). **A)** analyzes variation for $\delta^{15}N$ and **B)** analyzes variation for $\delta^{13}C$. Upper and lower limits correspond to 95% confidence intervals.

A)

$\delta^{15}N$					
Group A	**Group B**	**Lower Limit**	**Mean Difference**	**Upper Limit**	**P-value**
> 400 m	< 400 m	-0.159	4.123	8.405	0.063
> 400 m	Nighttime	-1.950	1.926	5.803	0.562
> 400 m	Daytime	-1.842	2.079	5.999	0.507
< 400 m	Nighttime	-4.740	-2.196	0.348	0.115
< 400 m	Daytime	-4.654	-2.044	0.566	0.176
Nighttime	Daytime	-1.719	0.152	2.024	0.996

B)

$\delta^{13}C$					
Group A	**Group B**	**Lower Limit**	**Mean Difference**	**Upper Limit**	**P-value**
> 400 m	< 400 m	-1.169	0.041	1.251	0.999
> 400 m	Nighttime	-0.839	0.256	1.351	0.927
> 400 m	Daytime	-0.386	0.721	1.829	0.325
< 400 m	Nighttime	-0.504	0.215	0.934	0.860
< 400 m	Daytime	-0.057	0.681	1.418	0.081
Nighttime	Daytime	-0.063	0.465	0.994	0.104

Table 8. Tukey-Kramer test to analyze variation for migrating mesopelagic fishes between day-time/night-time tows and depth (above and below 400 m). Table **A)** analyzes variation for $\delta^{15}N$ and table **B)** analyzes variation for $\delta^{13}C$. Upper and lower limits correspond to 95% confidence intervals and "A-B" corresponds to the difference in means in $\delta^{13}C$ and $\delta^{15}N$ between the two groups.

A)

$\delta^{15}N$					
Group A	**Group B**	**Lower Limit**	**Mean Difference**	**Upper Limit**	**P-value**
Daytime	Nighttime	4.478	-1.470	1.538	0.578
Daytime	>400m	3.787	-1.665	0.456	0.176
Daytime	<400m	4.298	1.955	0.387	0.135
Nighttime	>400m	2.503	-0.196	2.112	0.996
Nighttime	<400m	2.997	0.486	2.026	0.957
>400m	<400m	1.615	0.290	1.036	0.940

B)

$\delta^{13}C$					
Group A	**Group B**	**Lower Limit**	**Mean Difference**	**Upper Limit**	**P-value**
Daytime	Nighttime	1.600	-0.520	0.561	0.591
Daytime	>400m	0.748	0.014	0.776	0.999
Daytime	<400m	0.980	0.139	0.702	0.973
Nighttime	>400m	0.295	0.534	1.363	0.336
Nighttime	<400m	0.521	0.381	1.283	0.687
>400m	<400m	0.629	0.153	0.323	0.835

Table 9. A) Summary of genera and species total sample size (genera ≥ 4 were used), mean $\delta^{13}C$, variance of $\delta^{13}C$ within each group, and average depth range that the species/genera can inhabit. **B)** ANOVA analyzing the variance of $\delta^{13}C$ across genera and species sampled.

A)

Summary					
Groups	Count	Average δ13C	Variance	Average Depth Range (m) *	Migration Status*
δ13C Cyclothone acclinidens	17	-20.155	0.540	300-1500	Non-migrator
δ13C Cyclothone pseudopallida	43	-20.156	0.733	300-900	Non-migrator
δC13 Cyclothone signata	39	-20.382	0.212	100-800	Migrator
***δ13C Diaphus* spp.**	4	-20.960	1.135	0-1800	Migrator
***δ13C Diogenichthys* sp.**	8	-20.849	0.212	0-1050	Migrator
***δ13C Gonostoma* spp.**	11	-20.234	1.045	100-1500	Migrator
***δ13C Stenobrachius* sp.**	9	-19.978	0.164	30-1200	Migrator
***δ13C Sternoptyx* sp.**	4	-20.440	0.342	0-1500	Migrator
***δ13C Electrona* sp.**	4	-21.252	0.008	90-1500	Migrator
***δ13C Valenciennellus* sp.**	4	-20.255	0.092	200-400	Non-migrator

*See Table 3 for citations for classifying taxa by migration status and depth range.

B)

ANOVA for δ13C and Genera Variance					
Source Of Variation	Sum of Squares	Degrees of Freedom	F	P-value	F crit
Between Groups	10.325	9	2.331	0.018	1.951
Within Groups	65.445	133			
Total	75.769	142			

Table 10. A) Summary of genera and species total sample size (genera with sample sizes of 4 or greater were used), mean $\delta^{15}N$, variance of $\delta^{15}N$ within each group, and average depth range the species/genera can inhabit. **B)** ANOVA analyzing the variance of $\delta^{15}N$ among genera and species sampled.

A)

Summary					
Groups	*Count*	*Average*	*Variance*	*Average Depth Range (m)**	*Migration Status**
δ15N Cyclothone acclinidens	17	8.706	12.581	300-1500	Non-migrator
δ15N Cyclothone pseudopallida	43	8.533	6.441	300-900	Non-migrator
δ15N Cyclothone signata	39	6.410	0.532	100-800	Migrator
***δ15N Diaphus* spp.**	4	4.304	0.484	0-1800	Migrator
***δ15N Diogenichthys* sp.**	8	5.231	2.643	0-1050	Migrator
***δ15N Gonostoma* spp.**	11	8.473	13.955	100-1500	Migrator
***δ15N Stenobrachius* sp.**	9	5.609	0.759	30-1200	Migrator
***δ15N Sternoptyx* sp.**	4	6.792	2.066	0-1500	Migrator
δ15N Electrona sp.	4	3.813	0.003	90-1500	Migrator
***δ15N Valenciennellus* sp.**	4	6.649	5.273	200-400	Non-migrator

*See Table 3 for citation information on average depths and migration status.

B)

ANOVA for δ15N and genera variance					
Source of Variation	Sum of Squares	Degrees of Freedom	F	P-value	F crit
Between Groups	291.924	9	6.347	≤0.0001	1.951
Within Groups	679.668	133			
Total	971.592	142			

Table 11 A) Core sediment trap data from station ALOHA KM1910 cruise. Collection Date: 6/19/19. Water was filtered onto a glass fiber filter with a 25-mm diameter. **B)** Ring net data for zooplankton samples (zoo=zooplankton) from station ALOHA KM1910 cruise. Collection date: 6/20/19**. C)** Average $\delta^{13}C$ and $\delta^{15}N$ of primary producers sampled in the pelagic and benthic ocean layers of the NPSG. POM = particulate organic matter.

(Table 10C Source: Davenport and Bax, 2002)

A)

Trap Number	Depth(m)	δ15N	δ13C
1	75	0.68	-22.07
2	75	0.94	-21.95
3	75	1.27	-22.23
1	150	3.57	-22.32
2	150	2.75	-22.01
3	150	2.71	-22.11
1	300	2.31	-21.91
2	300	2.09	-20.86
3	300	2.71	-21.46

B)

Sample	Depth (m)	δ13C	δ15N
zoo a	0-200	-21.08	2.08
zoo b	0-200	-21.52	-----
zoo c	0-200	-21.12	2.07
zoo d	0-200	-21.44	2.11

C)

Primary Producer	δ15N	δ13C
Pelagic		
Phytoplankton	6.2	-20.5
POM	6.1	-21.5
Zooplankton	7.7	-21.3
Benthic		
Sediment	7.0	-21.8
POM	6.1	-21.5

Table 12 Tukey-Kramer test to analyze variation between $\delta^{13}C$ and $\delta^{15}N$ among genera and species. **A)** analyzes variation for $\delta^{13}C$ and **B)** analyzes variation for $\delta^{15}N$. Upper and lower limits correspond to 95% confidence intervals. Mean difference corresponds to the difference in means in $\delta^{13}C$ and $\delta^{15}N$ between the two groups.

A)

δ13C					
Group A	**Group B**	**Lower Limit**	**Mean Difference**	**Upper Limit**	**P-value**
C.acclinidens	*C.pseudopallida*	-0.651	-0.012	0.627	1.000
C.acclinidens	*C. signata*	-0.425	0.223	0.871	0.986
C.acclinidens	*Diaphus* sp.	-0.423	0.816	2.055	0.539
C.acclinidens	*Diogenichthys*	-0.265	0.691	1.647	0.397
C.acclinidens	*Gonostoma* sp.	-0.767	0.096	0.959	1.000
C.acclinidens	*Stenobrachius* sp.	-1.100	-0.181	0.738	1.000
C.acclinidens	*Sternoptyx* sp.	-0.973	0.266	1.505	1.000
C.acclinidens	*Electrona* sp.	-0.173	1.066	2.305	0.165
C.acclinidens	*Valenciennellus* sp.	-1.148	0.091	1.330	1.000
C.pseudopallida	*C.signata*	-0.258	0.236	0.729	0.888
C.pseudopallida	*Diaphus* sp.	-0.337	0.828	1.994	0.423
C.pseudopallida	*Diogenichthys* sp.	-0.155	0.703	1.562	0.221
C.pseudopallida	*Gonostoma* sp.	-0.645	0.108	0.862	1.000
C.pseudopallida	*Stenobrachius* sp.	-0.986	-0.169	0.649	1.000
C.pseudopallida	*Sternoptyx* sp.	-0.887	0.278	1.444	0.999
C.pseudopallida	*Electrona* sp.	-0.087	1.078	2.244	0.098
C.pseudopallida	*Valenciennellus* sp.	-1.062	0.103	1.269	1.000
C. signata	*Diaphus* sp.	-0.578	0.593	1.764	0.848
C. signata	*Diogenichthys* sp.	-0.398	0.468	1.333	0.790
C. signata	*Gonostoma* sp.	-0.889	-0.128	0.634	1.000
C. signata	*Stenobrachius* sp.	-1.229	-0.404	0.420	0.871
C. signata	*Sternoptyx* sp.	-1.128	0.043	1.214	1.000
C. signata	*Electrona* sp.	-0.328	0.843	2.014	0.404
C. signata	*Valenciennellus* sp.	-1.303	-0.132	1.039	1.000
Diaphus sp.	*Diogenichthys* sp.	-1.491	-0.125	1.241	1.000
Diaphus sp.	*Gonostoma* sp.	-2.022	-0.720	0.582	0.766
Diaphus sp.	*Stenobrachius* sp.	-2.337	-0.997	0.343	0.354
Diaphus sp.	*Sternoptyx* sp.	-2.127	-0.550	1.027	0.985
Diaphus sp.	*Electrona* sp.	-1.327	0.250	1.827	1.000

Diaphus sp.	*Valenciennellus* sp.	-2.302	-0.725	0.852	0.910
Diogenichthys sp.	*Gonostoma* sp.	-1.632	-0.595	0.441	0.724
Diogenichthys sp.	*Stenobrachius* sp.	-1.956	-0.872	0.211	0.244
Diogenichthys sp.	*Sternoptyx* sp.	-1.791	-0.425	0.941	0.993
Diogenichthys sp.	*Electrona* sp.	-0.991	0.375	1.741	0.997
Diogenichthys sp.	*Valenciennellus* sp.	-1.966	-0.600	0.766	0.931
Gonostoma sp.	*Stenobrachius* sp.	-1.279	-0.277	0.726	0.997
Gonostoma sp.	*Sternoptyx* sp.	-1.132	0.170	1.472	1.000
Gonostoma sp.	*Electrona* sp.	-0.332	0.970	2.272	0.351
Gonostoma sp.	*Valenciennellus* sp.	-1.307	-0.005	1.297	1.000
Stenobrachius sp.	*Sternoptyx* sp.	-0.893	0.447	1.787	0.989
Stenobrachius sp.	*Electrona* sp.	-0.093	1.247	2.587	0.094
Stenobrachius sp.	*Valenciennellus* sp.	-1.068	0.272	1.612	1.000
Sternoptyx sp.	*Electrona* sp.	-0.777	0.800	2.377	0.846
Sternoptyx sp.	*Valenciennellus* sp.	-1.752	-0.175	1.402	1.000
Electrona sp.	*Valenciennellus* sp.	-2.552	-0.975	0.602	0.630

B)

δ15N					
Group A	**Group B**	**Lower Limit**	**Mean Difference**	**Upper Limit**	**P-value**
C.acclinidens	*C.pseudopallida*	-1.874	0.171	2.216	1.000
C.acclinidens	*C. signata*	0.221	2.296	4.370	0.017
C.acclinidens	*Diaphus* sp.	0.439	4.406	8.372	0.016
C.acclinidens	*Diogenichthys*	0.408	3.468	6.529	0.012
C.acclinidens	*Gonostoma* sp.	-2.538	0.224	2.986	1.000
C.acclinidens	*Stenobrachius* sp.	0.152	3.095	6.037	0.030
C.acclinidens	*Sternoptyx* sp.	-2.036	1.931	5.897	0.876
C.acclinidens	*Electrona* sp.	0.914	4.881	8.847	0.004
C.acclinidens	*Valenciennellus* sp.	-1.911	2.056	6.022	0.829
C.pseudopallida	*C.signata*	0.546	2.125	3.703	0.001
C.pseudopallida	*Diaphus* sp.	0.504	4.235	7.966	0.012
C.pseudopallida	*Diogenichthys* sp.	0.549	3.297	6.046	0.006

C.pseudopallida	*Gonostoma* sp.	-2.359	0.053	2.465	1.000
C.pseudopallida	*Stenobrachius* sp.	0.307	2.924	5.540	0.015
C.pseudopallida	*Sternoptyx* sp.	-1.971	1.760	5.491	0.896
C.pseudopallida	*Electrona* sp.	0.979	4.710	8.441	0.003
C.pseudopallida	*Valenciennellus* sp.	-1.846	1.885	5.616	0.849
C. signata	*Diaphus* sp.	-1.637	2.110	5.858	0.747
C. signata	*Diogenichthys* sp.	-1.598	1.173	3.943	0.945
C. signata	*Gonostoma* sp.	-4.508	-2.072	0.365	0.178
C. signata	*Stenobrachius* sp.	-1.840	0.799	3.439	0.994
C. signata	*Sternoptyx* sp.	-4.112	-0.365	3.383	1.000
C. signata	*Electrona* sp.	-1.162	2.585	6.333	0.469
C. signata	*Valenciennellus* sp.	-3.987	-0.240	3.508	1.000
Diaphus sp.	*Diogenichthys* sp.	-5.308	-0.938	3.433	1.000
Diaphus sp.	*Gonostoma* sp.	-8.349	-4.182	-0.014	0.048
Diaphus sp.	*Stenobrachius* sp.	-5.600	-1.311	2.978	0.994
Diaphus sp.	*Sternoptyx* sp.	-7.522	-2.475	2.572	0.871
Diaphus sp.	*Electrona* sp.	-4.572	0.475	5.522	1.000
Diaphus sp.	*Valenciennellus* sp.	-7.397	-2.350	2.697	0.903
Diogenichthys sp.	*Gonostoma* sp.	-6.561	-3.244	0.072	0.061
Diogenichthys sp.	*Stenobrachius* sp.	-3.842	-0.374	3.095	1.000
Diogenichthys sp.	*Sternoptyx* sp.	-5.908	-1.538	2.833	0.984
Diogenichthys sp.	*Electrona* sp.	-2.958	1.413	5.783	0.991
Diogenichthys sp.	*Valenciennellus* sp.	-5.783	-1.413	2.958	0.991
Gonostoma sp.	*Stenobrachius* sp.	-0.337	2.871	6.079	0.126
Gonostoma sp.	*Sternoptyx* sp.	-2.461	1.707	5.874	0.955
Gonostoma sp.	*Electrona* sp.	0.489	4.657	8.824	0.015
Gonostoma sp.	*Valenciennellus* sp.	-2.336	1.832	5.999	0.930
Stenobrachius sp.	*Sternoptyx* sp.	-5.453	-1.164	3.125	0.998
Stenobrachius sp.	*Electrona* sp.	-2.503	1.786	6.075	0.950
Stenobrachius sp.	*Valenciennellus* sp.	-5.328	-1.039	3.250	0.999

Sternoptyx sp.	*Electrona* sp.	-2.097	2.950	7.997	0.704
Sternoptyx sp.	*Valenciennellus* sp.	-4.922	0.125	5.172	1.000
Electrona sp.	*Valenciennellus* sp.	-7.872	-2.825	2.222	0.754

Chapter 2 Figures

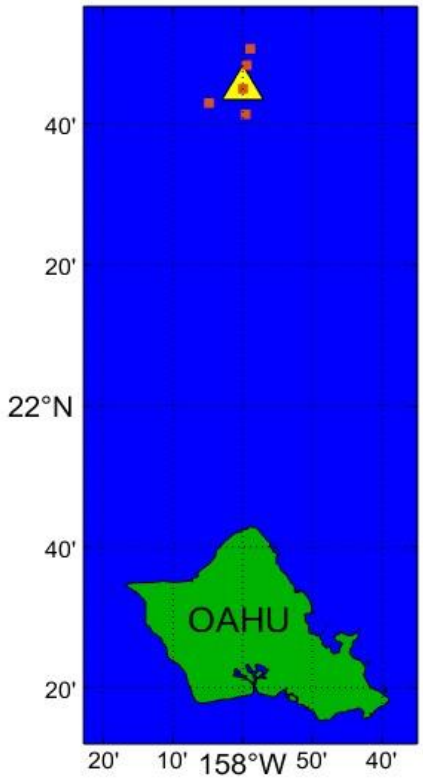

Figure 1 Map of study location station ALOHA (yellow triangle) in relation to Oahu, Hawaii. Location of MOCNESS tows (red circles) are marked within station ALOHA.

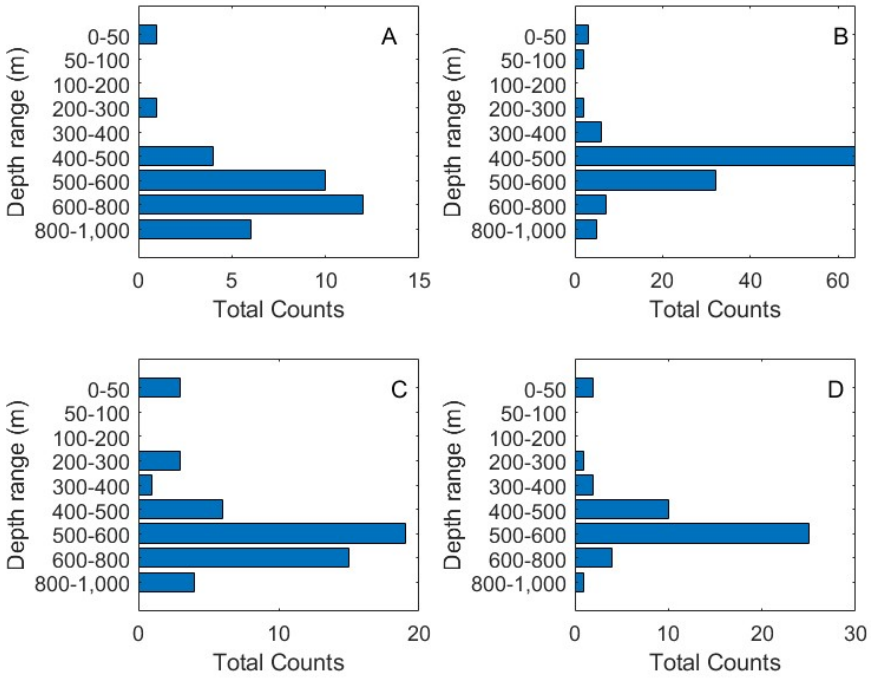

Figure 2A. Frequency of dissected mesopelagic fishes at sampled depth ranges with a MOCNESS net at station ALOHA for: **A)** Day-time, non-migrating species; **B)** Day-time, migrating species; **C)** Night-time, non-migrating species, and **D)** Night-time, migrating species.

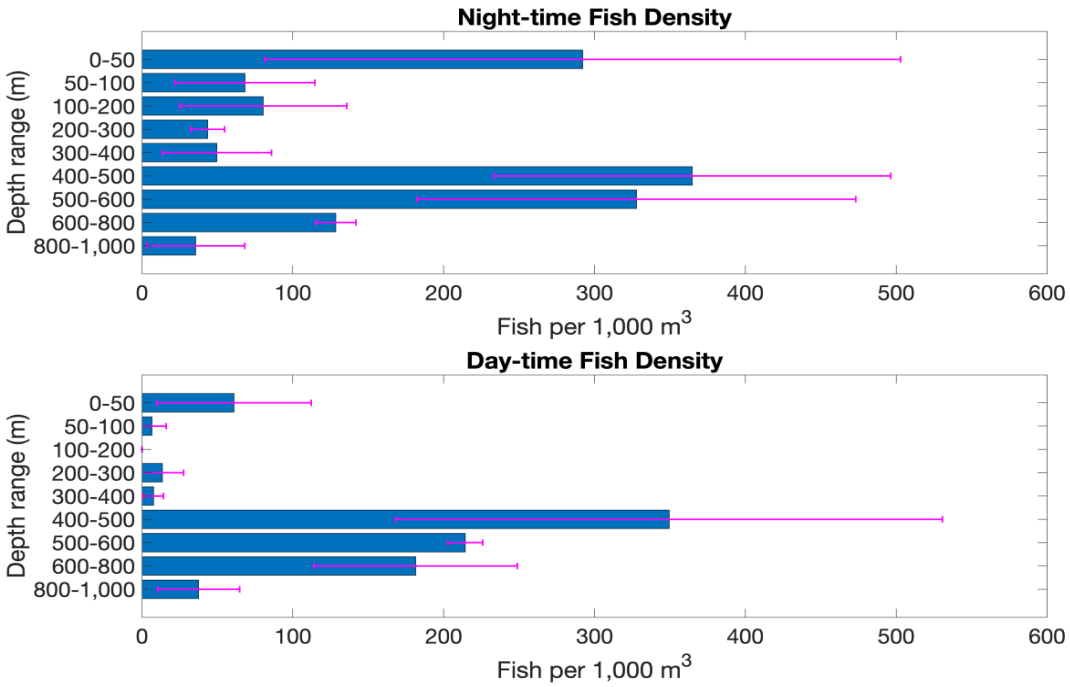

Figure 2B. Frequency of mesopelagic fishes, with 95% confidence intervals, collected aboard the research cruise at depth ranges from the MOCNESS net at day- and night-time tows. Frequency of dissected fishes processed for SIA is detailed in Figure 2A.

A)

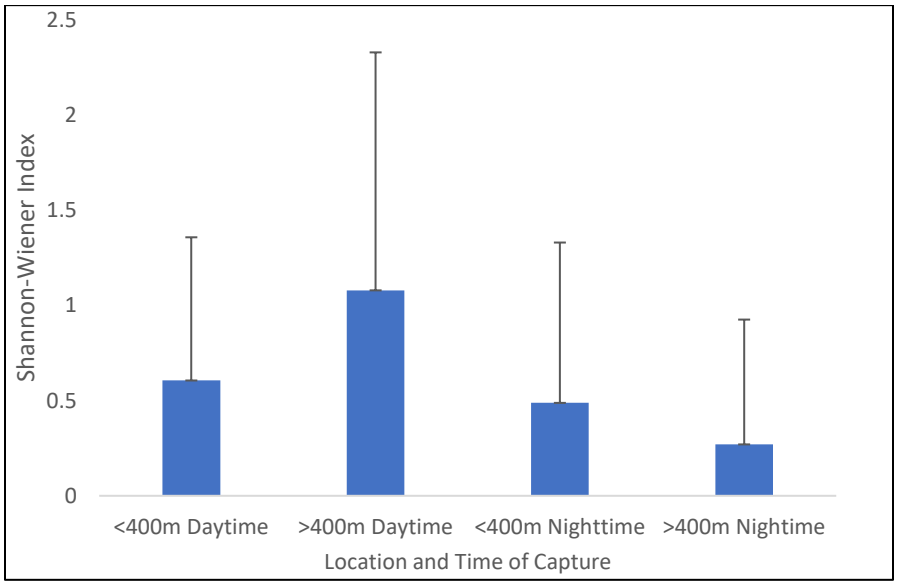

B)

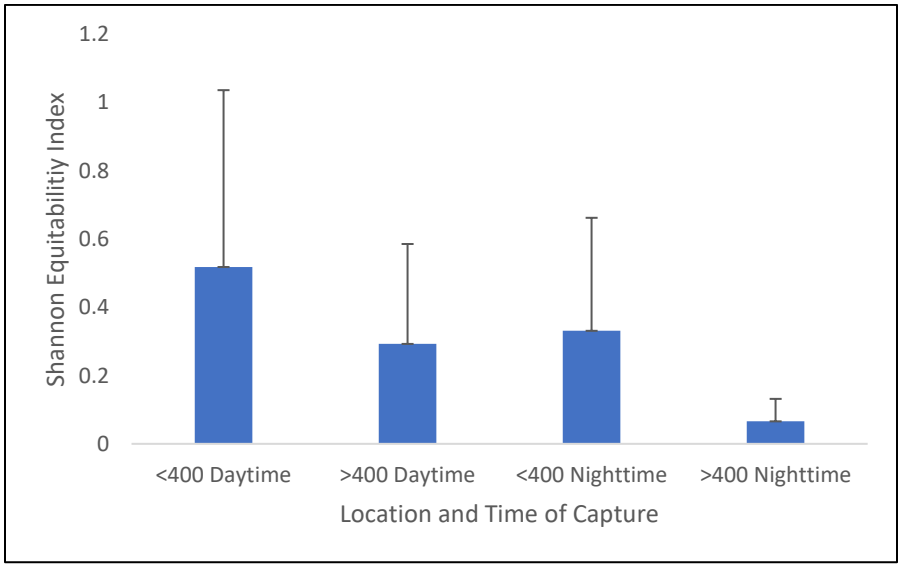

Figure 3 A) Shannon diversity and **B)** Shannon Equitability Index, with upper 95 % confidence intervals for dissected mesopelagic fishes sampled at an ocean depth below and above 400 m at day-time and night-time tows.

A.

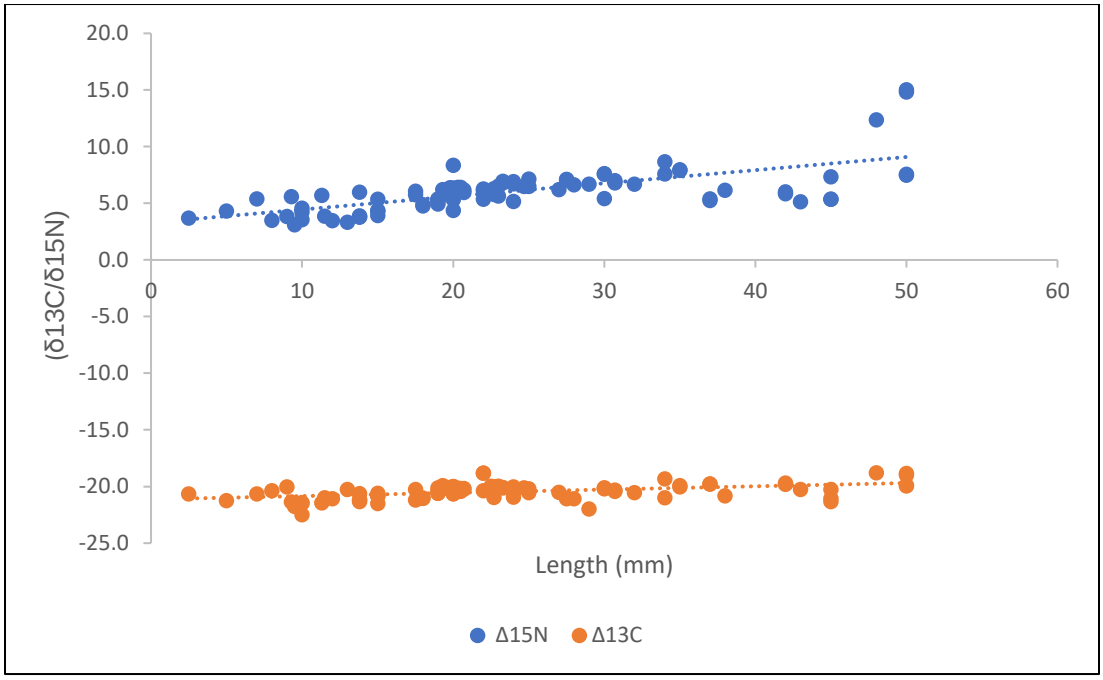

B.

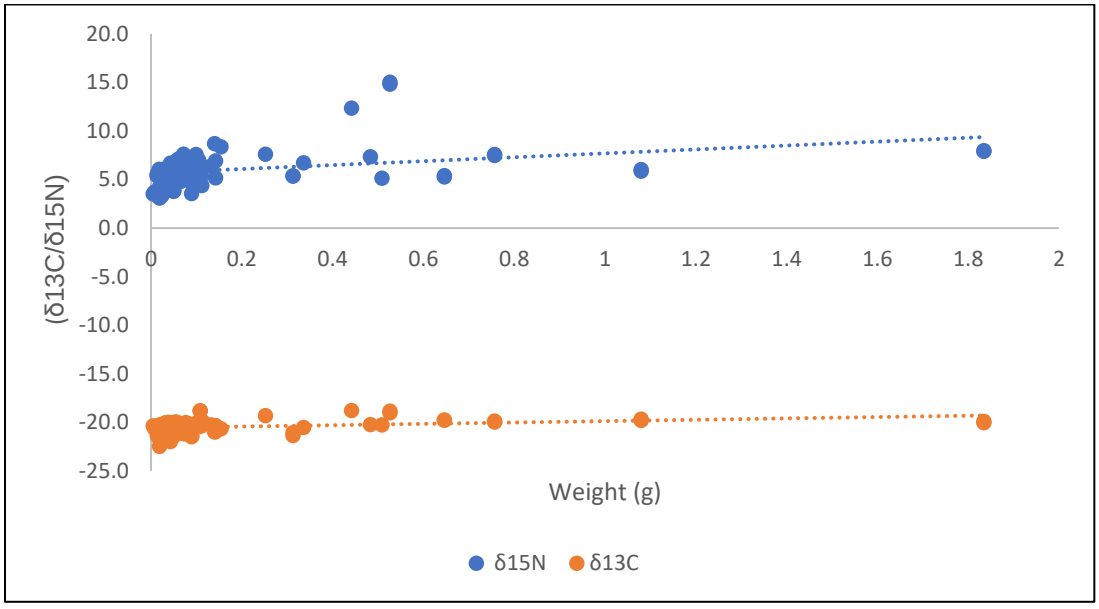

Figure 4. A) Linear regression of the relationship of $\delta^{13}C$ and $\delta^{15}N$ and standard length (mm) of mesopelagic fishes classified as migrators. **B)** Linear regression of the relationship of $\delta^{13}C$ and $\delta^{15}N$ and wet weight (g) of mesopelagic fishes classified as migrators.

A.

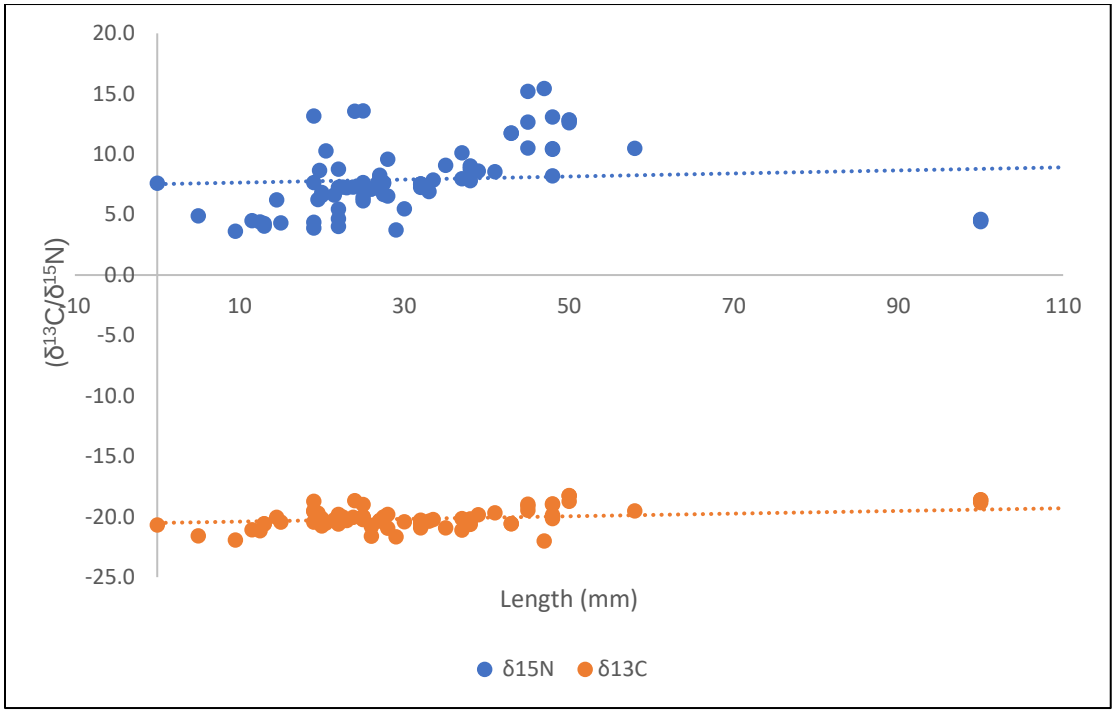

B.

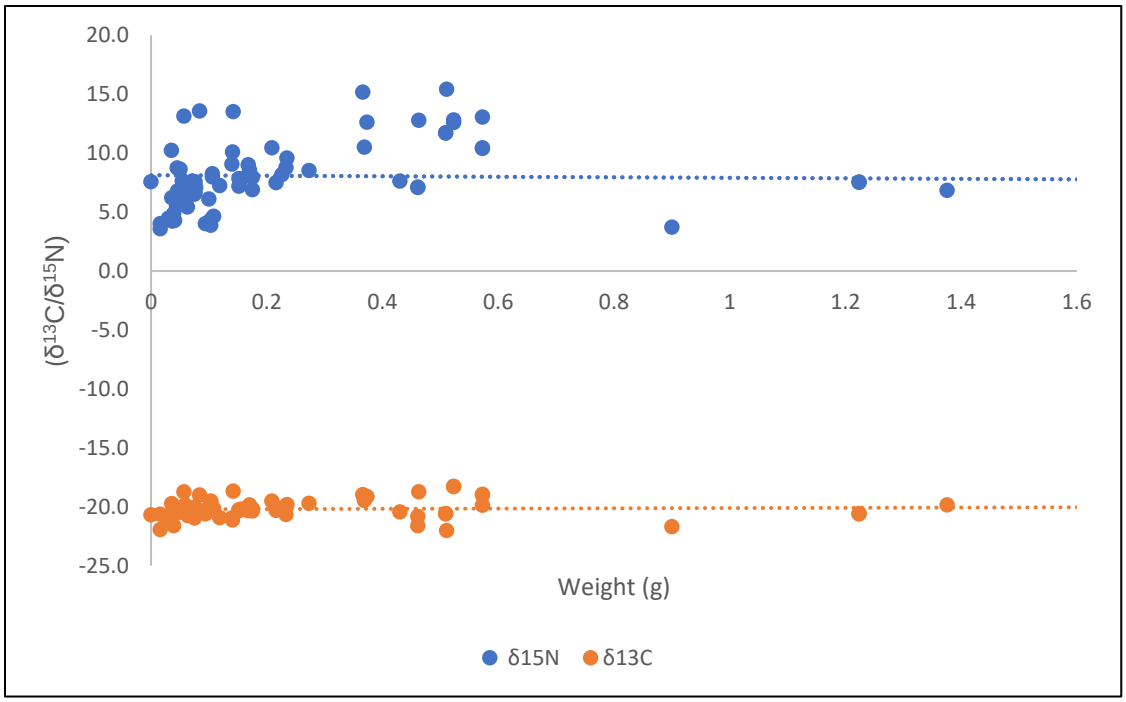

Figure 5. A) Linear regression of the relationship of $\delta^{13}C$ and $\delta^{15}N$ and standard length (mm) of mesopelagic fishes classified as non-migrators. **B)** Linear regression of the relationship of $\delta^{13}C$ and $\delta^{15}N$ and wet weight (g) of mesopelagic fishes classified as non-migrators.

A)

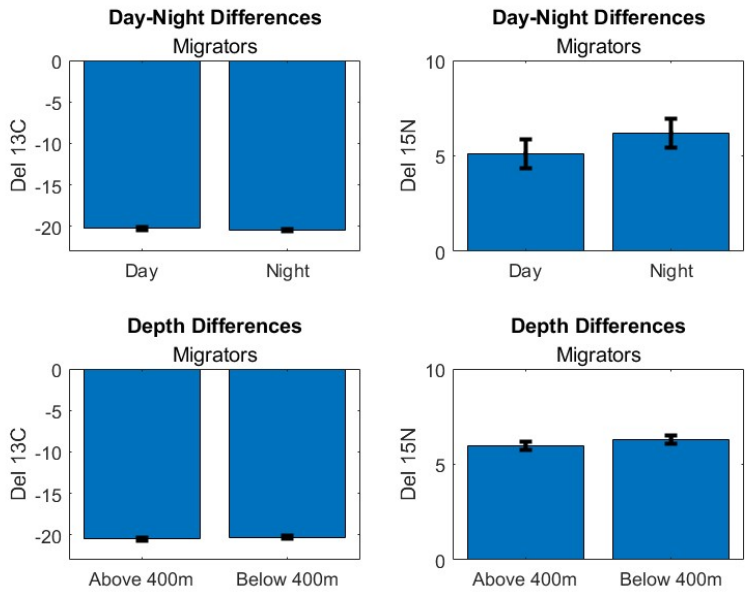

B)

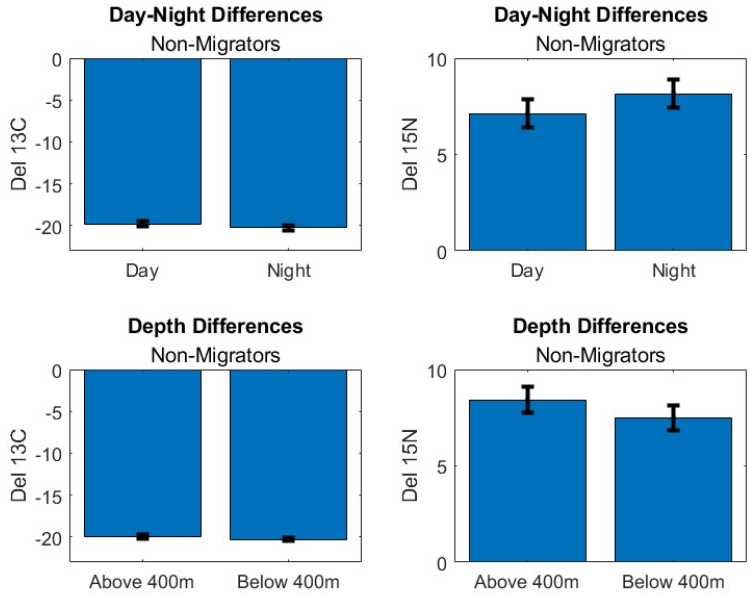

Figure 6. The relationship of **A)** migrating and **B)** non-migrating mesopelagic fish species to analyze time of day and depth variability in $\delta^{15}N$ and $\delta^{13}C$. For depth, fishes were categorized if they were sampled below or above 400m at time of capture. For time of day, fishes were categorized if they were sampled during a daytime or nightime tow. Error bars indicate 95% confidence intervals.

A)

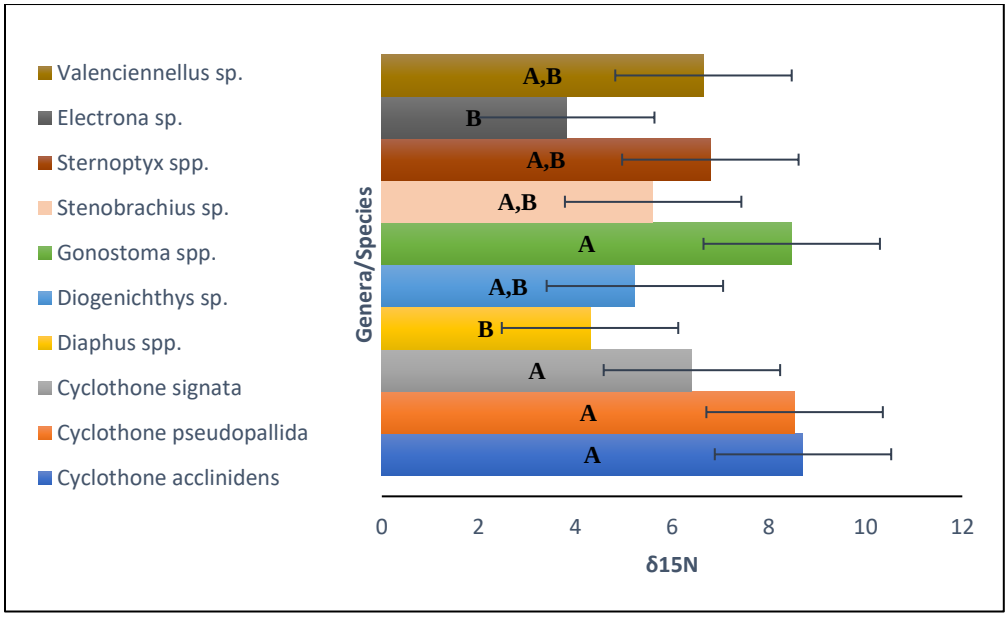

B)

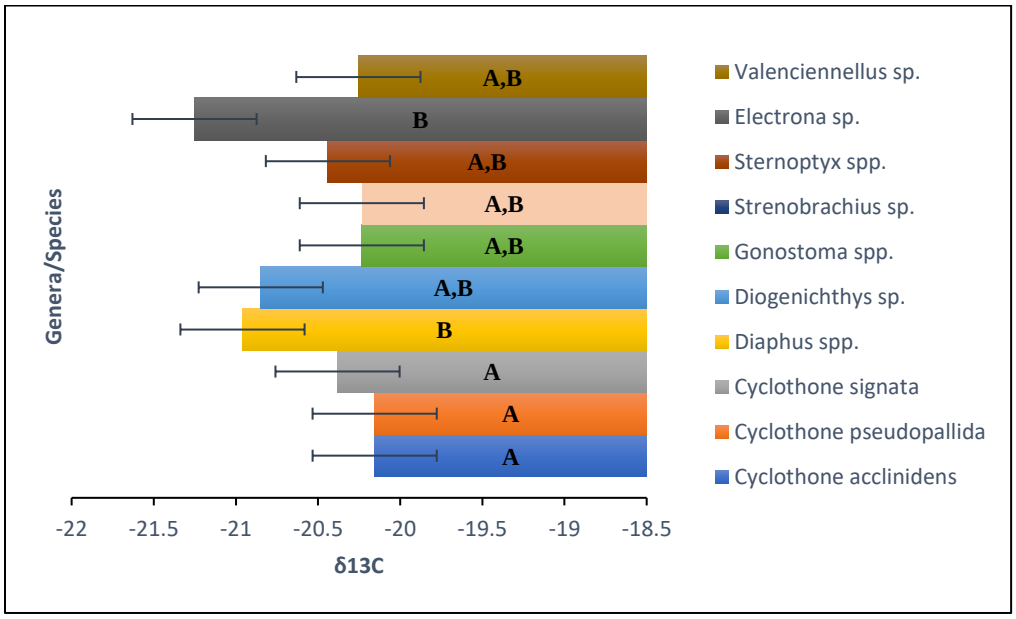

Figure 7. Relationship of mesopelagic fish species/genera and **A)** $\delta^{15}N$ and **B)** $\delta^{13}C$, with 95% confidence intervals shown. The genus *Cyclothone* was differentiated to species level for analysis since *Cyclothone pseudopallida* and *Cyclothone acclinidens* were classified as non-migrators and *Cyclothone signata* was classified as a migrator. A post-hoc Tukey-Kramer test (Table 12) was also included to analyze where variation in isotope composition ($\delta^{15}N$ and $\delta^{13}C$) between species/genera existed.

Chapter 3 Tables

Table 1. Description of fish specimens used to develop allometric relationships. This table includes information on sampling location, latitude/longitude coordinates, collection dates, species collected, standard length range of collected fishes, weight of collected fishes, number of species collected and dissected, and the number of samples encapsulated to undergo SIA.

Location	Location Coordinates	Collection Date	Species Collected	Standard Length Range (mm)	Weight Range(g)	Number of Species Collected	Number of Fishes Dissected	Number of Samples Submitted for SIA
Wanchese	35°50'42"N, 75°38'22"W	10/2022, 11/2022	Naked Gobies (*Gobiosoma bosc*)	22-32	0.055-0.520	70	41	15
Goose Creek State Park	35°28'55"N, 76°54'5"W	7/2022	Bay Anchovies (*Anchoa mitchilli*)	35-68	0.390-2.844	148	75	37
Beaufort	34°43'5"N, 76°39'49"W	9/2020	Atlantic Silversides (*Menidia menidia*)	39-61	0.525-1.743	75	37	19

Table 2 Descriptive statistics [mean, standard deviation (stdev), standard error (sterr), and 95% confidence interval (95 CI)] for carbon (C) content (mg) for ethanol (EtOH) and ice preserved fish gut contents (GC).

Column1	EtOH GC C13	EtOH GC N15	Ice GC C13	Ice GC N15
mean	0.369	0.08875	0.7565	0.153
stdev	0.219699795	0.038947614	0.24395184	0.042426407
sterr	0.1098	0.0194	0.1725	0.03
95 CI	0.215208	0.038024	0.3381	0.0588
95 CI Range	0.153-0.584	0.051-0.127	0.418-1.095	0.094-0.212

	EtOH GC C	EtOH SL C	Ice GC C	Ice SL C
mean	0.369	0.233	0.756	0.378
stdev	±0.219	±0.130	±0.244	±0.261
sterr	±0.109	±0.080	±0.172	±0.407
95 CI	±0.215	±0.157	±0.338	±0.798

Table 3 Descriptive statistics [mean, standard deviation (stdev), standard error (sterr), and 95% confidence interval (95 CI)] for nitrogen content (N) (mg) for ethanol (EtOH) and ice preserved fish stomach linings (SL).

	EtOH GC N	EtOH SL N	Ice GC N	Ice SL N
mean	0.089	0.049	0.153	0.071
stdev	±0.039	±0.035	±0.042	±0.055
sterr	±0.019	±0.024	±0.030	±0.032

95% CI	±0.038	±0.047	±0.059	±0.063

Table 4. Descriptive statistics [mean, standard deviation (stdev), standard error (sterr), and 95% confidence interval (95 CI)] of $\delta^{13}C$ for ethanol (EtOH) and ice preserved fish stomach lining (SL) and gut contents (GC).

	Ice GC δ13C	EtOH GC δ13C	Ice SL δ13C	EtOH SL δ13C
mean	-25.329	-25.423	-25.979	-24.536
stdev	±0.471	±0.732	±0.881	±0.733
sterr	±0.333	±0.327	±0.293	±0.277
95% CI	±4.228	±0.909	±0.677	±0.678

Table 5. Descriptive statistics [mean, standard deviation (stdev), standard error (sterr), and 95% confidence interval (95 CI)] of $\delta^{15}N$ for ethanol (EtOH) and ice preserved fish stomach lining (SL) and gut contents (GC).

	Ice GC δ15N	EtOH GC δ15N	Ice SL δ15N	EtOH SL δ15N
mean	10.239	9.502	10.424	11.016
stdev	±0.291	±0.288	±0.395	±0.743

sterr	±0.205	±0.129	±0.132	±0.281
95% CI	±2.61	±0.358	±0.304	±0.687

Table 6 Linear regression statistics on the relationship between carbon content (mg) and fish size [standard length (mm) and wet weight (g)] for Atlantic silversides, bay anchovies, and naked gobies.

Weight				
Species	**p-value**	**R^2**	**Slope**	**Intercept**
Atlantic Silversides	0.030	0.260	-7.892	2.811
Bay Anchovies	0.110	0.070	-0.253	0.000
Naked Gobies	0.040	0.260	-0.543	0.000
Length				
Species	**p-value**	**R^2**	**Slope**	**Intercept**
Atlantic Silversides	0.020	0.270	1.530	0.000
Bay Anchovies	0.080	0.090	-0.135	-0.358
Naked Gobies	0.040	0.250	1.150	0.000

Chapter 3 Figures

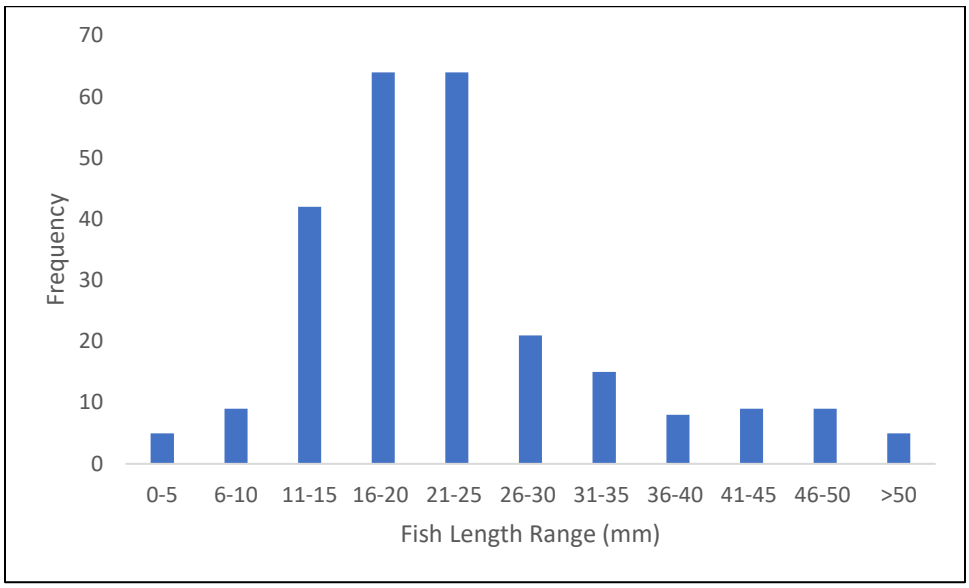

Figure 1. Standard length frequency distribution of dissected mesopelagic fishes

A

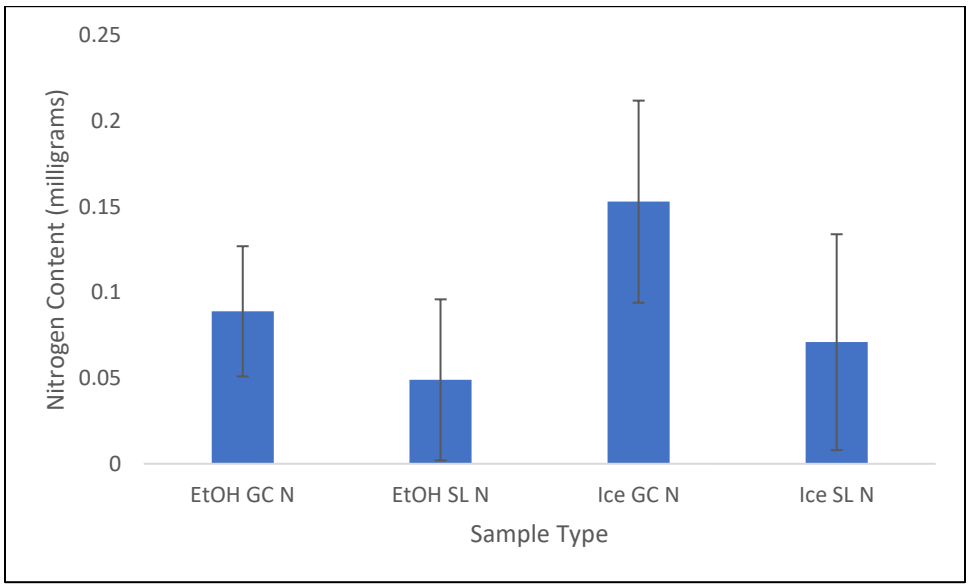

B)

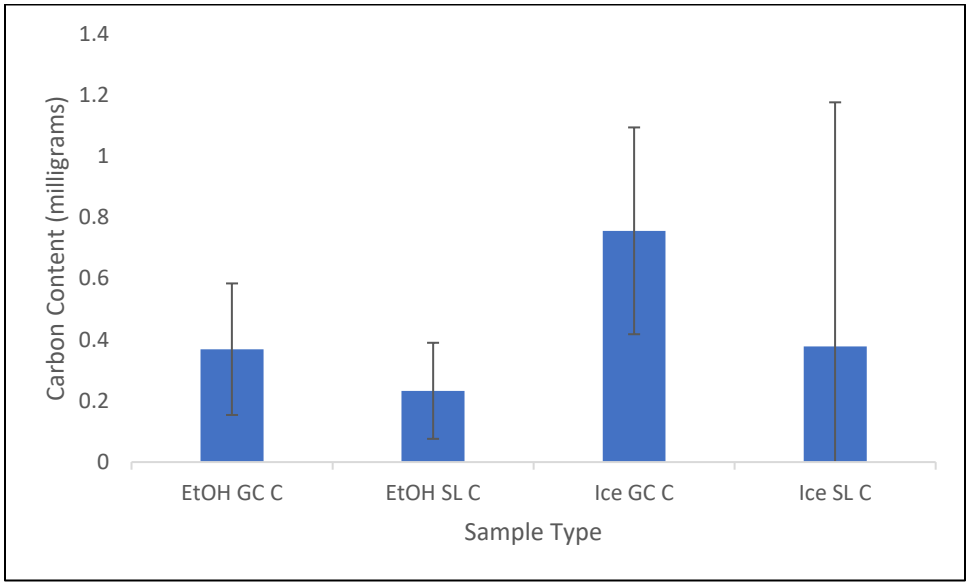

Figure 2. A) The impacts of preservation method [ice or ethanol (EtOH)] upon grams of nitrogen (N) in bay anchovy gut contents (GC) and stomach lining (SL) with 95% confidence intervals**. B)** The impacts of preservation method (ice or ethanol) upon grams of carbon (C) in bay anchovy gut contents and stomach lining with 95% confidence intervals.

A)

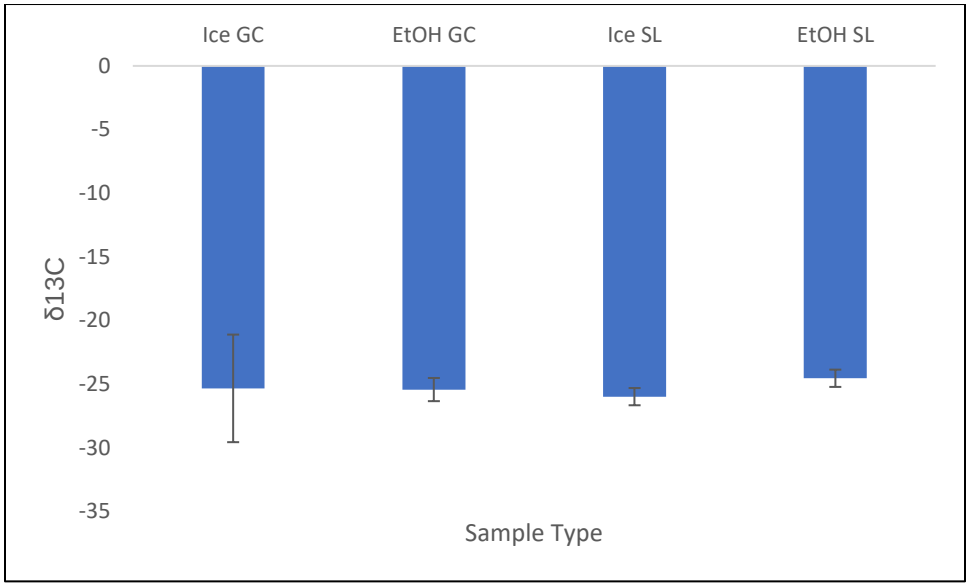

B)

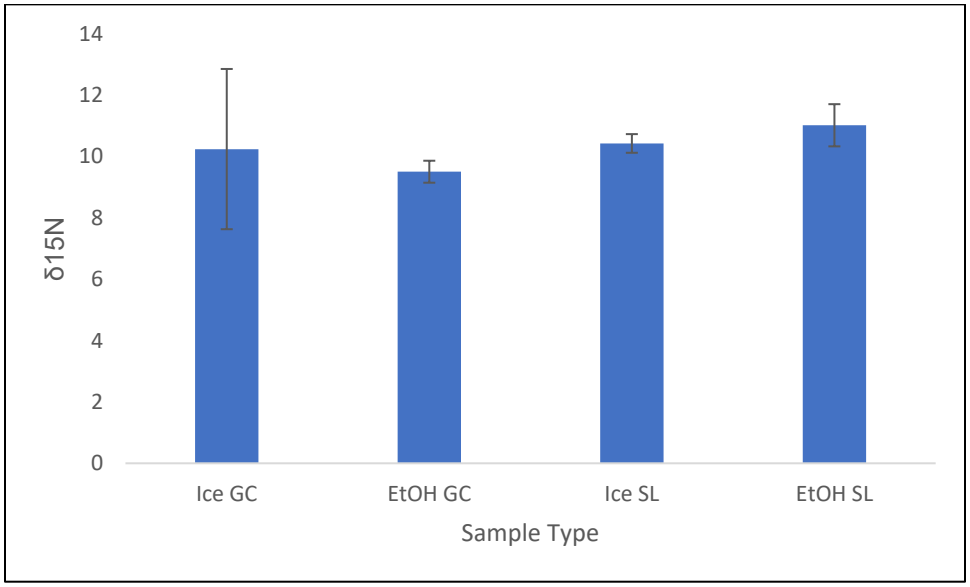

Figure 3. A) The impacts of preservation method (ice or ethanol (EtOH)) upon $\delta^{13}C$ in bay anchovy gut contents (GC) and stomach lining (SL) with 95% confidence intervals**. B)** The impacts of preservation method (ice or ethanol) upon $\delta^{15}N$ in bay anchovy gut contents and stomach lining with 95% confidence intervals.

A)

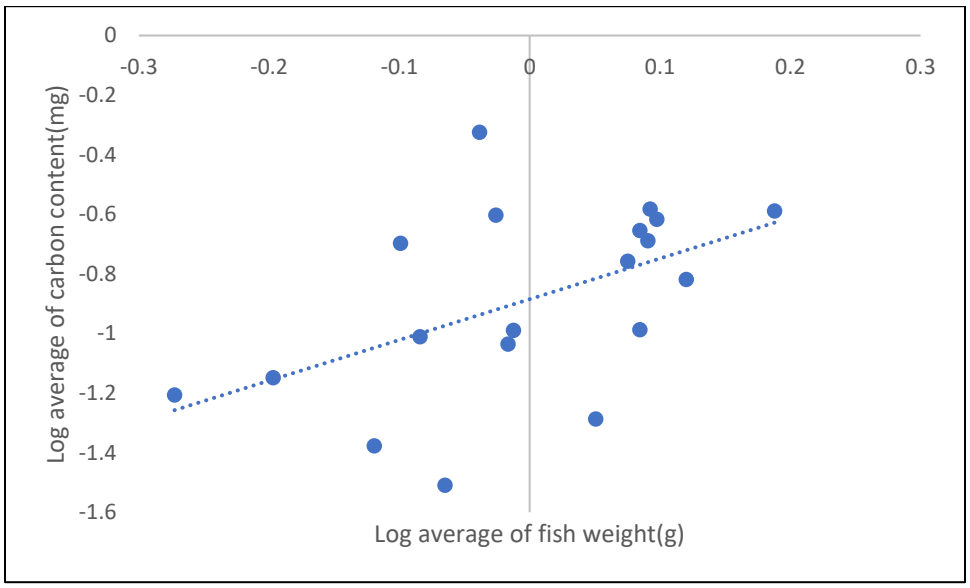

.

B)

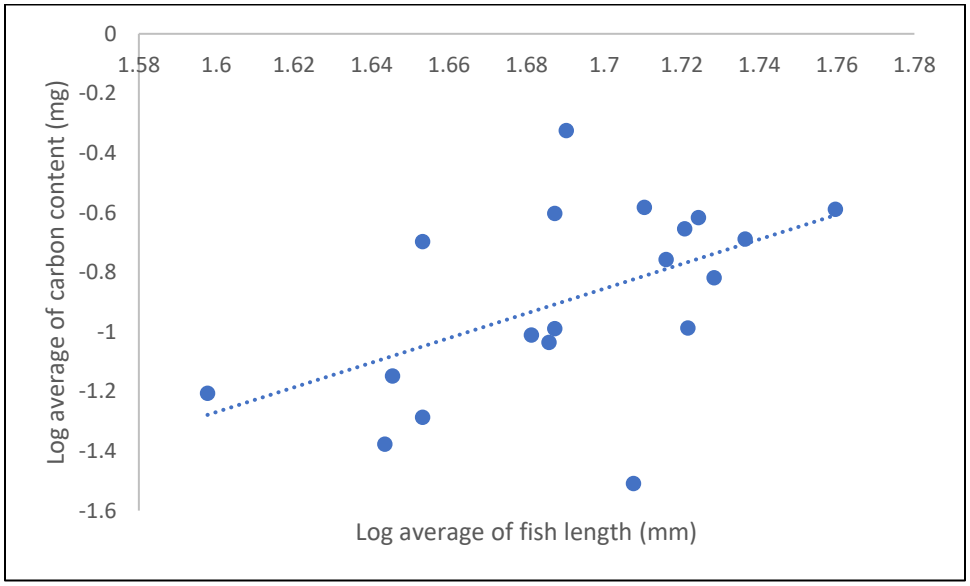

Figure 4. A) Log average of carbon (mg) in Atlantic silversides (*Menidia menidia*) in relation to fish weight in grams.

B) Log average of carbon (mg) in Atlantic Silversides in relation to fish standard length in millimeters.

A)

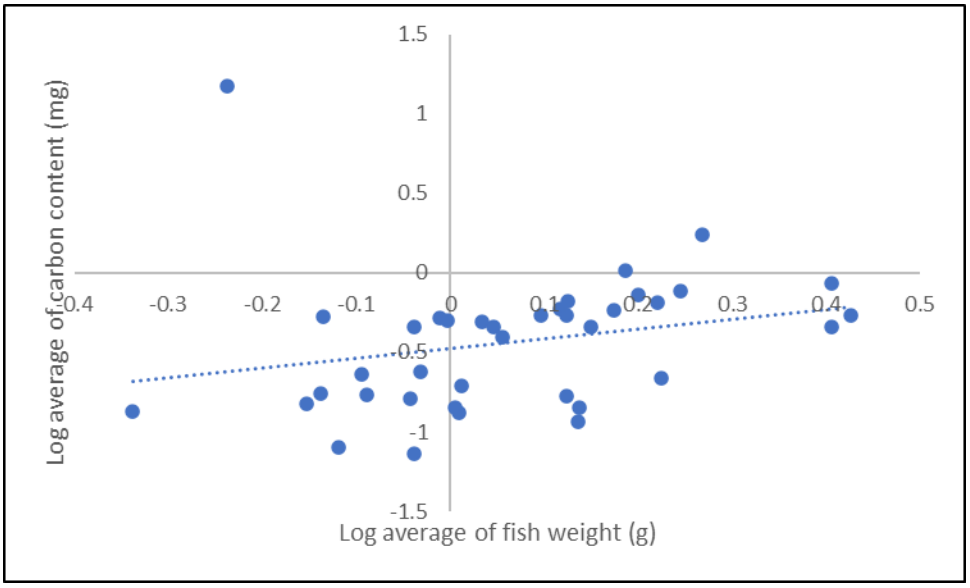

B)

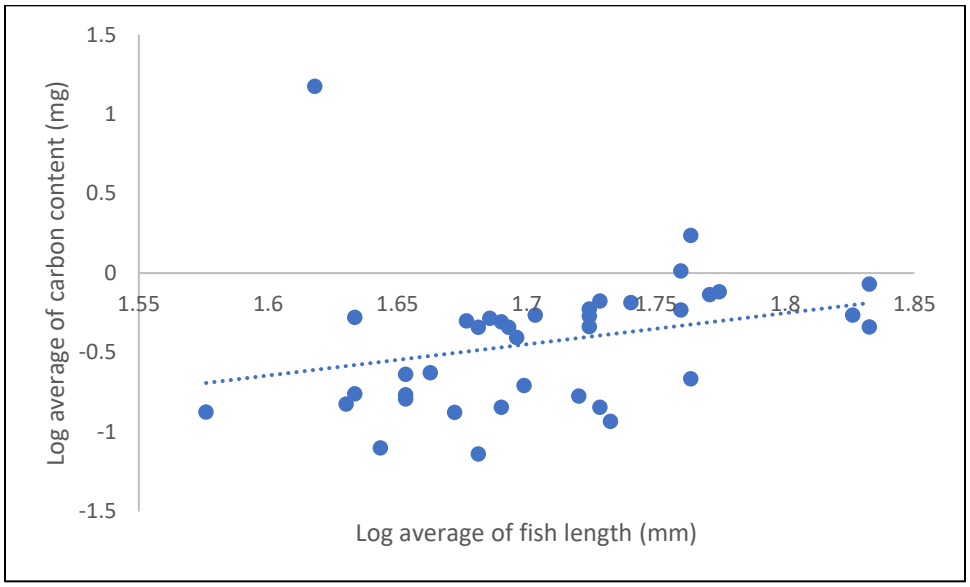

Figure 5. A) Log average of carbon (mg) in bay anchovies (*Anchoa mitchilli*) in relation to fish weight in grams.

B) Log average of carbon (mg) in bay anchovies in relation to fish standard length millimeters.

A)

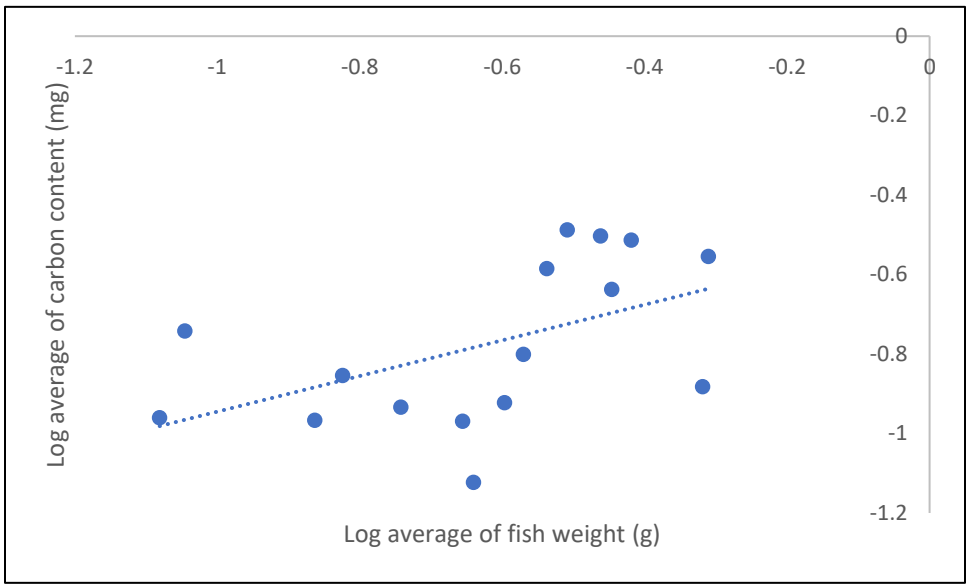

B)

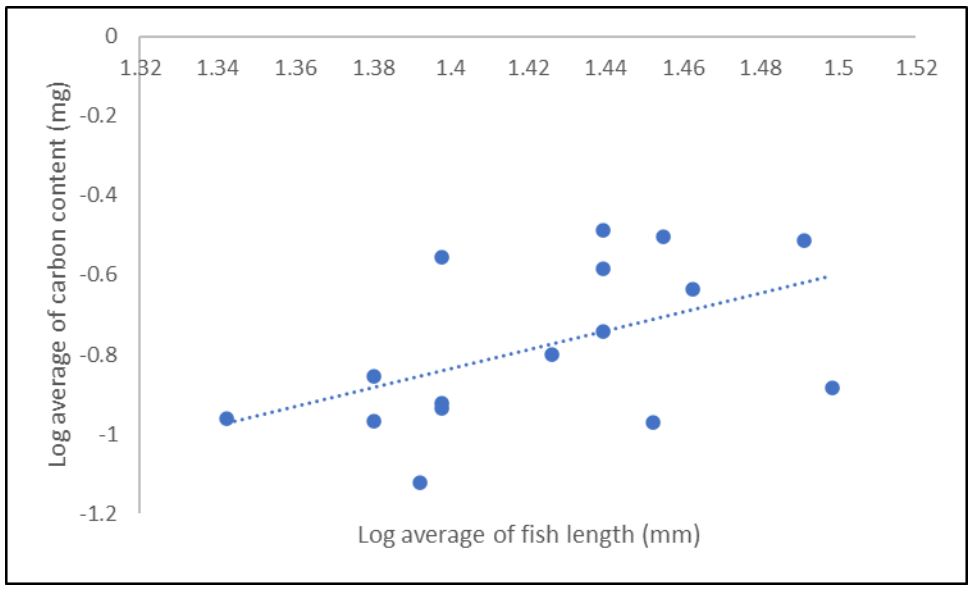

Figure 6. A) Log average of carbon (mg) in naked gobies (*Gobiosoma bosc*) in relation to fish weight in grams.

B) Log average of carbon (mg) in naked gobies in relation to fish standard length in millimeters.

Appendix: IACUC Permission Letter

Animal Care and Use Committee
003 Ed Warren Life Sciences Building | East Carolina University | Greenville NC 27834 – 4354
252-744-2436 office | 252-744-2355 fax

May 20, 2022

Rebecca Asch, Ph.D.
Department of Biology, ECU

Dear Dr. Asch:

Your Animal Use Protocol entitled, "Collection of juvenile fishes from Goose Creek State Park, North Carolina for allometric relationship development to estimate carbon in gut contents based on fish biomass and length" (AUP#D379) was reviewed by this institution's Animal Care and Use Committee on 05/18/2022. The following action was taken by the Committee:

"Approved as submitted"

****Please contact Aaron Hinkle prior to any hazard use****

A copy of the protocols is enclosed for your laboratory files. Please be reminded that all animal procedures must be conducted as described in the approved Animal Use Protocol. Modifications of these procedures cannot be performed without prior approval of the ACUC. The Animal Welfare Act and Public Health Service Guidelines require the ACUC to suspend activities not in accordance with approved procedures and report such activities to the responsible University Official (Vice Chancellor for Health Sciences or Vice Chancellor for Academic Affairs) and appropriate federal Agencies. **Please ensure that all personnel associated with this protocol have access to this approved copy of the AUP/Amendment and are familiar with its contents.**

Sincerely yours,

Susan McRae, Ph.D.
Chair Animal Care and Use Committee

SM/GD

enclosure